

UCSF

UC San Francisco Electronic Theses and Dissertations

Title

Functional genetic studies of the murine integrin beta8 subunit

Permalink

<https://escholarship.org/uc/item/0dg170gn>

Author

Proctor, John Michael

Publication Date

2006

Peer reviewed|Thesis/dissertation

Functional Genetic Studies of the Murine Integrin β 8 Subunit

by

John Michael Proctor

DISSERTATION

Submitted in partial satisfaction of the requirements for the degree of

DOCTOR OF PHILOSOPHY

in

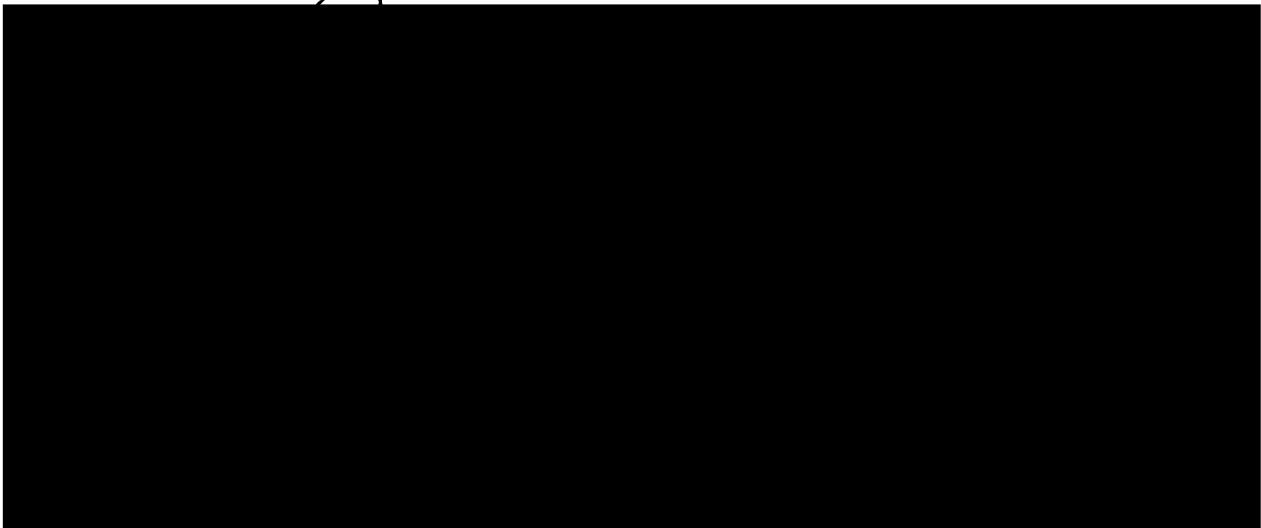
Neuroscience

in the

GRADUATE DIVISION

of the

UNIVERSITY OF CALIFORNIA, SAN FRANCISCO



Date

University Librarian

Degree Conferred:.....

Copyright 2006

by

John Michael Proctor

Preface

When I moved to San Francisco in July of 2000, I was unaware of the many lives that would touch my own in the five and half years to come. I was even more ignorant of the impact each person would have on my personal development. Regrettably, I will not be able to mention them all by name in this short preface. My appreciation, however, belongs to all those who shared parts of their lives and experiences with me. I am forever grateful and will cherish the memories we've made and those we have yet to make.

My professional development during my tenure at UCSF has taken place under the kind guidance of Lou Reichardt. Known to many as the director of Neuroscience at UCSF, I know him simply as Lou. He is no less than a brilliant neuroscientist, an admirable advisor, and a good friend. His passion for science, his knowledge of climbing, and his never-ending energy inspired me daily. Even the most dedicated doctoral student needs motivation to persevere and finish a Ph.D. Lou never let me lose sight of the goal and constantly challenged me to prioritize my time and experiments. I thank him for traveling along with me on this journey. It has truly been an honor and a pleasure to have been a part of the Reichardt lab.

The Reichardt lab was more than a place of work or study. Indeed, much of my success was due to the wonderful members of the lab that shared their insights, enthusiasm, and friendship during my dissertation. My bench mate and good friend James Linton was always available to discuss anything science, baseball, or football making even the slowest of times bearable. Shernaz Bamji and Zhen Huang provided me with endless information about microscopy and integrin biology and became good friends in the process. Denise Marciano has helped me think about my future and I thank her for

her positive energy and daily laughter. Keling Zang shared her many years of technical experience in labs at UCSF to help me be successful in my project. I also want to thank her for her constant kindness and concern for my personal happiness and well-being while in the lab. I want to especially thank Will Walantus for heroically ensuring that my mice safely arrived at Mission Bay. I am most appreciative, though, of his incredible friendship. I am deeply thankful for being able to spend more than one Thanksgiving with he and his family and for all the great times we shared on his land in Calveras County.

I also want to thank my thesis committee, John Rubenstein, Larry Tecott, Rong Wang, and Marc Tessier-Lavigne. On the formal occasions they were never short on encouragement or helpful suggestions. At informal meetings I appreciated the care each of them showed for my graduate experience, always asking about me before my project. In particular, I have appreciated my chair, John Rubenstein who was always straightforward and kind. He has an elegant way of injecting calmness into seemingly turbulent situations. I thank them all for being a positive influence on me and my thesis.

The fond memories I have of UCSF and San Francisco originate with my wonderful classmates. Matt Caywood, a man believed to this day to be my twin brother by some less observant faculty members, may well be the best debater I know. His uncanny wit and dry humor were a welcome part of my graduate experience. Ammon Corl and Kaiwen Kam have been great friends that I could always count on to rescue the dull atmosphere of Asilomar with a board game or an in depth discussion of life. Cory Blaiss, while certainly the most gifted vocal performer in our class, managed also to be

one of the most caring individuals I know. I thank them all for their wonderful friendship.

My success would not have been possible without the support of my loving parents Billie and Lucy Proctor. Their enduring encouragement has always been inspirational and their patience and understanding throughout the tough times of my tenure in San Francisco was amazing. The insights they continue to give me illuminate the life I want for myself and my own family one day. I cannot find words for the love and appreciation I have for them and their active role in my life. As a small token of thanks, I dedicate this thesis to them both.

Functional Genetic Studies of the Murine Integrin $\beta 8$ Subunit

by

John Michael Proctor

A handwritten signature in black ink, appearing to read 'John Rubenstein', is written over a horizontal line. The signature is stylized and cursive.

John Rubenstein

Chair, Thesis Committee

Abstract

Central to understanding development of multicellular organisms is a thorough understanding of intercellular communication. The intricate process of vascular development within the central nervous system highlights the importance of molecules that can mediate both intercellular communication and interaction between vascular endothelial cells and cells within the neuroepithelium. The integrin family of cell adhesion molecules functions in many aspects of development and the integrin $\alpha v \beta 8$ functions specifically in vascular development of the brain, yolk sac, and placenta. Animals lacking either the *integrin αv* (*itgav*) subunit gene or the $\beta 8$ (*itg $\beta 8$*) subunit gene

die either at midgestation because of insufficient vascularization of the placenta and yolk sac, or shortly after birth with severe intracerebral hemorrhage. To specifically focus on the role of integrins containing the $\beta 8$ subunit in the brain, and to avoid early lethality, we utilized a targeted deletion strategy to delete *itg $\beta 8$* only from cell types within the brain. Ablating *itg $\beta 8$* from vascular endothelial cells or from migrating neurons did not result in cerebral hemorrhage. Targeted deletion of *itg $\beta 8$* from the neuroepithelium, however, resulted in bilateral hemorrhage at postnatal day zero, although the phenotype was less severe than in *itg $\beta 8$* -null animals. Newborn mice lacking *itg $\beta 8$* from the neuroepithelium had hemorrhages in the cortex, ganglionic eminence, and thalamus as well as abnormal vascular morphogenesis, and disorganized astroglial processes. We herein propose that defective association between vascular endothelial cells and astroglia lacking *itg $\beta 8$* is responsible for the leaky vasculature seen during development. Interestingly, adult mice lacking *itg $\beta 8$* from cells derived from the neuroepithelium did not show signs of hemorrhage. However, these adult mutant animals began to display abnormal gait in their hind limbs approximately six to twelve weeks after birth. They also developed severe urinary dysfunction which may have ultimately contributed to their premature death. Although morphological cortical abnormalities were not observed in these mutants, the brains of adult *itg $\beta 8$* neuroepithelial cell mutants have an abnormal distribution of astrocytes indicating that the $\alpha \nu \beta 8$ integrin may play a role in proper cortical astrocyte localization in the adult animal. We discuss potential signaling mechanisms to explain these anatomical results.

TABLE OF CONTENTS

Preface	iii
Abstract	vi
List of Figures and Tables	xi
CHAPTER ONE: Introduction	1
Integrin Structure and Signaling.....	2
The Integrin $\alpha\beta 8$	5
Endothelial Cell Biology and Integrin $\alpha\beta 8$	10
Statement of Purpose.....	14
CHAPTER TWO: Vascular Development of the Brain Requires $\beta 8$ Integrin Expression in the Neuroepithelium	15
Acknowledgements.....	16
Abstract.....	18
Introduction.....	19
Materials and Methods.....	20
Results.....	27
Discussion.....	35
Figures.....	42
CHAPTER THREE: Functional Analysis of the Integrin $\beta 8$ Pathway Using a Microarray Approach	59
Acknowledgements.....	60
Abstract.....	61
Introduction.....	62

Materials and Methods.....	63
Results.....	69
Discussion.....	72
Figures and Tables.....	80
CHAPTER FOUR: Integrin β8 is Required in the Adult Mouse for Proper	
Locomotion, Urinary Function, and Cortical Astrocyte Localization.....	91
Acknowledgements.....	92
Abstract.....	92
Introduction.....	93
Materials and Methods.....	94
Results.....	95
Discussion.....	100
Summary.....	104
Figures and Tables.....	106
CHAPTER FIVE: Discussion, Final Summary, and Future Perspectives.....	114
Discussion.....	115
CNS Vascular Development.....	116
Summary of Chapters.....	121
Future Perspectives.....	124
REFERENCES.....	127
APPENDIX: Generation and Characterization of Polyclonal Antisera	
Against the Murine Integrin β8 Subunit.....	150
Acknowledgements.....	151

Abstract.....	151
Introduction.....	152
Materials and Methods.....	154
Results.....	161
Discussion.....	165
Figures.....	169

LIST OF FIGURES AND TABLES

CHAPTER TWO

Figure 2-1: Phenotypic defects observed after conditional deletion of <i>itgβ8</i> from the neuroepithelium using <i>nestin-cre</i> .	42
Figure 2-2: Conditional deletion of <i>itgβ8</i> from vascular endothelial cells using <i>tie2-cre</i> does not result in cerebral hemorrhage.	44
Figure 2-3: Conditional deletion of <i>itgβ8</i> from post-mitotic neurons using <i>nex-cre</i> does not result in cerebral hemorrhage.	46
Figure 2-4: Conditional deletion of <i>itgβ8</i> in the neuroepithelium leads to endothelial cell irregularities in the P0 neonatal cortex.	48
Figure 2-5: <i>itgβ8 nestin-cre</i> mutants have abnormally organized cortical glia.	50
Figure 2-6: Adult <i>itgβ8 nestin-cre</i> mutants show no sign of brain hemorrhage.	52
Supplementary Figure 2-1: Generation of conditional <i>itgβ8</i> mice.	54
Supplementary Figure 2-2: <i>β-Galactosidase</i> expression analysis of smooth-muscle cells in E15.0 embryo cortices obtained from a cross of a <i>nestin-cre</i> positive animal and the <i>R26R</i> reporter line.	57
Supplementary Figure 2-3: Conditional deletion of <i>itgβ8</i> from the neuroepithelium using <i>nescre8</i> results in cerebral hemorrhage.	58

CHAPTER THREE

Figure 3-1: Analysis of the <i>nescre8</i> transgenic line using the <i>R26R</i> reporter line.	80
---	----

Figure 3-2: RT-PCR and Northern blot analysis of RNA from <i>itgβ8</i> mutants.	81
Table 3-1: Quantification of RNA collected and amplified from E12.5 <i>itgβ8 nescre8</i> mutants and control forebrains.	83
Figure 3-3: Quality analysis of total RNA and amplified RNA from E12.5 <i>itgβ8 nescre8</i> mutants and control forebrains.	84
Figure 3-4: Gene expression analysis of E12.5 <i>itgβ8 nescre8</i> mutant and control forebrains using MEEBO microarrays.	86
Figure 3-5: Secondary analysis of gene expression in E12.5 <i>itgβ8 nescre8</i> mutant and control forebrains using MEEBO microarrays.	88

CHAPTER FOUR

Table 4-1: Age of onset of phenotypes identified during adulthood and lifespan of conditional <i>itgβ8</i> mutants generated using various cre lines.	106
Figure 4-1: Adult <i>itgβ8 nestin-cre</i> mutants and the <i>itgβ8 nescre8</i> mutants display abnormal hindlimb coordination during locomotor activity.	107
Figure 4-2: <i>R26R</i> reporter analysis of the <i>nescre8</i> transgenic mouse line.	109
Figure 4-3: Adult <i>itgβ8 nestin-cre</i> mutants show no sign of brain hemorrhage.	110
Figure 4-4: Adult <i>itgβ8 nestin-cre</i> mutants have abnormally organized cortical astrocytes, but do not have leaky blood vessels.	112

APPENDIX

Figure A-1: ELISA results for serum obtained from rabbits immunized with the GST-tagged mouse integrin β8 cytoplasmic tail.	169
---	-----

Figure A-2: Western blot and immunocytochemistry of HT1080 cells transfected with human integrin $\beta 8$.	172
Figure A-3: Affinity purification of antibodies against the mouse integrin $\beta 8$ cytoplasmic tail tagged with GST from serum obtained from rabbit 1673.	174
Figure A-4: Immunoprecipitation using affinity purified antibodies against the mouse integrin $\beta 8$ cytoplasmic tail.	176

Chapter 1

Introduction

Development of multicellular organisms requires two fundamental processes: cell-cell communication and intercellular adhesion. Several highly conserved families of molecules function across species and phyla boundaries to mediate these critical functions. Of these, the integrin family of cell adhesion molecules is known to function as receptors for extracellular matrix (ECM) molecules and play critical roles during development, immune responses, homeostasis, and cancer (Hynes, 2002a). In this chapter, I will discuss portions of the vast body of knowledge regarding integrin biology amassed in the last two decades. I will pay particular attention to how members of this family of molecules function during vascular development of the embryo and brain.

Integrin Structure and Signaling

Integrins are a family of cell-surface transmembrane glycoproteins that act as receptors for ECM molecules and cell-surface bound molecules. Each integrin is a heterodimer that consists of a noncovalently associated α subunit and β subunit each with a large extracellular domain and a short cytoplasmic tail. To date there are 18 distinct α and 8 distinct β subunits known that combine to produce 24 different heterodimers known in mammals (Hynes, 2002a). The specific α/β subunit pairings specify the ligand, such as laminin, collagen, or short peptide sequences such as the arginine-glycine-asparagine (RGD) sequence, to which the integrin can bind. However, specific arrangement of the three-dimensional structure of the integrin is required for ligand binding.

The extracellular ligand binding domains (also known as the headpieces) of the α and β subunits associate noncovalently in a “bent” conformation (Takagi et al., 2002; Xiong et al., 2002). Integrins in this bent conformation are “inactive” and have low

affinity for ligands, although they are still capable of ligand binding (Adair et al., 2005). Upon activation of the integrin, the headpieces move upward in a switch-blade like motion into the so-called “active” conformation that optimizes the position of the ligand-binding domains within the α and β subunits increasing the integrin’s affinity for binding its target ligand (Springer and Wang, 2004; Arnaout et al., 2005).

Integrin activation is essential for normal development of the embryo because it directly regulates processes such as cell adhesion, migration, and assembly of the ECM (Wu et al., 1995; Huttenlocher et al., 1996; Palecek et al., 1997). In fact, deregulated integrin activation disrupts embryonic development (Martin-Bermudo et al., 1998), cardiac function (Keller et al., 2001) and the immune response (McDowall et al., 2003). Thus, proper integrin function is dependent on proper regulation of activation. In addition, proper activation of the integrin depends on the cytoplasmic tails of the α and β subunits (Calderwood, 2004). There are specific domains within the cytoplasmic tails of the integrin subunits which seem to play critical roles in integrin activation. Deletion of the membrane-proximal sequences of either the α subunit (GFFKR sequence) the or β subunit (LLxxxHDRRE) results in constitutive activation of an integrin (O’Toole et al., 1994; Lu and Springer, 1997; Lu et al., 2001). One prominent model favors the idea that interaction of the membrane proximal sequences of the α and β subunits maintain the integrin in the inactive, low-affinity, state while separation of these domains causes the conformational change in the extracellular domains to “activate” the integrin in the high-affinity state (Woodside et al., 2001; Calderwood, 2004). In addition, mutations outside the membrane-proximal sequence of the β subunit seem to block activation. Specifically, mutations in the NPxY motif not only block integrin activation, but perturb binding of

numerous cytoskeletal proteins to the integrin β tail (Liu et al., 2000). Activation through this motif on the integrin β subunit is mediated largely through binding of a large homodimer called talin, although other molecules have been identified that may directly activate integrins (Kolanus et al., 1996; Kashiwagi et al., 1997; Tsuboi, 2002; Tadokoro et al., 2003).

Activation of integrins via talin binding to the cytoplasmic tail of the β subunit is commonly known as “inside-out” signaling. However, during critical cell processes such as adhesion, migration, differentiation, proliferation, and apoptosis integrins also transmit information from the extracellular environment into the cell. As activated integrins bind the ECM substrate, they become clustered in the membrane and interact with and regulate the actin cytoskeleton (Burrige and Chrzanowska-Wodnicka, 1996). Intracellularly, integrins bind signaling molecules like focal adhesion kinase (FAK) and paxillin, via the cytoplasmic tail of the β subunit, which connect the integrin to the actin cytoskeleton transmit biochemical information into the cell (Giancotti and Ruoslahti, 1999; Zamir and Geiger, 2001). While the β subunit is primarily responsible for this “outside-in” signaling function, the transmembrane domain of the α subunit may also activate specific intracellular signaling cascades via caveolin and protein kinase C (Wary et al., 1996; Hemler, 1998). Thus, by binding both intracellular and extracellular ligands, integrins mediate critical cellular functions by transmitting mechanical force and biochemical signals across the plasma membrane in either direction.

Lastly, in addition to their bidirectional signaling capabilities across the plasma membrane, integrins can interact and signal synergistically through cis interactions with growth factor receptors and other transmembrane proteins to regulate processes such as

blood vessel development and tumor growth (Eliceiri, 2001; Miranti and Brugge, 2002). In some cases, integrins interact directly with transmembrane proteins, such as with members of the tetraspan family (Serru et al., 1999; Sterk et al., 2000), but may also use intracellular FAK as a mediator to communicate with growth factor receptors such as the vascular endothelial growth factor receptor, the epithelial growth factor receptor, and the platelet derived growth factor receptors (Soldi et al., 1999; Sieg et al., 2000).

Integrins are a large family of transmembrane proteins that mediate a vital connection between the ECM and the intracellular cytoskeletal network of the cell. Their unique structure and signaling properties enables them to mediate cellular functions critical to development of multicellular organisms and serve important roles in tissue homeostasis and survival. However, not all integrins perform as stereotypically as described above. One integrin, in particular, is still vastly misunderstood.

The Integrin $\alpha v \beta 8$

The $\beta 8$ integrin subunit was the last of the mammalian subunits to be identified (Moyle et al., 1991). The $\beta 8$ subunit was shown to dimerize with the αv subunit *in vitro* and its expression seemed to be primarily restricted to the brain, kidney, and placenta. At that time, sequence analysis demonstrated that the integrin $\beta 8$ subunit was highly divergent from other members of the family. It was primarily distinguished by two important structural differences: a significant reduction in the number of consensus extracellular cysteine residues (50 of the 56 found in other members of the family) and a lack of polypeptide sequence homology in its transmembrane and cytoplasmic domains. While the reduction in cysteine residues in the extracellular domain implicates that it has three fewer disulfide bonds in the three dimensional structure of the extracellular protein,

this difference does not immediately indicate that the structure or function of the extracellular domain is vastly different than other members of the family. In fact, both the $\beta 7$ and the $\beta 4$ subunits also have reduced numbers of cysteine residues in their extracellular domains (54 and 48 cysteines respectively). However, the fact that the polypeptide sequences of the transmembrane and cytoplasmic domains of $\beta 8$ bear little homology to the other members of the integrin family has important functional implications for this integrin subunit.

The most striking difference in the sequence of the integrin $\beta 8$ subunit is the lack of the FAK binding LLxxxHDRRE sequence in the cytoplasmic membrane proximal region of the polypeptide and the lack of the NPxY domain within the cytoplasmic tail which is known to facilitate talin binding and integrin activation. This raises questions about how or if integrins containing the $\beta 8$ subunit are activated and whether it performs the canonical functions of integrins in cell adhesion, migration, and proliferation. Interestingly, in a comparison of 25 β subunits from sponges to humans, only the vertebrate integrin $\beta 8$ subunit contained the charged amino acid, asparagine, where all other integrins have a hydrophobic amino acid in the β -terminal motif of the extracellular domain (Jannuzi et al., 2004). There is also a loop within the β -terminal motif hypothesized to be required for maintenance of the integrin in the bent, low-affinity, conformation (Xiong et al., 2003) that is uniquely absent from the integrin $\beta 8$ subunit (Jannuzi et al., 2004). The asparagine polymorphism and the lack of the loop within the β -terminal motif suggests that integrins containing the $\beta 8$ subunit are easily, or perhaps constitutively, activated. If so, the integrin $\beta 8$ subunit may have evolved without a need for intracellular activation mediated by proteins such as talin.

Like other partners of αv , the extracellular domain of the $\beta 8$ subunit contains an RGD motif within its I-like ligand binding domain (Nishimura et al., 1994) so it stood to reason that integrins containing the $\beta 8$ subunit might promote adhesion on various RGD containing ligands. However, investigators found that while integrin $\alpha v\beta 8$ can bind vitronectin, the $\beta 8$ cytoplasmic domain does not promote cell adhesion on this substrate when it is coupled to the $\beta 3$ extracellular domain (Nishimura et al., 1994). Put another way, the extracellular domain of integrin $\beta 8$ subunit was only able to promote adhesion when coupled to the cytoplasmic domain of the integrin $\beta 3$ subunit (Nishimura et al., 1994). This indicates that the $\beta 8$ cytoplasmic domain does not promote cell adhesion using common integrin signaling pathways. However, just recently, two proteins have been identified to interact with the cytoplasmic domain of $\beta 8$ using the yeast-two-hybrid approach. The first, a protein called Band 4.1B, was identified from brain extracts and the authors hypothesized that it either controls activation of integrins containing the $\beta 8$ subunit, or it may function in outside-in signaling from the integrin $\beta 8$ cytoplasmic tail (McCarty et al., 2005a). The functional consequence of this interaction is yet to be determined, but it should be noted that this protein is not required for normal development (Yi et al., 2005). The second protein, Rho GDP dissociation inhibitor-1 (Rho-GDI), was identified in kidney mesangial cells (S. Lakhe-Reddy and J.R. Schelling, submitted to Journal of Biological Chemistry). By sequestering the Rho-GDI, this interaction permits selective activation of a small G-protein Rac1 by a guanine exchange factor. Activated Rac1 then activates downstream signaling mechanisms which prevent stress fiber and focal adhesion formation and thereby inhibit mesangial cell myofibroblast

differentiation (S. Lakhe-Reddy and J.R. Schelling, submitted to Journal of Biological Chemistry).

The integrin $\alpha v\beta 8$ has functions in a variety of epithelial tissues. In the most obscure case, $\alpha v\beta 8$ was identified as a receptor for the foot-and-mouth disease virus in human colon carcinoma cells (Jackson et al., 2004). In kidney epithelial cells, $\alpha v\beta 8$ expression is up-regulated by Fas activation and may play a role in renal fibrosis (Jarad et al., 2002). In addition, $\alpha v\beta 8$ has been implicated in preventing mesangial cell differentiation in the kidney as described above (S. Lakhe-Reddy and J.R. Schelling, submitted to the Journal of Biological Chemistry). Other *in vitro* studies have shown that $\alpha v\beta 8$ functions during astrocyte migration on vitronectin (Milner et al., 1999) and oligodendrocyte differentiation in the presence of neurons (Milner et al., 1997). In human glioblastomas, the $\beta 8$ integrin subunit is the most frequently up-regulated integrin subunit, particularly in perivascular areas, and may have a potential oncogenic function (Riemenschneider et al., 2005). Interestingly, $\alpha v\beta 8$ inhibits proliferation of normal airway epithelial cells and tumor cells *in vitro* and inhibits epithelial cell proliferation and bronchial tumor growth in nude mice (Cambier et al., 2000). *In vivo*, the $\beta 8$ subunit was localized to the suprabasal cell layer of the epidermis of eyelid prior to merger of the 3 types of epithelial cells present during eyelid development indicating that $\alpha v\beta 8$ may function in the formation of the epithelia of the ocular surface (Stepp, 1999). The primary function of $\alpha v\beta 8$ during development, however, seems to be regulation of vascular development of the embryo. Indeed, only integrins containing either the αv or $\beta 8$ subunits have been shown to be required for proper capillary development within the central nervous system (CNS), placenta, and yolk sac (Bader et al., 1998; McCarty et al.,

2002; Zhu et al., 2002). In fact, in the absence of αv or $\beta 8$, endothelial cells of the central nervous system become hyperproliferative and massive cerebral hemorrhages develop during early embryogenesis which may contribute to the neonatal death of these mutant animals (McCarty et al., 2002; Zhu et al., 2002). Although $\beta 8$ has been localized to both neuronal synapses and glia (Nishimura et al., 1998), $\alpha v\beta 8$ is only required on neuroepithelial glial cells for proper regulation of endothelial cell development within the brain (McCarty et al., 2005b; Proctor et al., 2005).

These data support a model in which $\alpha v\beta 8$ adheres to a ligand(s) within the extracellular matrix or a ligand(s) expressed directly by brain capillary vessels to mediate glial cell-endothelial cell contact and/or communication. This contact could provide instructive cues for proper vascular morphogenesis during early development and physical support during later aspects of CNS development. While $\alpha v\beta 8$ has been implicated to associate with RGD containing ECM components of basement membrane such as fibronectin and vitronectin (Nishimura et al., 1994), as well as the non-RGD ligands collagen IV and laminin-1 (Venstrom and Reichardt, 1995), no direct evidence has been presented to show integrin $\alpha v\beta 8$ directly interacts with these substrates. What's more, none of the known ECM ligands for $\alpha v\beta 8$ are required for vascular development of the CNS. Vitronectin null mice develop normally and are fertile (Zheng et al., 1995). None of the laminin isoform knock-out mice develop cerebral hemorrhage (Li et al., 2003), although laminin- $\alpha 5$ deficient mice have defective placental vasculature (Miner et al., 1998). Lastly, mice deficient for the primary isoform of collagen IV, $\alpha 1(IV)_2\alpha 2(IV)$, die at midgestation, but the capillary networks of the embryo, yolk sac, and placenta appear normal (Poschl et al., 2004). While these data do not eliminate the possibility that

any of these ligands contribute to $\alpha v\beta 8$'s function during capillary growth, they do suggest that other ligands for $\alpha v\beta 8$ are responsible for its regulatory function during CNS vasculature development.

Endothelial Cell Biology and Integrin $\alpha v\beta 8$

Blood vessels serve a dual function in the embryo. They deliver necessary nutrients that developing organs need to grow and they provide trophic signals that guide organ morphogenesis. Development of these capillary networks, termed angiogenesis, requires a coordinated effort involving growth and guidance factors such as ephrins, VEGF, and neuropilins (Carmeliet and Tessier-Lavigne, 2005; Coultas et al., 2005; Eichmann et al., 2005) as well as adhesion molecules such as VE-cadherin and integrins (Hynes, 2002b; Engelhardt, 2003). Angiogenesis of the brain, like other organs, occurs via a stereotypical fashion and results in a regularly patterned vascular plexus (Bar, 1983). In mice, radial vascular endothelial cell sprouts emerge from the perineural plexus along the pial surface between E9.0 and E10.0 and elongate along radial glial fibers toward the subventricular zone using a specialized cell called the tip cell (Gerhardt et al., 2004). As the CNS grows and expands, the vascular plexus expands through proliferation and by making lateral branches to create a very regular network of vessels throughout the brain. In addition, a tightly regulated structure, known as the blood-brain barrier (BBB) is established to selectively allow nutrients, trophic factors, and water to enter the brain parenchyma, while excluding macromolecules, glutamate, and ions such as potassium that could disturb the electrochemical balance of the CNS. This barrier is established by three main cell types: endothelial cells, astrocytes, and mural smooth-muscle cells. The complex interaction of these cell types is essential for homeostatic

regulation of the brain microenvironment and is necessary for development and healthy function of the CNS (Abbott, 2002; Engelhardt, 2003).

Vascular development within the CNS is, in part, regulated by cell-matrix and cell-cell interactions through molecules such as integrins. However, a majority of integrins studied in vascular biology are expressed in endothelial cells and exert their influence over vascular development cell-autonomously (Rupp and Little, 2001; Hynes, 2002b; Stupack and Cheresch, 2004). However, an exception to that statement is the integrin $\alpha\nu\beta 8$. This integrin seems to be expressed on neuroepithelial and glial cells, when deleted from those cells has a cell non-autonomous effect on endothelial cell development within the CNS.

One potential explanation for this cell non-autonomous effect is that the integrin $\alpha\nu\beta 8$ has been shown to bind the RGD containing latency-associated peptide of TGF- $\beta 1$ (LAP- $\beta 1$) in cultured human epithelial airway cells and cultured human astrocytes (Mu et al., 2002; Cambier et al., 2005). LAP- $\beta 1$ is a component of the TGF- β large latent complex (LLC), which is a secreted molecule found within the extracellular matrix. The LLC prevents TGF- $\beta 1$ from interacting with its receptors until it is liberated or “activated” by cleavage from the LLC and LAP by specific enzymes within the ECM (Annes et al., 2003; Todorovic et al., 2005). In the airway epithelium, $\alpha\nu\beta 8$ binds LAP- $\beta 1$ which is subsequently cleaved by the matrix metalloprotease, MT1-MMP, to activate or liberate, free TGF- $\beta 1$ (Mu et al., 2002). Lastly, $\alpha\nu\beta 8$ mediated activation of TGF- $\beta 1$ leads to an inhibition of epithelial cell proliferation *in vitro*.

TGF- β and its associated receptors are also known to play important roles in the regulation of migration and proliferation of endothelial cells during angiogenesis

(Goumans et al., 2003; Lebrin et al., 2005). The evidence presented above suggests a model in the brain in which $\alpha\nu\beta 8$ binds LAP- $\beta 1$ within the basal lamina between glial cells and endothelial cells, and through interaction with a MMP, liberates soluble TGF- $\beta 1$. TGF- $\beta 1$ could then interact cell non-autonomously with neighboring endothelial cells to activate pathways that would inhibit their proliferation and/or migration. This is an interesting model since a hallmark feature of loss of *itg $\beta 8$* from neuroepithelial cells is hyperproliferative endothelial cells (Zhu et al., 2002; Proctor et al., 2005). However, a caveat of this model is that TGF- β is known to both up-regulate endothelial cell proliferation by binding one of its receptors, ALK1, and down-regulate endothelial cell proliferation by binding its other receptor, TGF β R-1 (also known as ALK5) (Goumans et al., 2002). It remains unclear which of these receptor signaling pathways is dominant during $\alpha\nu\beta 8$ mediated TGF- $\beta 1$ activation. Worth noting, though, is that in co-culture with human astrocytes, immortalized mouse endothelial cells up-regulate the anti-angiogenic genes plasminogen activator inhibitor-1 (*PAI-1*) and thrombospondin-1 (*TSP-1*) (Cambier et al., 2005). These observations provide a potential pathway, centered around TGF- $\beta 1$, for $\alpha\nu\beta 8$ mediated regulation of endothelial cell proliferation and migration.

In spite of the biochemical evidence in favor of this TGF- β hypothesis, genetically it is not an attractive model. Only half of TGF- $\beta 1$ deficient mice have defective yolk sac vasculature, the remaining half surviving birth with no sign of cerebral hemorrhage and die due to a multifocal inflammatory disorder (Shull et al., 1992; Dickson et al., 1995). The LAP of TGF- $\beta 3$ also contains a RGD domain that $\alpha\nu\beta 8$ could presumably bind so it is possible that TGF- $\beta 3$ compensates for loss of TGF- $\beta 1$, but this is

unlikely since TGF- β 3 mice show no CNS vascular abnormalities and die due to delayed lung development (Kaartinen et al., 1995; Proetzel et al., 1995). Finally, while TGF- β 3 mRNA and protein has been localized to neuroepithelial cells in areas of the CNS such as the hippocampus and cerebellum, TGF- β 1 mRNA and protein has only been localized to the surrounding meninges and choroid plexus both in embryos and adults (Flanders et al., 1991; Unsicker et al., 1991). This suggests that other molecules may interact with α v β 8 and contribute to its role in brain angiogenesis.

From a genetic point of view, total deletion of *neuropilin-1* (*nrp-1*) is strikingly similar to *itg β 8* null mice. Deletion of *nrp-1* results in defective yolk sac and cerebral vessel development and early embryonic death (Kawasaki et al., 1999). Additionally, *nrp-1* mutants display aberrant endothelial cell clusters (Gerhardt et al., 2004) similar to those observed in the *itg β 8* null and neuroepithelial specific *itg β 8* mutants (Zhu et al., 2002; Proctor et al., 2005). Neuropilin-1 is a known receptor for the VEGF₁₆₅ isoform of VEGF-A (Breier et al., 1992; Soker et al., 1998). Moreover, the VEGF₁₆₅ binding site on neuropilin-1 is necessary for proper capillary development in the embryonic mouse brain (Gu et al., 2003). Increased capillary permeability and endothelial cell hyperproliferation are known effects of augmented VEGF expression (Cheng et al., 1997; Sundberg et al., 2001; Gora-Kupilas and Josko, 2005). Through possible direct contact, or indirect communication via an accessory ECM molecule, with neuropilin-1 expressed on endothelial cells, α v β 8 expressed on glial cells may down regulate expression or secretion of specific isoforms of VEGF, such as VEGF₁₆₅, from those glial cells. Thus through coordinated communication with neuropilin-1, α v β 8 could regulate vascular morphogenesis by inhibiting pathways that promote endothelial cell proliferation. Other

molecules such as Eph receptors and semphorins have been shown to interact with integrins and their signaling pathways (Zou et al., 1999; Pasterkamp et al., 2003; Serini et al., 2003), and thus may also play a role in regulating vascular development of the brain. Ultimately, understanding the pathway in which $\alpha v\beta 8$ functions will greatly increase our understanding of how this multifunctional family of adhesion molecules participates in vascular development of the brain.

Statement of Purpose

The purpose of my thesis is to gain a better understanding of how the integrin $\beta 8$ subunit participates in and regulates vascular development of the brain and to identify a role for integrin $\beta 8$ in the adult animal. Additionally, it is my intention to identify a pathway in which integrin $\beta 8$ may perform this vital function. In the chapters that follow, I describe the experiments that I performed to accomplish these goals. It is my hope that the progress I have made during this thesis impacts the field of integrin vascular biology significantly and that the information I contribute in this thesis is of value to those that read it.

Chapter 2

Vascular Development of the Brain Requires $\beta 8$

Integrin Expression in the Neuroepithelium

This chapter is largely a reprint of a published paper (Proctor et al., 2005 Journal of Neuroscience 25(43): 9940-9948), and is reproduced with permission from the Journal of Neuroscience (Copyright 2005 by the Society for Neuroscience). Supplementary material for this article is available online at <http://www.jneurosci.org/> but is included in this chapter as additional figures with detailed legends. I have also expanded the materials and methods section by including an “Unpublished Materials and Methods” detailing procedures that were abbreviated or omitted for space reasons in the original publication.

Acknowledgements

This work was supported by NIH grant R01-NS19090 (L.F.R). John M. Proctor is the recipient of a predoctoral fellowship from the National Science Foundation. Louis F. Reichardt is an investigator of the Howard Hughes Medical Institute. We thank Klaus-Armin Nave for the *nex-cre* mice; Zhen Huang, James Linton, and Ben Cheyette for critical reading of the manuscript, and members of the Reichardt Lab for helpful discussions. The RC2 antibody, developed by Miyuki Yamamoto, was obtained from the Developmental Studies Hybridoma Bank developed under the auspices of the National Institute of Child Health and Human Development and maintained by the Department of Biological Sciences, The University of Iowa (Iowa City, IA).

Vascular Development of the Brain Requires $\beta 8$ Integrin Expression in the Neuroepithelium

Authors: John M. Proctor¹, Keling Zang¹, Denan Wang¹, Rong Wang², and Louis F. Reichardt¹

Author's Address: ¹Howard Hughes Medical Institute and Department of Physiology, and ²Department of Surgery, University of California, San Francisco, CA 94143

Address for correspondence:

Louis F. Reichardt
Howard Hughes Medical Institute
UCSF Department of Physiology
1550 4th St., Room 284A
San Francisco, CA 94143-2611
Email: lfr@cgl.ucsf.edu
Phone: 415-476-3976
Fax: 415-476-9914

Author's Note: I designed and performed all experiments in this chapter. Keling Zang provided technical assistance to me during the ES cell transfection and colony selection. Denan Wang made the conditional integrin $\beta 8$ construct, but I confirmed its design by sequencing the entire construct. Rong Wang provided the *tie-2* cre line prior to publication of that line. However, since my paper was published, she has officially published analysis of the *tie-2* cre line (Braren et al., 2006 Journal of Cell Biology 172(1): 151-162).

Abstract

We showed previously that loss of the integrin $\beta 8$ subunit, which forms $\alpha v\beta 8$ heterodimers, results in abnormal vascular development in the yolk sac, placenta, and brain. Animals lacking the *integrin $\beta 8$ (itg $\beta 8$)* gene die either at midgestation because of insufficient vascularization of the placenta and yolk sac, or shortly after birth with severe intracerebral hemorrhage. To specifically focus on the role of integrins containing the $\beta 8$ subunit in the brain, and to avoid early lethality, we utilized a targeted deletion strategy to delete *itg $\beta 8$* only from cell types within the brain. Ablating *itg $\beta 8$* from vascular endothelial cells or from migrating neurons did not result in cerebral hemorrhage. Targeted deletion of *itg $\beta 8$* from the neuroepithelium, however, resulted in bilateral hemorrhage at postnatal day zero, although the phenotype was less severe than in *itg $\beta 8$* -null animals. Newborn mice lacking *itg $\beta 8$* from the neuroepithelium had hemorrhages in the cortex, ganglionic eminence, and thalamus as well as abnormal vascular morphogenesis, and disorganized glia. Interestingly, adult mice lacking *itg $\beta 8$* from cells derived from the neuroepithelium did not show signs of hemorrhage. We propose that defective association between vascular endothelial cells and glia lacking *itg $\beta 8$* is responsible for the leaky vasculature seen during development, but that an unidentified compensatory mechanism repairs the vasculature after birth.

Introduction

Vascular development of the central nervous system (CNS) depends on cells within the brain that secrete factors, such as vascular endothelial growth factor (VEGF), which promote and guide capillary growth (Ruhrberg et al., 2002; Gerhardt et al., 2003). To fully appreciate the complexity of vascular development within the CNS, however, requires a better understanding of the molecules utilized for endothelial cell and neuroepithelial cell communication. These complex interactions between endothelial cells of the vasculature and neuroepithelial cells are also essential for formation of the blood-brain barrier (BBB) which is important for homeostatic regulation of the brain microenvironment and is necessary for development and healthy function of the CNS (Abbott and Romero, 1996; Engelhardt, 2003).

Vascular development within the CNS is regulated by cell-matrix and cell-cell interactions. Integrins are important heterodimeric extracellular matrix (ECM) receptors that mediate cell adhesion, cell migration, and tissue organization (Calderwood, 2004). Several molecules have been identified that function during vasculogenesis and development of the BBB (Engelhardt, 2003; Park et al., 2003), but only integrins containing either the αv or $\beta 8$ subunits have been shown to be required for proper capillary development within the CNS (Bader et al., 1998; McCarty et al., 2002; Zhu et al., 2002; McCarty et al., 2005). The αv integrin subunit is the only known partner for $\beta 8$, and the integrin $\alpha v\beta 8$ has been shown to bind the latency-associated peptide of TGF- $\beta 1$ and vitronectin (Moyle et al., 1991; Nishimura et al., 1994; Mu et al., 2002). Other evidence suggests $\alpha v\beta 8$ may also bind laminin and collagen IV (Venstrom and Reichardt, 1995).

Deletion of the *integrin $\beta 8$* (*itg $\beta 8$*) gene during development results in severe cerebral hemorrhage, with death of null mice occurring during embryogenesis or shortly after birth (Zhu et al., 2002). Similarly, deletion of *integrin αv* (*itg αv*) also results in severe cerebral hemorrhage and neonatal death (Bader et al., 1998; McCarty et al., 2002). In addition to the $\beta 8$ subunit, αv can associate with several other β subunits including $\beta 1$, $\beta 3$, $\beta 5$, and $\beta 6$. These subunits, however, are not likely to be essential in vascular development of the neuroepithelium, because no vascular defects were observed in *itg $\beta 3$ /*itg $\beta 5$* double knockout mice or *itg $\beta 6$* mutants (Huang et al., 1996; McCarty et al., 2002). Furthermore, no cerebral hemorrhage has been observed in mice lacking *itg $\beta 1$* in neuroepithelial cells (Graus-Porta et al., 2001). This evidence strongly suggests that αv and $\beta 8$ function together as a heterodimer in the CNS during vasculogenesis.*

To determine the cellular basis for the cerebral hemorrhage observed in *itg $\beta 8$* null neonates, we have generated a conditional *itg $\beta 8$* knockout mouse (*itg $\beta 8$* flox). Using these mice, we have selectively ablated *itg $\beta 8$* from neuroepithelial cells, endothelial cells, and migrating neurons. Whereas deletion of *itg $\beta 8$* from the neuroepithelium results in intracerebral hemorrhage, deletion from endothelial cells or from neurons does not. Tissue-specific deletion of *itg $\beta 8$* from the neuroepithelium also resulted in morphologically abnormal capillaries and disorganized astroglial cells. Therefore, the presence of integrins containing the $\beta 8$ subunit on neuroepithelial-derived glial cells is essential for proper regulation of vascular morphogenesis in the developing CNS.

Materials and Methods

Generation of “flox” itg $\beta 8$ mice. Using standard procedures the targeting construct was generated by inserting a phosphoglycerate kinase-neomycin (*PGK-neo*) cassette,

flanked by *frt* sites and containing one *loxP* site at its 3' terminus, into the *EcoRV* restriction site between exons 4 and 5 in a genomic fragment of *itgβ8* containing exons 4, 5, and 6. A second *loxP/EcoRV* site was inserted into the intron between exons 3 and 4. The targeted allele was subsequently generated via homologous recombination by introducing the linearized targeting construct into undifferentiated SVJ129 mouse embryonic stem (ES) cells using standard methods. A 5' 670 bp and a 3' 700 bp genomic DNA fragment of *itgβ8* were used as probes for Southern blot identification of ES cells containing the targeted allele. Four independently targeted ES cell clones were identified. Two clones were injected into C57BL/6J blastocysts and then placed in pseudopregnant C57BL/6J females. One gave germline transmission which was confirmed by Southern blot. Chimeric mice carrying the floxed *itgβ8* allele were crossed to C57BL/6J mice. The progeny of that cross was crossed to mice carrying the enhanced *flp* recombinase gene (*flpE*) under the control of the ubiquitous *β-actin* promoter (Rodriguez et al., 2000) to remove the *PGK-neo* cassette. These mice were then interbred to obtain *itgβ8^{flox/flox}* mice. Total RNA for Northern blots was obtained from control and mutant *β-actin-cre itgβ8* postnatal day zero (P0) brains using the Qiagen RNeasy Mini Kit (Valencia, CA). A 700 bp fragment from the 3' untranslated region of *itgβ8* was used as a probe. A 500 bp fragment of *GAPDH* (glyceraldehydes-3-phosphate dehydrogenase) gene was used as a probe as a control for RNA load.

PCR genotyping of mice. Female *itgβ8^{flox/flox}* mice were crossed to male *itgβ8^{null/+};cre/+* mice to generate *itgβ8^{flox/null};cre/+* mutant progeny as well as heterozygous and wild-type littermate progeny. All progeny were genotyped by standard PCR analysis using DNA from tail tissue. Primers specific for each allele were used to identify progeny and are as

follows: *itgβ8* wild-type (250 bp) and floxed-allele (370 bp) (5'-GAGATGCAAGAGTGTTTACC-3') and (5'-CACTTTAGTATGCTAATGATGG-3'); *itgβ8* null-allele (450 bp) (5'-AGAGGCCACTTGTGTAGCGCCAAG-3') and (5'-GGAGGCATACAGTCTAAATTGT-3'); cre (400 bp) (5'-CTGGCAATTTTCGGCTATACGTAACAGGGTG-3') and (5'-GCCTGCATTACCGGTCGATGCAAC-3').

Mouse lines. The *β-actin-flpE* mice (Rodriguez et al., 2000), the *nestin-cre* mice (Tronche et al., 1999), the *nescre8* mice (Petersen et al., 2002), the *R26R* mice (Soriano, 1999), and the *itgβ8^{null/+}* (Zhu et al., 2002) have been described previously. The *tie2-cre* mice were generously provided by R. Wang at [University of California, San Francisco (UCSF)] (R. Braren and R Wang, unpublished observations). The *nex-cre* mice have been described previously (Beggs et al., 2003; Brockschneider et al., 2004), but were kindly provided before publication by K.A. Nave (Max-Planck-Institute, Gottingen, Germany). The *β-actin-cre* were generously provided by G. Martin at UCSF and have been previously described (Lewandoski, 1997). Mice were cared for according to animal protocols approved by the UCSF Committee on Animal Research.

Morphological and histological analysis. Whole brains, dissected from P0 mice, were photographed using a CCD camera mounted on a dissecting microscope. Brains were then submerged in 4% paraformaldehyde in PBS overnight at 4°C followed by submersion in 30% sucrose at 4°C until saturated and then frozen in Tissue Tek OCT (Miles, Elkart, IN) for cutting 20 μm sections using a cryostat. Embryos used for immunohistochemistry were decapitated and the heads were then fixed in 4% paraformaldehyde in PBS 1-2 hours, cryoprotected in 30% sucrose, embedded in OCT

and cut on the cryostat (20 μm sections). For LacZ staining, whole embryos or P0 brains were fixed for two hours in 0.2% glutaraldehyde at 4°C, washed in PBS containing 0.02% NP-40 for 15 minutes, and stained with a freshly made X-gal (5-bromo-4-chloro-3-indolyl- β -D-galactopyronoside) solution according to the standard protocol. These embryos were subsequently fixed in 4% paraformaldehyde in PBS overnight, crotoprotected in 30% sucrose, embedded in OCT and cut on the cryostat (15 μm sections). All sections were counterstained with Nuclear Fast Red. Adult mice were anesthetized with 2.5% avertin in 0.9% NaCl using 15 μl per gram mouse weight and perfused with 4% paraformaldehyde in PBS. This tissue was frozen directly in 30% sucrose for cutting 40 μm sections using a sliding microtome. Nissl stain was used according to standard procedures.

Immunohistochemistry. Primary antibodies were used as follows: GFAP polyclonal (pAb) (1:250, Dako, High Wycombe, UK), platelet-endothelial cell adhesion molecule (PECAM) (CD31) monoclonal (mAb) (1:150, Pharmingen, San Diego, CA), RC2 mAb (1:4, Hybridoma Bank, Iowa City, IA), collagen IV pAb (1:1000, Cosmobio Corporation, Tokyo, Japan), Englebreth-Holm-Swarm (EHS) laminin pAb (1:3000, Sigma, St. Louis, MO) α -smooth-muscle-actin (α -SMA) mAb (1:500, Sigma), β -galactosidase (1:5000, ICN Biochemicals, Costa Mesa, CA). All sections stained with the RC2 monoclonal antibody were subjected to heat-based antigen retrieval at 94°C in 10 mM sodium citrate buffer, pH 6.0 at 94°C for 10 minutes, using the 34700 BioWave Microwave (Ted Pella, Redding, CA). OCT embedded frozen sections were placed in 5% goat serum, 5% BSA, and 0.3% Triton X-100 for 2 hours at room temperature. Sections were incubated with primary antibodies overnight at 4°C followed by fluorescent labeling with mouse or

rabbit Alexa 488 (1:250, Invitrogen, Eugene, OR) or Texas Red (1:500, Invitrogen) in blocking buffer. For the isolectin B4 staining: paraformaldehyde-fixed sections were blocked as above for primary antibodies followed by permeabilization in PBS containing 1% Triton X-100, 1 mM CaCl₂, 1 mM MgCl₂, 0.1 mM MnCl₂. These sections were then incubated with biotin-conjugated isolectin B4 (20 ng/μL, Sigma L-2140) overnight at 4°C in permeabilization solution. After 5 washes in PBS, sections were incubated with streptavidin-conjugated Alexa 594 (1:500, Molecular Probes) in blocking buffer. Some sections were counterstained with the nuclear marker TO-PRO-3 (1:4000, Molecular Probes). All sections were analyzed using a Zeiss LSM 5 Pascal confocal microscope. Radial glia morphology near the pial surface was analyzed by first collecting a z-series of images and then, using the Pascal program, collapsing the images into one projection image.

Unpublished Materials and Methods

itgβ8 conditional construct verification by sequence analysis. I used mouse genomic DNA information for *itgβ8* from Kristine Venstrom (Reichardt Lab) to design 24 primers to sequence the entirety of the *itgβ8* conditional construct. The primers are as follows:

5ARM1 (5'-GATTCATCAGGCTACAGATGG- 3'); 5ARM2 (5'-GAATCAGAGTGTTACAGAAG- 3'); 5ARM3 (5'-GAATCAGCTGATGAGCTTCC- 3'); 5ARM4 (5'-CAGTCTGAACTATTTAACC- 3'); 5ARM5 (5'-GAGATGATGCTAGATGTGTC- 3'); EXON4A (5'-CTAATGTATGGCGAGACAG- 3'); EXON4B (5'-CTGGTTGATGTGTCAGCATG- 3'); NEOA0 (5'-TAGAGGCTCTTACTATTGC- 3'); INTRON4B2 (5'-

TACATTGTAAACAGTATAGC- 3'); NEOB0 (5'-GATCTATAGATCATGAGTGG-3'); PGK2F (5'-TCGGCCATTGAACAAGATGGATTGC- 3'); PGK1R (5'-AGCAATATCACGGGTAGCC- 3'); NEOA1 (5'-ACTAGTCTCGTGCAGATGG- 3'); INTON4A1 (5'-GGAATTCAGTGTAAGTAGC- 3'); PGK2R (5'-TCCCTTCCCGCTTCAGTGACAACG- 3'); NEOB1 (5'-AGGAGCAAAGCTGCTATTGG- 3'); EXON5A (5'-CAGCCTGAAGCATGGCATC-3'); EXON5B (5'-CTACAATTTAGACTGTATGC- 3'); INTRON5B (5'-ATAGTCAGGAAGTAGAGTGG- 3'); EXON6A (5'-TGGTTGTCGATTTGACGTAAC- 3'); EXON6B (5'-ATTGCTGCTGGTGATGACAG- 3'); 3ARM1 (5'-TTCATGTGATTCGAAGGTC- 3'); 3ARM2 (5'-AGGTAGAGACAAGAAGATCAG- 3'). All exon/intron boundaries were verified for Exons 4, 5, and 6 by comparison to the genomic sequence provided by K. Venstrom. The position and sequence of the loxP sites, frt sites, and the PGK-neo selection cassette were also verified. Lastly, Vector NTI software (Invitrogen, Carlsbad, CA) was used to assemble an electronic full-length sequence of the conditional *itgβ8* knock-out construct.

Embryonic stem cell culture, transfection, and injection. The conditional *itgβ8* knock-out construct was housed in the pGEM-5 vector (Promega, Madison, WI). After purification on a CsCl gradient (see standard protocol in “Molecular Cloning” 2001 third edition Volume 1 by Sambrook and Russell), the targeting vector was linearized using the Not1 restriction enzyme [New England BioLabs (Ipswich, MA)] and purified by phenol/chloroform extraction.

Embryonic stem (ES) cells were grown on mitomycin-c (Sigma M4287, St. Louis, MO) inactivated mouse embryonic fibroblast (MEF) feeder cells in Dulbecco's Modification of Eagle's Medium (Mediatech, Herndon, VA) containing 1% Pen/strep, 1% glutamine, 1% 2-mercaptoethanol, 1% non-essential amino acids, 15% fetal bovine serum, and 0.1% leukemia inhibitory factor (all available from UCSF Cell Culture Facility). Note this medium will, from here on, be referred to as ES cell medium. Feeder cells used were SNL 76/7 cells from Allan Bradley (Sanger Centre, Cambridge, England). The targeted allele was subsequently generated via homologous recombination by introducing the linearized targeting construct into undifferentiated SVJ129 (JM1) mouse ES cells using the following procedure. The ES cells were cultured until just subconfluent, at which time they were trypsinized using 0.25% trypsin (Cell Culture Facility, UCSF) for 7 minutes at 37°C and counted. Approximately 1.4×10^7 cells were transferred to a 15 mL culture tube, pelleted at 250 X g for 5 min at room temperature, and resuspended in 0.8 ml of phosphate-buffered saline (PBS). Twenty five micrograms of linear DNA was added to the cells, mixed, and placed on ice for 5 minutes. The cells/DNA was then placed into an electroporation cuvette. The cells were electroporated room temperature using a Bio-Rad (Richmond, CA) Gene Pulser unit set at 240 mV, and 500 μ F. The Gene Pulser read a time constant of 8.7. The cuvette was then placed on ice for 10 minutes. The transfected cells were diluted in 5 mL ES cell medium and plated on six 10 cm culture dishes with feeders. The cells were cultured undisturbed for 2 days to allow attachment and recovery. The medium was then replaced with 300 μ g/mL G418 (Geneticin, GIBCO, No. 860-1811) selection medium. Cells were kept under selection for 11 days changing the medium daily. G418-resistant colonies were visible

macroscopically after 5 days of culture and colonies were transferred beginning day 7 to duplicate 96 well plates using sterile technique. Both plates were allowed to expand in ES cell medium. After two days, one plate was treated with 20 μ L trypsin per well for 5 minutes at 37°C. Then 180 μ L Freezing Medium (UCSF Cell Culture Facility) was added to each well and the cells were frozen at -80°C. The other plate of cells was allowed to grow to confluency for collection of DNA from each well via cell lysis.

ES cell DNA was digested with restriction enzymes: either EcoRV (5' digest) or Pst1 and Sac1 (3' digest) [note: all restriction enzymes were products of (NEB)]. The DNA was blotted onto nitrocellulose and probed with 5' and 3' probes which detected both the wild-type allele (4.5kb and 6.3kb respectively) and mutant targeted allele (3.3kb and 4.7kb respectively). Four independently targeted ES cell clones were identified. Two clones were injected into C57BL/6J blastocysts and then placed in pseudopregnant C57BL/6J females by technicians at the Stanford Transgenic Research Facility (Palo Alto, CA). One gave germline transmission which was confirmed by Southern blot of isolated tail DNA using the probes mentioned above.

Results

Targeting strategy for conditional inactivation of the *itg β 8* gene

In a previous study, we observed that two-thirds of *itg β 8* null mutant homozygotes die during mid-gestation due to defects in vascularization of the yolk sac and placenta. In the remaining third, *itg β 8* null mice were born with severe cerebral hemorrhages, and died shortly after birth (Zhu et al., 2002). To gain a better understanding of the cell types responsible for the cerebral hemorrhage in the *itg β 8* null mutant, we generated a conditional “floxed” allele of *itg β 8* using cre/loxP technology.

The *itgβ8* locus was targeted in ES cells using a construct containing loxP sites flanking exon 4 and a *PGK-neo* selection cassette inserted into the intron between exons 4 and 5 (Supplementary Fig. 2-1A). Exon 4 encodes the integrin I-like domain, which has been shown to contribute to ligand binding in other integrin heterodimers (Tuckwell and Humphries, 1997; Green et al., 1998; Xiong et al., 2001). Cre mediated deletion of exon 4 results in a translational frameshift that generates a premature stop codon. As a result, *itgβ8* mRNA is destabilized by the mRNA surveillance mechanism that degrades mRNA containing untranslated exons (Mendell et al., 2004). Thus, there is no detectable mRNA expressed in recombined cells as assessed by Northern blot (Supplementary Fig. 2-1C). This is consistent with our previous observation that disruption of exon 4, in *itgβ8* null animals, leads to a lack of *itgβ8* mRNA expression (Zhu et al., 2002). Therefore, we predict that there are no functional αvβ8 heterodimers expressed by mutant cells in *itgβ8* conditional mutants. Homozygous *itgβ8^{lox/lox}* mice were viable, fertile, and showed no obvious phenotype.

Loss of *itgβ8* from neuroepithelial cells results in cerebral hemorrhage

Integrin αvβ8 is expressed in neurons and glia in the mouse central nervous system (Milner et al., 1997; Nishimura et al., 1998). While *itgav* and *itgβ8* mRNA are both strongly expressed in neuroepithelial cells, neither has been detected on the endothelial cells of the vasculature (Pinkstaff et al., 1999; Zhu et al., 2002). Nevertheless, it remained possible that undetectable amounts of *itgβ8* expression in the CNS vasculature could contribute to the hemorrhagic phenotype in mice resulting from complete deletion of *itgβ8*. To determine which cell types were responsible for the hemorrhage observed in *itgβ8* null animals, *itgβ8* was separately ablated from

neuroepithelial cells, endothelial cells, and cortical neurons. Deletion of *itgβ8* was accomplished by crossing female *itgβ8^{lox/lox}* mice with male *itgβ8^{null/+}* mice expressing cre-recombinase in the specified cell type (Supplementary Fig. 2-1D) resulting in mutant animals hemizygous for the *cre* transgene and carrying one *itgβ8* floxed allele and one *itgβ8* null allele.

To address the hypothesis that *itgβ8* expression in neuroepithelial cells is necessary for proper vascular morphogenesis in the mouse brain, we first ablated *itgβ8* specifically from the neuroepithelium using a *nestin-cre* transgenic mouse line which expresses cre under the control of the neural enhancer element of the *nestin* promoter (Tronche et al., 1999). Since only the neural enhancer element, and not the entirety of the *nestin* promoter-enhancer region, is used to drive *cre* expression, not all cells that express *nestin* endogenously express *cre*. It has been reported that neural precursor cells that give rise to both neurons and glia are recombined as early as embryonic day 10.5 (E10.5) using this *nestin-cre* transgene and that endothelial cells remain unrecombined (Graus-Porta et al., 2001). In contrast to a control animal (Fig. 2-1A), examination of whole brains from postnatal day zero (P0) mice demonstrate that excision of *itgβ8* from the neuroepithelium using *nestin-cre* results in cerebral hemorrhage (Fig. 2-1D; n=6). All mutant animals observed had bilateral hemorrhages distributed across their cortices. Brain morphology in coronal sections was examined using both Nissl (Fig. 2-1) and Hematoxylin and Eosin (H&E) staining (data not shown). We found that 100% of *nestin-cre* mutant brains had visible hemorrhages throughout the dorsal cortex (Fig. 2-1E) as well as large hemorrhages present within the thalamus (Fig. 2-1F) and in the ganglionic eminence near the deep mesencephalic nucleus (data not shown). This phenotype is less

severe and less widespread across the cortex than that observed in the *itgβ8* null animals (Fig. 2-1G). The reduced severity of the hemorrhagic phenotype using this *nestin-cre* line may be due to incomplete recombination of the neuroepithelium. To address this possibility, we crossed the *nestin-cre* line with the R26R reporter strain and collected embryos at E15.0, just one half day after the onset of hemorrhage in this mutant (Fig. 2-1H). Recombination appeared complete throughout the cortex and ganglionic eminence (Fig. 2-1I), and no β-galactosidase was detected in endothelial cells (Fig. 2-1J-L') or vascular smooth-muscle cells (Supplementary Fig. 2-2).

A second explanation for the reduction in severity of hemorrhage seen in the *nestin-cre* mutants may be the perdurance of a small amount of *itgβ8* mRNA produced prior to deletion of *itgβ8* by *nestin-cre*. Since expression of this transgene begins at E10.5 (Graus-Porta et al., 2001), we used the *nescre8* transgenic mouse line, which expresses *cre* under control of the entire *nestin* promoter/enhancer beginning at E8.5 (Petersen et al., 2002). Hemorrhages in these mutants appeared by day E12.5 (Supplementary Fig. 2-3B), the same time at which *itgβ8* null animals develop intracerebral hemorrhage, but two days earlier than observed using the *nestin-cre* line. However, all *nescre8* mutants observed at P0 had hemorrhages more similar to those obtained using *nestin-cre* than those seen in the *itgβ8* null animal (Supplementary Fig. 2-3C; n=5) suggesting that factors in addition to loss of *itgβ8* in the neuroepithelium contribute to the more severe hemorrhage observed in *itgβ8* null animals.

To determine whether integrin β8 expressed in endothelial cells is also necessary for normal development of brain vasculature, we ablated *itgβ8* specifically from endothelial cells using *cre* driven by the *tie2* promoter (Fig. 2-2). This transgene drives

cre expression in most endothelial cells by E7.5 (R. Braren and R. Wang, unpublished observations). By E9.0 *tie2* driven *cre* expression is very strong in the head vasculature prior to invasion of the neuroepithelium (Fig. 2-2E-F). Mutants generated using the *tie2-cre* transgene showed no sign of hemorrhage in the cortex or thalamus nor were other brain defects observed (Fig. 2-2G-I; n=7). This data indicates that loss of $\alpha\beta8$ protein from endothelial cells does not account for the hemorrhagic phenotype observed in *itg β 8 nestin-cre* mutants or *itg β 8* null animals.

To determine whether absence of *itg β 8* from cortical neurons contributed to the hemorrhage defect seen in *itg β 8* null animals, *nex-cre* (Beggs et al., 2003; Brockschneider et al., 2004) was used to delete *itg β 8* from those cells (Fig. 2-3). The *cre* cDNA was inserted using a knock-in strategy into the *nex* locus ensuring *nex* cell-specific expression of *cre* (Brockschneider et al., 2004). This gene encodes a basic helix-loop-helix transcription factor and its promoter was used to drive *cre* expression primarily in pyramidal, postmitotic migrating neurons in the future cortical plate by E11 resulting in robust expression throughout the forebrain by E12.5 (S. Goebbels and K. Nave, unpublished observations). When *itg β 8^{flx/flx}* animals were crossed to *itg β 8^{null/+};nex-cre/+* mice, mutant progeny showed no sign of cerebral hemorrhage or other brain defects (Fig. 2-3A-C; n=3), indicating that expression of $\beta8$ in cortical neurons is not necessary for proper vascular morphogenesis in the CNS.

Together these data indicate that *itg β 8* in the neuroepithelium is essential for proper vascular formation during development. Deletion of *itg β 8* specifically from endothelial cells or from migrating cortical neurons does not result in hemorrhage. Additionally, deletion of *itg β 8* specifically from cells in the neuroepithelium using *nestin-*

cre or *nescre8* does result in cerebral hemorrhage during development that closely resembles, but is less severe than, the hemorrhage identified in the complete *itgβ8* null mice (Zhu et al., 2002).

Loss of *itgβ8* in neuroepithelial cells results in endothelial cell abnormalities in the developing cortex

To further characterize the nature of the defect observed in the *itgβ8 nestin-cre* mutants, we utilized confocal microscopy to visualize cortical vasculature in coronal sections of the cortex by immunostaining with an antibody recognizing PECAM, a membrane glycoprotein expressed on the surface of endothelial cells. During development, a uniformly-sized primary capillary plexus is formed in the neural tube through angiogenesis (Yancopoulos et al., 2000). Anti-PECAM immunostaining of endothelial cells in sections of the forebrain from control mice labels this uniform plexus at P0 (Fig. 2-4A,B). A normal plexus also developed in mice from which *itgβ8* had been deleted in endothelial cells using *tie2-cre* (Fig. 2-4K,L). However, deletion of *itgβ8* from the neuroepithelium using *nestin-cre* resulted in vessels with large irregular endothelial cell clusters (Fig. 2-4F,G). These clusters are similar to those observed in *itgβ8* null embryonic neuroepithelium (Zhu et al., 2002). We hypothesize that these abnormal clusters of endothelial cells may reflect aberrant endothelial cell migration or hyperproliferation during development of the brain and may permit leakage and subsequent hemorrhage of the vasculature.

The presence of endothelial cell clusters in *nestin-cre* mutant vessels suggested that improper basement membrane deposition or organization could result in the improper clustering of endothelial cells. However, anti-collagen IV immunostaining of

the basement membrane of vessels in the cortex was normal in the *itgβ8 nestin-cre* mutants, even in areas of bulbous endothelial cell clusters, (Fig. 2-4H,J). Anti-laminin immunostaining of the vessel basement membranes also appeared normal in the *itgβ8 nestin-cre* mutants compared to control animals (data not shown). This confirms our earlier finding in the *itgβ8* null animals that loss of *itgβ8* does not cause a general defect in basement membrane assembly, although discontinuities were observed possibly due to secondary effects of hemorrhage (Zhu et al., 2002).

Pericytes also appeared to be recruited normally to endothelial cells in *nestin-cre* mutant brains as detected by anti- α -smooth-muscle-actin immunostaining (Fig. 2-4I,J). Pericytes were recruited to both stalk cells of the vessels and to cells within the bulbous endothelial cell clusters. This finding is consistent with the normal recruitment of pericytes we previously reported in the *itgβ8* null animals (Zhu et al., 2002).

Conditional deletion of *itgβ8* from the neuroepithelium results in glial disorganization in the mouse brain

The known juxtaposition of glial cells and endothelial cells in the brain (Kacem et al., 1998; Simard et al., 2003) suggested that a primary defect in glial cells could give rise to a secondary endothelial cell phenotype in the *itgβ8 nestin-cre* mutant. Using confocal microscopy, we examined astroglia and radial glia in control and *itgβ8 nestin-cre* mutant P0 cortex. Cortical astroglial processes in wild-type P0 neonates were arrayed in a very regular pattern and were parallel to and in close association with blood vessels (Fig. 2-5A, A'). In a matched section from an *itgβ8 nestin-cre* mutant, astroglia appeared disorganized. They did not have the regular parallel organization seen in the control. Furthermore, in contrast to the wild-type, blood vessels in the mutant did not run parallel

to these glial processes (Fig. 2-5E, E'). The lack of alignment of the blood vessels and astroglial processes observed in the *itgβ8 nestin-cre* mutant may be explained by our previous observation that endothelial cells in the *itgβ8* null mice were not well attached to the surrounding brain parenchyma as observed by electron microscopy (Zhu et al., 2002).

Radial glia are precursors cells that give rise to both neurons and glial cell types (Doetsch, 2003) and have been shown to express αv integrins (Hirsch et al., 1994). To examine whether radial glia were also disorganized in the *nestin-cre* mutant, we stained E14.5 coronal forebrain sections for RC2, an early radial glia marker (Misson et al., 1988). E14.5 corresponds to the earliest time that hemorrhage was observed in the *nestin-cre* mutants. Control animals showed the expected radial pattern of glia in the ganglionic eminence of the neuroepithelium (Fig. 2-5B). However, in the *itgβ8 nestin-cre* mutants, radial glia were very disorganized in the ganglionic eminence (Fig. 2-5F). Since all *nestin-cre* mutants had visible hemorrhage in the ganglionic eminence at this time, we looked in areas of the developing cortex where hemorrhage had not yet occurred. Radial glial processes appeared normal and pial attachment did not appear altered in the *nestin-cre* mutants (Fig. 2-5G,H). This data suggests that radial glial disorganization closely coincides with but may be a secondary consequence of hemorrhage of the vasculature within the CNS of these mutants.

Adult *itgβ8 nestin-cre* mutants lack hemorrhages

Since *itgβ8* null animals die before or shortly after birth, we utilized our conditional *itgβ8* floxed allele to look at phenotypes in adult mutants. Adult *itgβ8 nestin-cre* mutants were examined six to ten weeks after birth by Nissl stain (Fig. 2-6). Similar to control animals, this mutant showed no sign of cortical or thalamic hemorrhage

compared to controls (Fig. 2-6D,E; n=6). Additionally, no cortical lamination defect was observed (Fig. 2-6F), which was not surprising since radial glial attachment to the pial surface did not appear altered in the mutants during development. This suggests that the cerebrovascular defects observed in these animals at P0 were transient and were later repaired. The repair of the vascular defects observed at P0, however, was unexpected since no *itgβ8* null animal survived more than a few days postnatally.

Discussion

We generated a floxed allele of *itgβ8* to examine the functions of integrins containing the β8 subunit in the CNS. Targeted deletion of *itgβ8* from the embryonic neuroepithelium causes abnormal vascular development resulting in cerebral hemorrhage. Ablation of *itgβ8* from embryonic endothelial cells or neurons does not result in abnormal development of brain vasculature. Expression of integrins containing the β8 subunit appears to be required on non-neuronal cells within the neuroepithelium for proper blood vessel development in the CNS. Moreover, neuroepithelial derived astroglia lacking *itgβ8* are disorganized, particularly in relation to the vasculature within the forebrain. These findings complement our earlier work on *itgβ8* null mice, and further define the cell types that must express β8 within the CNS to promote normal vascular development during embryogenesis. In addition, adult animals lacking *itgβ8* in cells generated within the neuroepithelium did not have intracerebral hemorrhages even though hemorrhages occurred earlier during development. This result indicates that *itgβ8* is not required postnatally for proper cerebral blood vessel function.

Comparison of *itgβ8* null mutants to conditional *itgβ8 nestin-cre* mutants

All *itgβ8* null animals that survive gestation die within hours after birth with severe cerebral hemorrhage throughout the forebrain. While *itgβ8 nestin-cre* mutants also show widespread cortical hemorrhage the day of birth, the hemorrhage is not as severe as in *itgβ8* null animals and they survive birth to become adults. This marked difference may be a result of several possibilities. First, the complete *itgβ8* null animals may develop under abnormal environmental conditions, such as hypoxia-induced oxidative stress, since *itgβ8* is required for proper vascular development of the placenta (Zhu et al., 2002). These environmental stress factor(s) may contribute indirectly, by inducing cell death and brain tissue damage, to increase the severity of hemorrhage in this mutant. Secondly, *nestin-cre* may have a slightly mosaic spatial expression pattern that prevents recombination of 100% of all neuroepithelial cells. The presence of a few cells that express β8 may reduce the severity of the hemorrhage observed at P0. Additionally, if *itgβ8* mRNA is produced before the onset of cre expression (and thus *itgβ8* deletion) enough β8 protein may be made to initiate aspects of proper vascular development. This latter possibility seems unlikely because the *nescre8* mutant has a very similar phenotype to that of the neural-specific *nestin-cre* mutant used in the bulk of our analyses, but expresses cre two days earlier (Petersen et al., 2002).

CNS function of integrin αvβ8

Null alleles and floxed alleles of *itgβ8* and *itgαv* have been generated to elucidate the function of these integrin subunits *in vivo*. Null alleles of both *itgαv* and *itgβ8* have two stages of lethality with a majority of each mutant dying during embryogenesis and a minority surviving until birth with severe cerebral hemorrhage (Bader et al., 1998; McCarty et al., 2002; Zhu et al., 2002). This evidence strongly suggests that these two

subunits function together as a heterodimer during CNS vascular development. Indeed, αv and $\beta 8$ may function exclusively together during vascular development since no vascular defects were observed in *itg β 3/itg β 5* double knockout mice (McCarty et al., 2002), *itg β 6* knockout mice (Huang et al., 1996), or *nestin-cre* derived *itg β 1* deficient mice (Graus-Porta et al., 2001).

Both floxed alleles of *itg β 8* and *itgav* have been crossed to *nestin-cre* and *tie2-cre* (Fig. 2-1, 2-2) and (McCarty et al., 2005; present study). Neither mutant obtained from the *tie2-cre* cross developed cerebral hemorrhage. Similarly, both mutants derived from the *nestin-cre* cross developed bilateral hemorrhage similar to, but less severe than either null mutant. Our current study further defines non-neuronal cell types within the neuroepithelium responsible for proper capillary development within the CNS (Fig. 2-3). Moreover, our observation that astroglia in the *itg β 8 nestin-cre* mutant are disorganized (Fig. 2-5) implies that $\alpha v\beta 8$ expressed on glial cell processes facilitates proper CNS blood vessel development. Cre expression driven by a glial lineage-specific promoter early during development would strengthen these findings; however, this may not be possible since radial glia differentiate to form both glial cells and neurons (Doetsch, 2003). The *itgav* floxed mice were crossed to mice expressing cre driven by the human *GFAP* promoter (*hGFAP*) in an attempt to recombine primarily CNS glia originating from *GFAP* positive radial glia. The resulting mutants, however, developed only a mild cerebral hemorrhage due, most likely to, the late onset (~E15) of cre expression (McCarty et al., 2005). Although *GFAP* positive radial glia are known to give rise to astrocytes and other glial cell types, almost all cortical projection neurons and some striatal neurons also originate from this radial glial lineage (Doetsch, 2003). At least

some of these neurons are also likely to have lost *itgav* as a result of recombination mediated by *hGFAP-cre*; thus they may contribute to any hemorrhage observed in this mutant. Our observation that *itgβ8 nestin-cre* mutants do not develop cerebral hemorrhage (Fig. 2-3) indicates that cortical neurons do not contribute to the cerebral hemorrhage observed in *itgβ8 nestin-cre* mutants or *itgβ8* null animals at P0. Taken together this evidence suggests that deletion of $\alpha\beta 8$ on glial cells within the neuroepithelium is responsible for the hemorrhage observed in the *itgβ8* and *itgav* null animals.

Since neither the *itgav* or *itgβ8* null animals survive long after birth, use of the floxed *itgβ8* allele has enabled investigation of the postnatal functions of $\beta 8$. Surprisingly, we discovered that adult *itgβ8 nestin-cre* mutants do not have cerebral hemorrhage (Fig. 2-6). While a majority of *itgav nestin-cre* mutants also survive neonatal hemorrhage to become mature adults, a few do not fully repair the hemorrhage and die within two to three weeks after birth (McCarty et al., 2005). The absence of premature death in *itgβ8 nestin-cre* mutants could reflect differences in the background strains of these two mutants. Lastly, *itgβ8 nestin-cre* mutant animals begin to display abnormal gait in hind limbs eight weeks after birth (J.M.P and L.F.R, unpublished observations). While we are currently investigating this adult phenotype in more detail, it is worth noting that adult *itgav nestin-cre* mutants also display abnormal gait with a similar time of onset (McCarty et al., 2005).

Brain vascular development and integrin $\alpha\beta 8$

The cerebral hemorrhage observed in the conditional *itgβ8 nestin-cre* mutants suggests a severe defect in vascular development and function. Analysis of mutant brains revealed aberrant capillary vessel morphology and abnormal clustering of endothelial

cells (Fig. 2-4). However, vessels maintained an intact basement membrane and normal endothelial cell associated pericytes (Fig. 2-4). The defect in glial alignment and possible lack of association with endothelial cells observed in the *itgβ8 nestin-cre* mutants (Fig. 2-5) suggests that $\alpha v\beta 8$ regulates vascular morphogenesis through its expression on neuroepithelial cells, particularly glia. These data support a model in which $\alpha v\beta 8$ adheres to ligand(s) within the extracellular matrix or ligand(s) expressed directly in brain capillary vessels to mediate glial cell-endothelial cell contact. This contact could provide instructive cues for proper vascular morphogenesis during early development and physical support during later aspects of CNS development. None of the known ligands for $\alpha v\beta 8$, however, are required for vascular development of the CNS. For example, half of TGF- $\beta 1$ deficient mice have defective yolk sac vasculature, but the remaining half survive birth with no sign of cerebral hemorrhage and die due to a multifocal inflammatory disorder (Shull et al., 1992; Dickson et al., 1995). Knock-out mice of ECM ligands such as vitronectin develop normally and are fertile (Zheng et al., 1995). None of the laminin isoform knock-out mice develop cerebral hemorrhage (Li et al., 2003), although laminin- $\alpha 5$ deficient mice have defective placental vasculature (Miner et al., 1998). Lastly, collagen IV deficient mice die at midgestation, but the capillary networks of the embryo, yolk sac, and placenta appear normal (Poschl et al., 2004). Taken together, these data suggest that the $\alpha v\beta 8$ ligand responsible for its regulatory function in CNS vasculature development has not been identified.

Strikingly similar to *itgβ8* null mice, total deletion of *neuropilin-1* (*nrp-1*) results in defective yolk sac and cerebral vessel development and early embryonic death (Kawasaki et al., 1999). Neuropilin-1 is a known receptor for the VEGF₁₆₅ isoform of

VEGF-A (Breier et al., 1992; Soker et al., 1998). One putative mechanism by which $\alpha\text{v}\beta\text{8}$ expressed on glial cells could regulate vascular development is by indirectly regulating release of secreted factors, such as VEGF, through cross talk with endothelial cell receptors such as neuropilin-1. The VEGF₁₆₅ binding site on neuropilin-1 has been shown to be necessary for proper capillary development in the embryonic mouse brain (Gu et al., 2003). Additionally, *nrp-1* mutants display aberrant endothelial cell clusters (Gerhardt et al., 2004) similar to those observed in the *itg β 8* null and *nestin-cre* mutants. Increased capillary permeability and endothelial cell hyperproliferation are known effects of augmented VEGF expression (Cheng et al., 1997; Sundberg et al., 2001; Gora-Kupilas and Josko, 2005). Bromodeoxyuridine labeling of endothelial cells in the *itg β 8* null animals demonstrates that these cells are in fact hyperproliferative in this mutant (Zhu et al., 2002). Through possible communication with neuropilin-1, $\alpha\text{v}\beta\text{8}$ may regulate expression or secretion of specific isoforms of VEGF, such as VEGF₁₆₅, and thereby regulate vascular morphogenesis. Other molecules such as Eph receptors and semphorins have been shown to interact with integrins and their signaling pathways (Zou et al., 1999; Pasterkamp et al., 2003; Serini et al., 2003), and thus may also play a role in regulating vascular development of the brain. We are currently pursuing the mechanism by which $\alpha\text{v}\beta\text{8}$ functions in the developing mouse brain.

Our current study defines neuroepithelial cells and glia as the primary cell types in which *itg β 8* expression is essential for proper development of capillary growth in the embryonic brain. It is essential now to identify the ligand(s) for $\alpha\text{v}\beta\text{8}$ in the CNS and to develop reagents that will facilitate our understanding of the mechanism by which $\alpha\text{v}\beta\text{8}$ promotes proper vascular development. Use of the *itg β 8* floxed allele in elucidating the

WEST LIBRARY

signaling pathways through which integrin $\alpha v\beta 8$ functions should help define the regulatory mechanisms necessary to establish an organized capillary network in the developing brain.

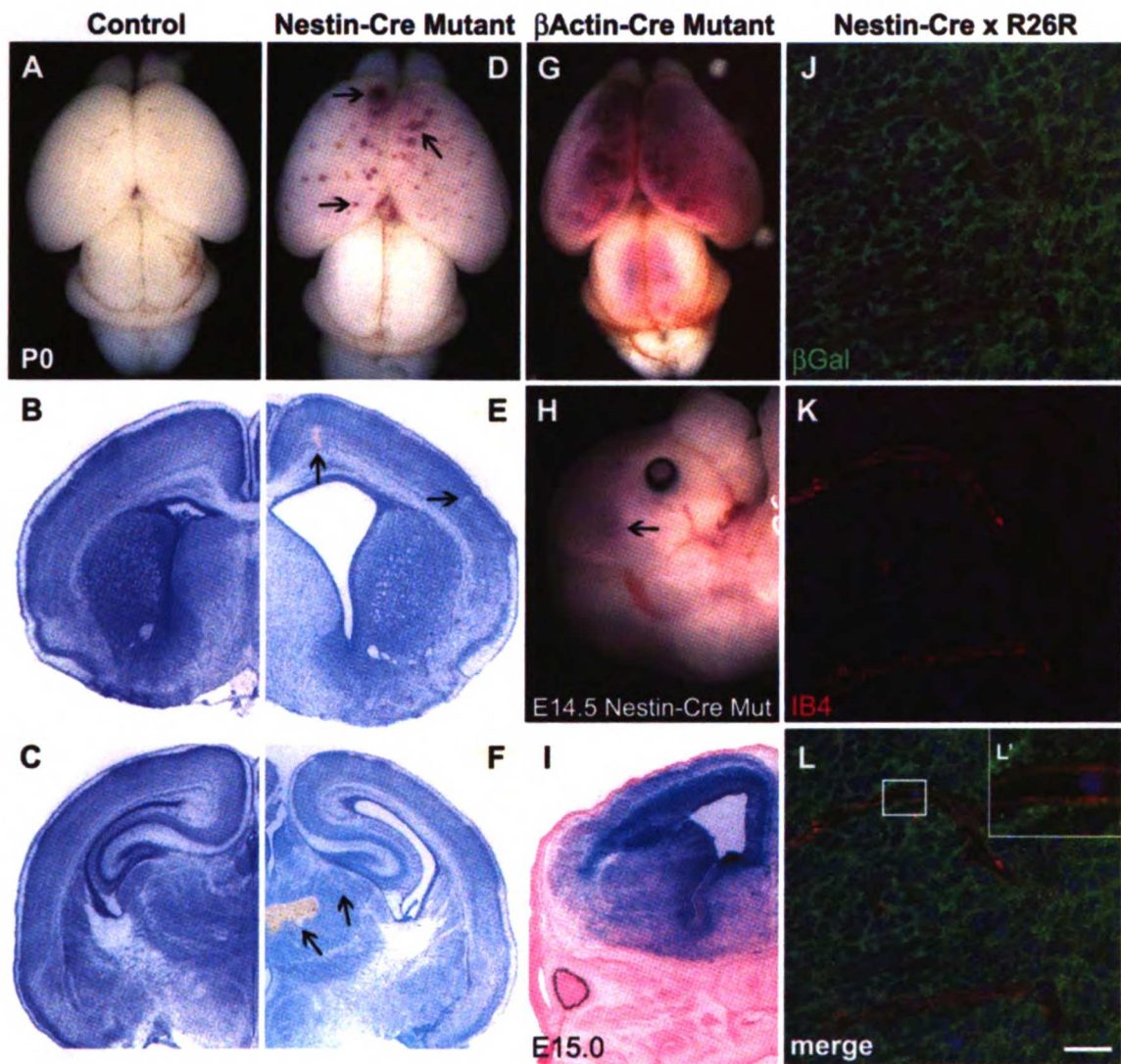


Figure 2-1. Phenotypic defects observed after conditional deletion of *itgb8* from the neuroepithelium using *nestin-cre*.

Figure 2-1. Phenotypic defects observed after conditional deletion of *itgβ8* from the neuroepithelium using *nestin-cre*. *A*, wild-type brain from P0 neonate. *B,C* Nissl stained sections of a control brain. *D*, P0 brain lacking *itgβ8* due to conditional deletion mediated by neuroepithelial-specific *nestin-cre*. Note blood produced from hemorrhages throughout the dorsal and rostral cortices (arrowheads). *E,F* Nissl stained sections of a *nestin-cre* mutant brain. Notice the hemorrhages (arrowheads) throughout the cortex (*E*) in addition to the massive hemorrhage in the thalamus (*F*). *G*, P0 mutant animal generated using the *β-actin-cre* line. Mutants generated with this *cre* line display phenotypes not obviously different from the null animal. An avascularized yolk-sac and placenta is seen in the majority of embryos that die by E11.5 and severe hemorrhage in the brain of embryos that survive to birth. *H*, E14.5 brain lacking *itgβ8* from the neuroepithelium due to conditional deletion mediated by neuroepithelial-specific *nestin-cre*. Note blood produced from hemorrhages throughout the dorsal and rostral cortices (arrowhead). *I*, LacZ stained section from an E15.0 *nestin-cre* positive animal crossed to the R26R reporter strain. Note that the neuroepithelium is almost entirely recombined. *J-L'*, β-Galactosidase (βGal) expression analysis of E15.0 embryo cortices (one half day after hemorrhage was observed in *nestin-cre* mutants) obtained from a cross of a *nestin-cre* positive animal and the R26R reporter line. Note the strong expression of βGal (green) in cells of the neuroepithelium but the lack of βGal immunolabeling of the endothelial cells labeled with isolectin B4 (red) (*L'*). Cell nuclei were counterstained with TO-PRO-3 (blue). βGal, β-Galactosidase; Mut, mutant; IB4 isolectin B4. Scale bar: *L*, 20 μm.

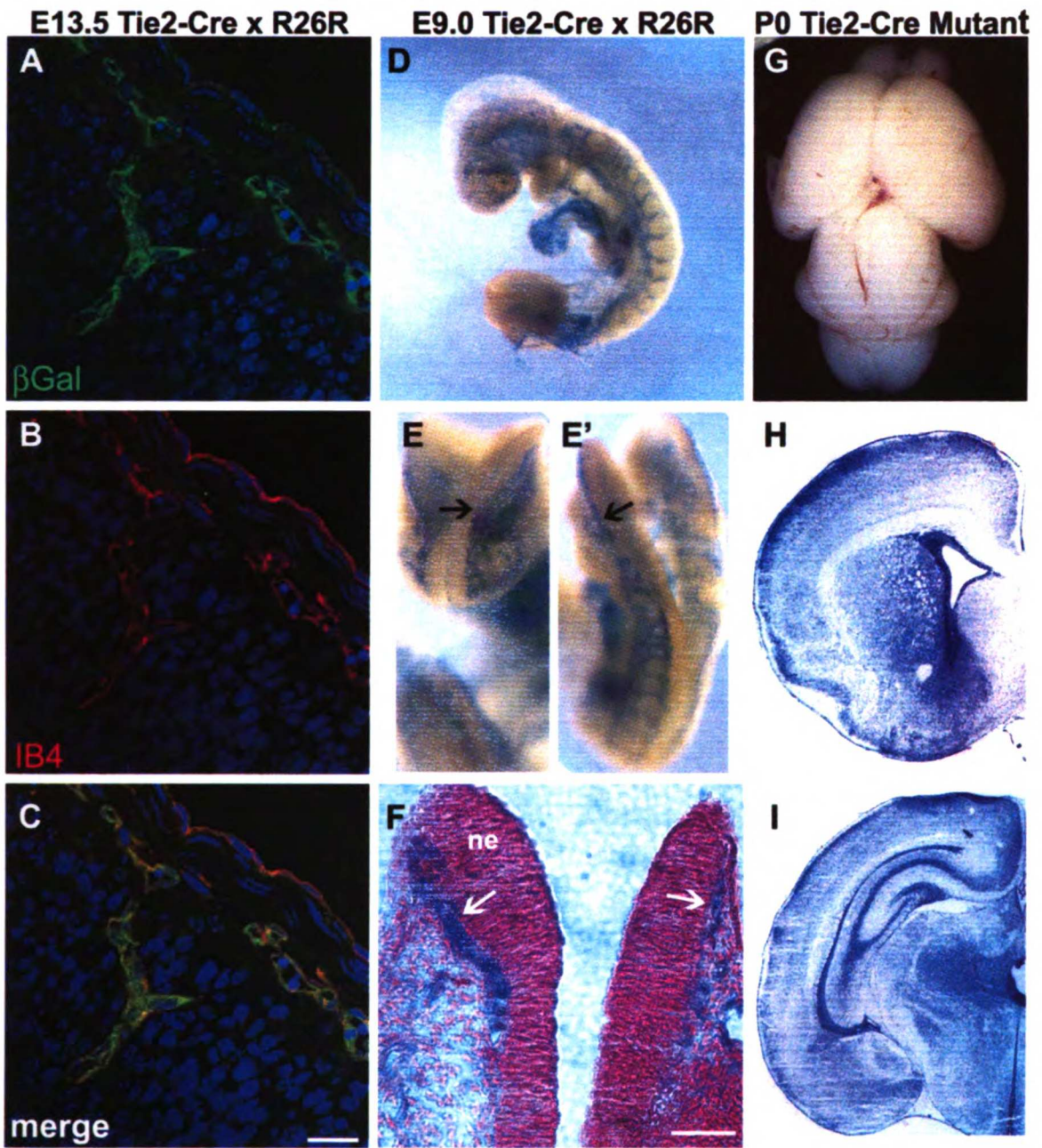


Figure 2-2. Conditional deletion of *itg β 8* from vascular endothelial cells using *tie2-cre* does not result in cerebral hemorrhage.

Figure 2-2. Conditional deletion of *itgβ8* from vascular endothelial cells using *tie2-cre* does not result in cerebral hemorrhage. *A-C*, β-galactosidase expression analysis of E13.5 embryo cortices obtained from a cross between a *tie2-cre* positive animal and the R26R reporter line. Note that β-Galactosidase (green) expression is very strong and perfectly overlaps with the isolectin B4 (red) (B,C) immunolabeling of endothelial cells. Cell nuclei were counterstained with TO-PRO-3 (blue). *D-F*, LacZ reporter analysis of E9.0 embryos obtained from a cross between a *tie2-cre* positive animal and the R26R reporter line. Notice that cre mediated recombination is very strong in the head vasculature prior to invasion of the neuroepithelium (arrows E, E'). *F*, Coronal slice of embryo from (E) counterstained with Nuclear Fast Red. Notice that LacZ positive vessels (blue) have not yet invaded the neuroepithelium (ne) at 9.0 days post conception. *G*, P0 brain lacking *itgβ8* in vascular endothelial cells due to conditional deletion mediated by *tie2-cre*. *H,I*, Nissl stained sections of a *tie2-cre* mutant P0 brain. Note absence of hemorrhage. βGal, β-Galactosidase; IB4, isolectin B4. Scale bar: *C*, 20 μm; *F*, 40 μm.

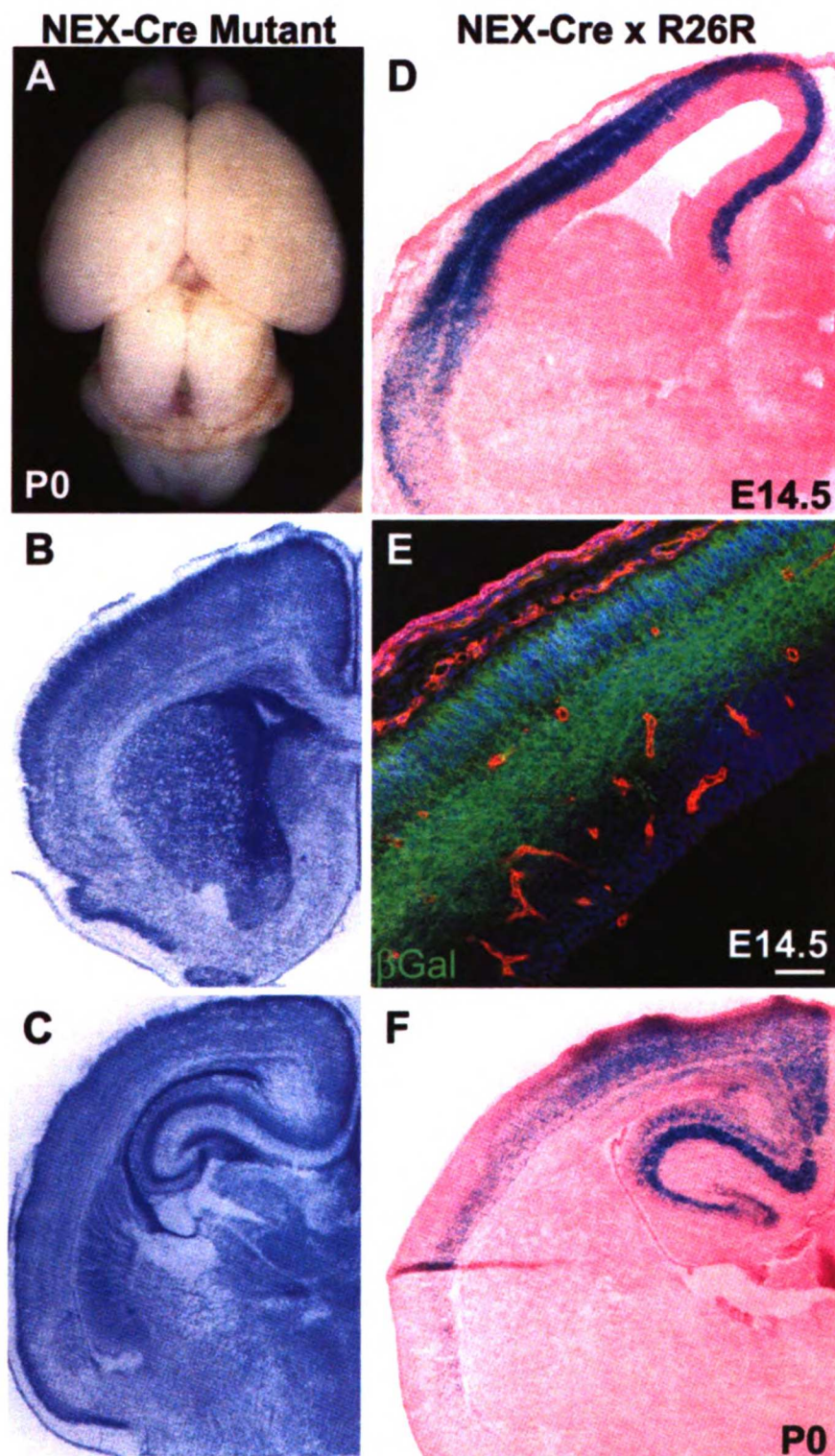


Figure 2-3. Conditional deletion of *itgβ8* from post-mitotic neurons using *nex-cre* does not result in cerebral hemorrhage.

Figure 2-3. Conditional deletion of *itgβ8* from post-mitotic neurons using *nex-cre* does not result in cerebral hemorrhage. *A*, P0 brain lacking *itgβ8* in post-mitotic neurons due to conditional deletion mediated by *nex-cre*. *B,C*, Nissl stained sections of a *nex-cre* mutant P0 brain. *D,F*, LacZ stained sections from an E14.5 embryo cortex and P0 cortex obtained from a cross between a *nex-cre* positive animal and the R26R reporter line. *cre* mediated recombination is very strong in the future cortical plate by E14.5 when hemorrhage is observed in the *nestin-cre* mutant and remains strong after birth. *E*, β-Galactosidase (βGal) expression analysis of E14.5 embryo cortex. Note that βGal (green) immunolabeling is limited to cells within the future cortical plate. Endothelial cells were immunolabeled with isolectin B4 (red) and were not recombined by this *cre* line. Cell nuclei were counterstained with TO-PRO-3 (blue). Scale bar: *E*, 50 μm.

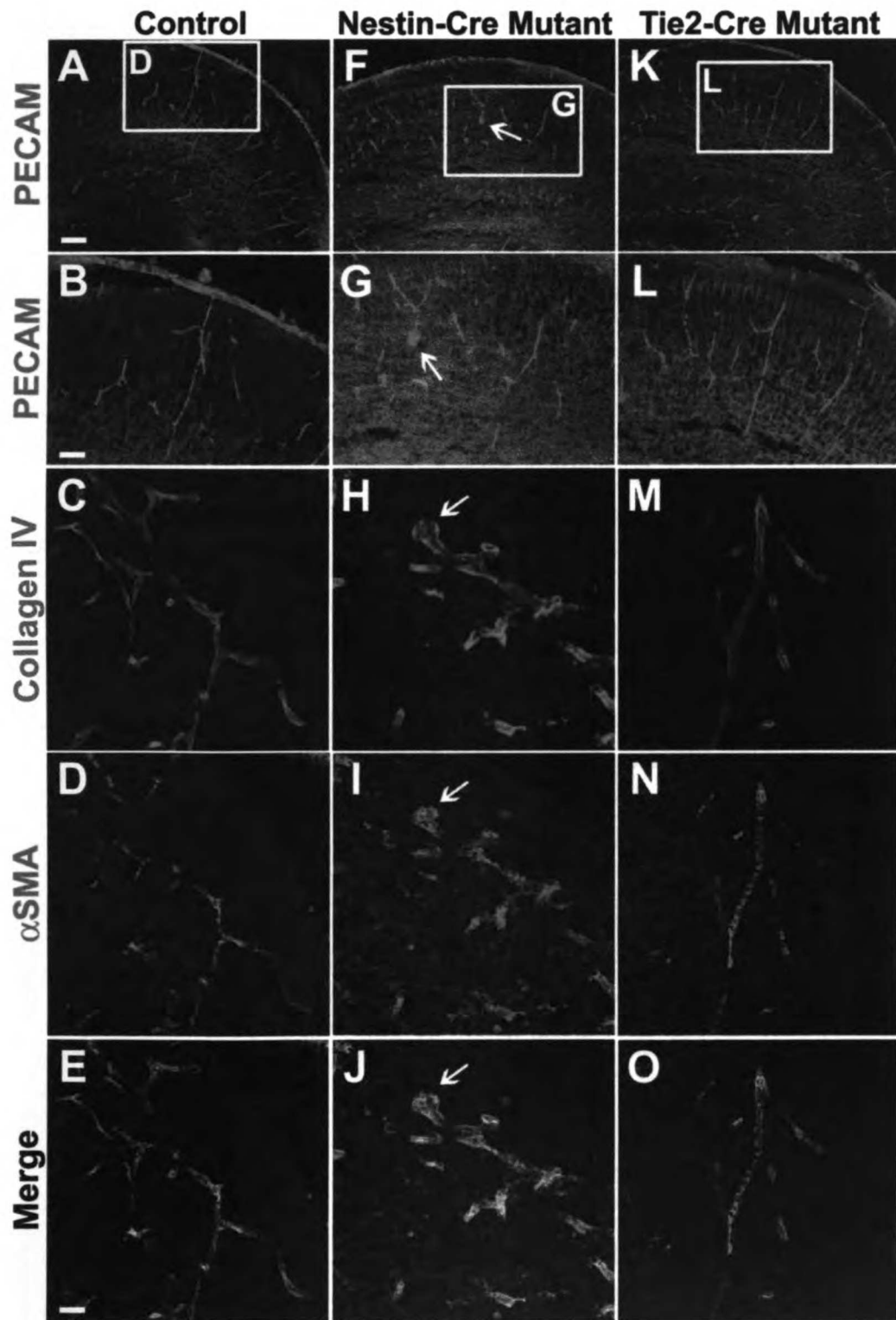


Figure 2-4. Conditional deletion of *itg β 8* in the neuroepithelium leads to endothelial cell irregularities in the P0 neonatal cortex.

Figure 2-4. Conditional deletion of *itgβ8* in the neuroepithelium leads to endothelial cell irregularities in the P0 neonatal cortex. Anti-PECAM immunolabeling of P0 coronal sections of the forebrain to visualize vascular endothelial cells. *A,B*, control; *F,G*, *nestin-cre* targeted mutant; *K,L*, *tie2-cre* targeted mutant. Notice the bulbous organization of endothelial cell clusters in the cortex (arrows) of the *nestin-cre* targeted mutant in (F) and (G). Anti-collagen IV immunolabeling of P0 coronal sections of the neuroepithelium to visualize the basal lamina surrounding the vasculature. *C,E*, control; *H,J*, *nestin-cre* targeted mutant; *M,O*, *tie2-cre* targeted mutant. Notice the intact basement membrane in the area of an endothelial cell cluster (arrowhead) in the *nestin-cre* targeted mutant in (H) and (J). Anti- α -smooth-muscle-actin (α SMA) immunolabeling of pericytes in P0 coronal sections of the neuroepithelium. *D,E*, control; *I,J*, *nestin-cre* mutant; *N,O*, *tie2-cre* mutant. Note normal recruitment of pericytes to the vasculature in both mutants. Scale bar: *A*, 80 μ m; *B,E*, 40 μ m.

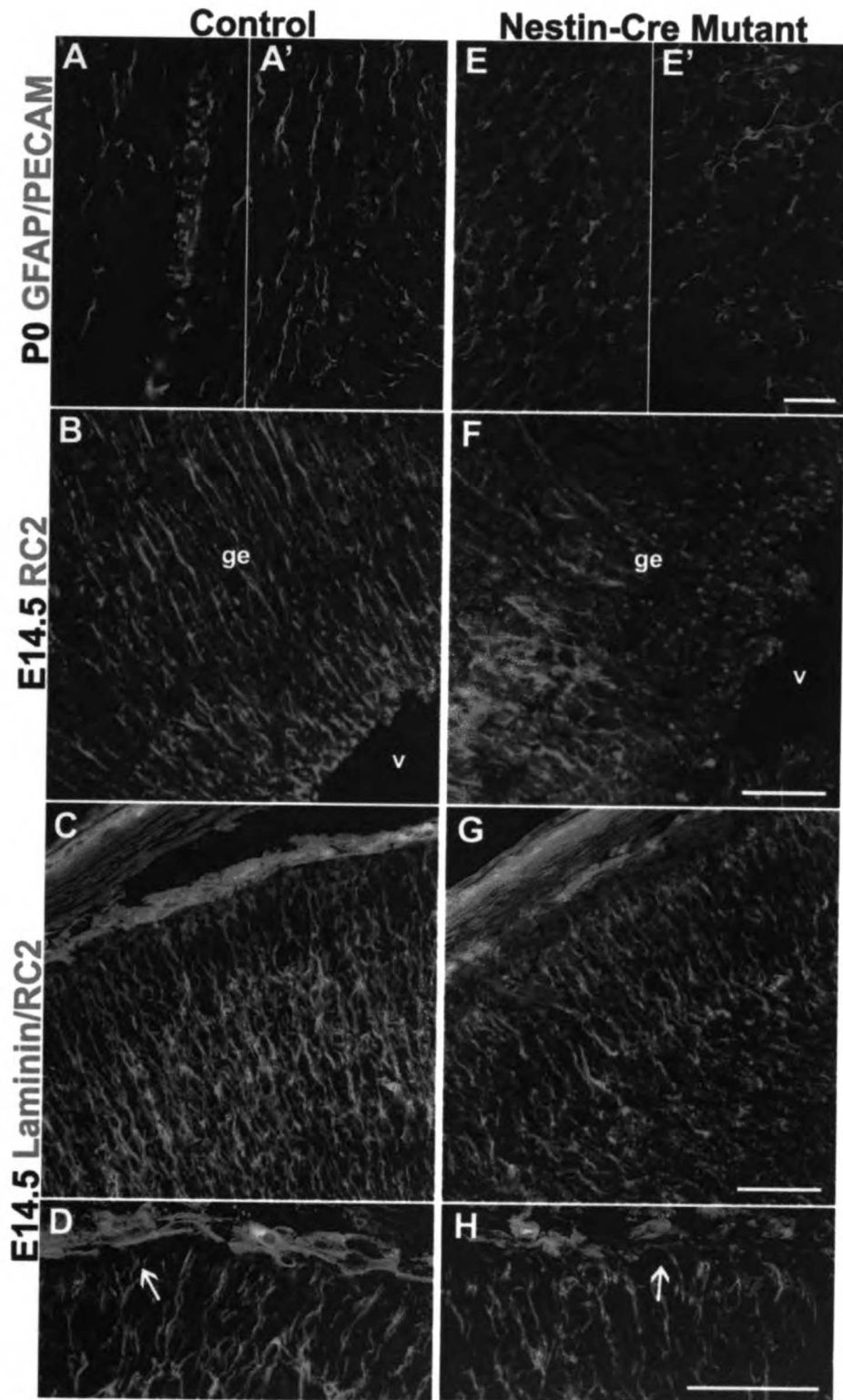


Figure 2-5. *itgβ8* *nestin-cre* mutants have abnormally organized cortical glia.

Figure 2-5. *itgβ8 nestin-cre* mutants have abnormally organized cortical glia. Anti-PECAM/GFAP immunostaining of endothelial cells and glia, respectively, in P0 coronal sections of the dorsal forebrain. *A,A'*, control; *E,E'*, *nestin-cre* mutant. Notice the disorganization of the astroglia, and the lack of alignment between endothelial cells and the astroglial processes in (*E*) and (*E'*). Anti-RC2 immunostaining of radial glia in E14.5 coronal sections of the ganglionic eminence is shown. *B*, control; *F*, *nestin-cre* targeted mutant. Radial glia in (*F*) are badly disorganized most likely due to hemorrhage within the ganglionic eminence (*ge*) near the lateral ventricles (*v*). Anti-RC2 and anti-laminin immunolabeling of E14.5 coronal sections demonstrating radial glia cell morphology in cortices of control *C,D*, and *nestin-cre* mutant *G,H*. Attachment of the radial glia to the pial surface in the *nestin-cre* mutant does not appear altered (arrow in *H*) and glial processes display normal organization. Scale bar: *E'*, 20 μm; *F,G,H*, 50 μm.

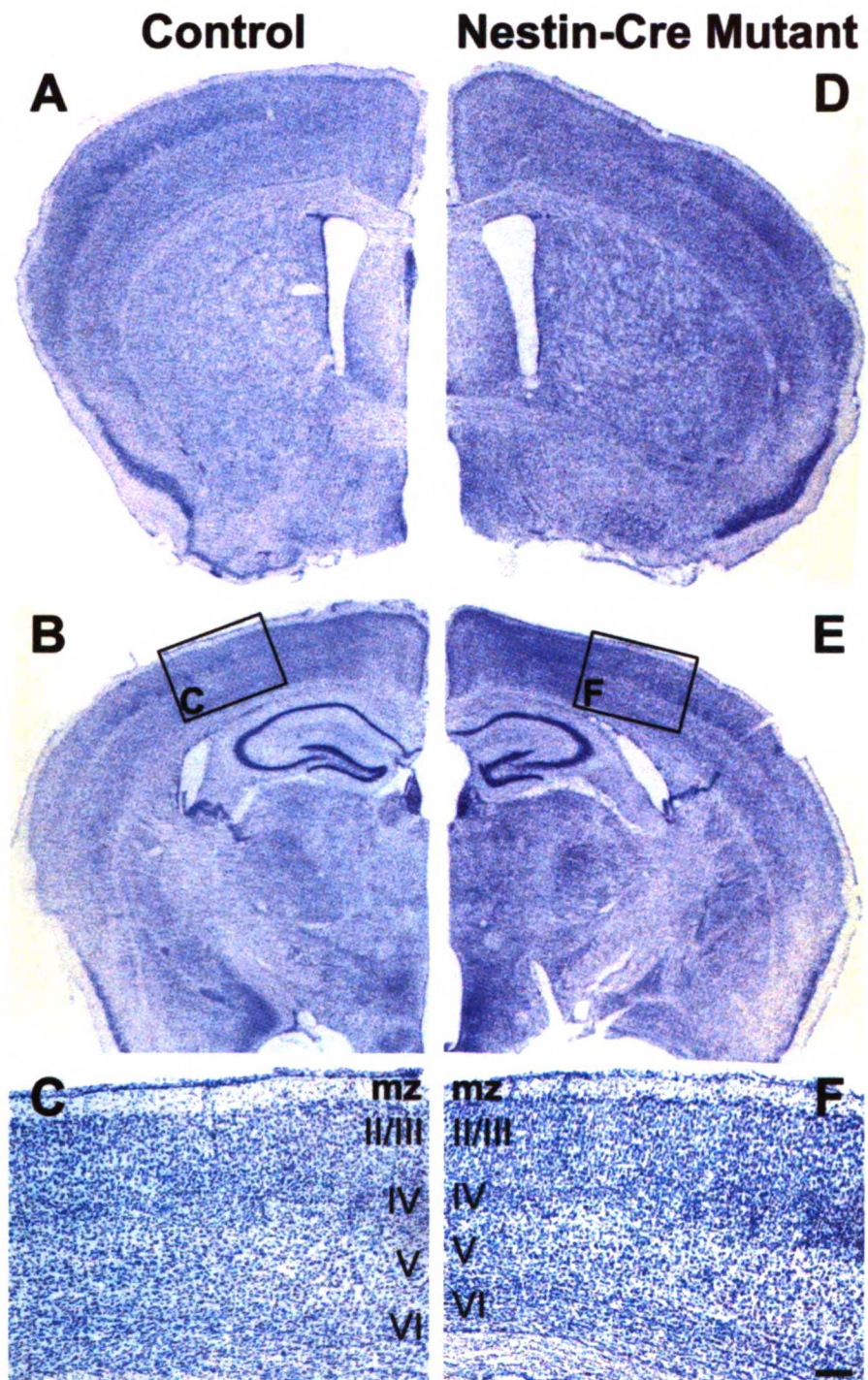
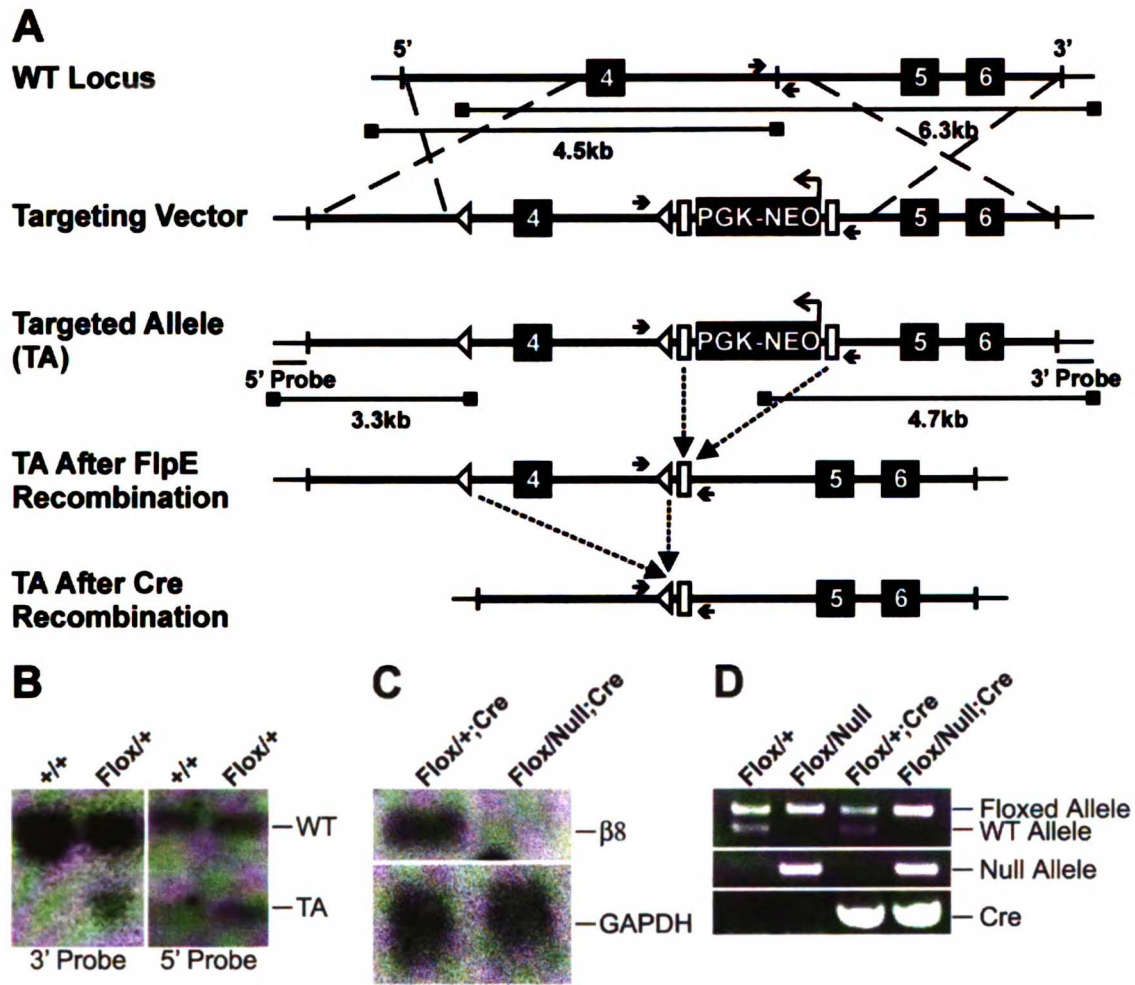


Figure 2-6. Adult *itgβ8 nestin-cre* mutants show no sign of brain hemorrhage.

Figure 2-6. Adult *itgβ8·nestin-cre* mutants show no sign of brain hemorrhage. *A*, six-week old control *D*, six-week old *nestin-cre* targeted mutant coronal sections at the level of the lateral ventricles in the forebrain stained with Nissl. *B*, control; *E*, *nestin-cre* mutant coronal sections at the level of the hippocampus stained with Nissl. Note lack of hemorrhage or other obvious defect in the cortex or thalamus. *C,F*, High magnification of cortical sections boxed in *B,E*. All cortical layers are present and in the correct order in the mutant. mz, Marginal zone Scale bar: *F*, 100 μm.

bioRxiv preprint doi: <https://doi.org/10.1101/101111>; this version posted January 10, 2017. The copyright holder for this preprint (which was not certified by peer review) is the author/funder, who has granted bioRxiv a license to display the preprint in perpetuity. It is made available under aCC-BY-NC-ND 4.0 International license.



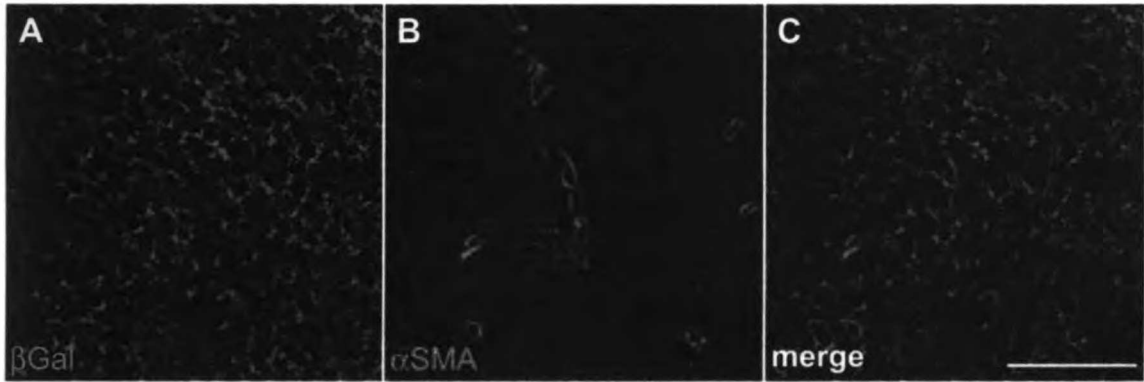
Supplementary Figure 2-1. Generation of conditional *itgβ8* mice.

www.nature.com

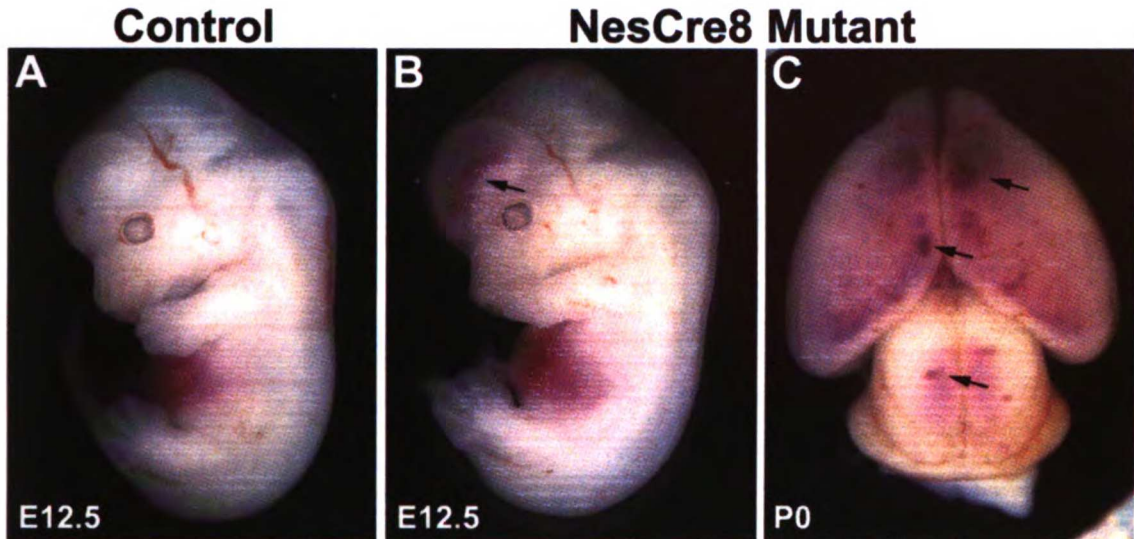
Supplementary Figure 2-1. Generation of conditional *itgβ8* mice. *A*, Schematic drawing of gene targeting strategy used to generate *itgβ8* flox mice. Black boxes with white numbers represent exons 4-6. Exon 4, which contains the integrin-I-like domain that functions in ligand binding, is flanked by *loxP* sites (open triangles). The large horizontal rectangle represents the *PGK-neo* selection cassette which is flanked by *frt* sites (small vertical open rectangles). After the targeting construct was incorporated into the mouse germline, the selection cassette was removed by crossing to mice expressing germline *flpE*-recombinase under the control of the ubiquitous *β-actin* promoter to yield *itgβ8^{flox/+}* mice. Both 5' and 3' probes used for Southern blot analysis, in addition to the relative length bands (square ended lines) they detect, are indicated. Deletion of exon 4 was accomplished using *cre*-recombinase under the control of various region specific promoters. Deletion of exon 4 induces a frameshift mutation that results in premature translational termination and mRNA degradation. Small arrows indicate primers used for PCR genotyping of tail DNA from wild-type and mutant animals. *B*, Southern blot identification of an ES cell clone containing the targeted allele (TA). ES cell DNA was probed with 5' and 3' probes which detected both the wild-type allele (4.5kb and 6.3kb respectively) and mutant targeted allele (3.3kb and 4.7kb respectively). Note: the wells of ES cells used to make DNA for the 3' probe southern contained a large number of feeder cells which contributed to the density of the wild-type band. *C*, Northern blot analysis of RNA acquired from the forebrain of a P0 *itgβ8^{flox/mull}*; *β-actin-cre* mutant and *itgβ8^{flox/+}*; *β-actin-cre* heterozygote littermate control. A probe designed within the 3' UTR was used to detect *itgβ8* transcript while a GAPDH probe was used as a loading control. Note that no *itgβ8* transcript was detected. (Legend continued on next page).

D, PCR of mouse tail DNA obtained from the progeny of a cross between *itgβ8^{flox/flox}* and *itgβ8^{null/+};cre*. Primers used to identify the wild-type and floxed alleles are indicated in the targeted locus diagram in (A). Separate primer sets were used to detect the *itgβ8 null* allele and *cre*.

WASH STATE LIBRARY



Supplementary Figure 2-2. *β-Galactosidase* expression analysis of smooth-muscle cells in E15.0 embryo cortices obtained from a cross of a *nestin-cre* positive animal and the *R26R* reporter line. *A*, β -Gal (green); *B*, α -smooth-muscle actin (red); *C*, merged image. Note the strong expression of β -Gal in cells of the neuroepithelium but the lack of β -Gal immunolabeling of the smooth-muscle cells. Scale bar: *C*, 50 μ m.



Supplementary Figure 2-3. Conditional deletion of *itgβ8* from the neuroepithelium using *nescre8* results in cerebral hemorrhage. *A*, E12.5 control; *B*, E12.5 *nescre8* mutant; *C*, P0 *nescre8* mutant. The early onset (E8.5) of the *nescre8* line compared to the later onset of the *nestin-cre* (E10.5) results in hemorrhage occurring two days earlier in *itgβ8 nescre8* mutants (E12.5, arrow in *B*) than in *nestin-cre* mutants. However, the hemorrhage (arrows in *C*) at P0 is less severe than seen in the *itgβ8* null animal and similar to the hemorrhage seen in the *nestin-cre* mutant.

Chapter 3

Functional Analysis of the Integrin $\beta 8$ Pathway Using a Microarray Approach

UNIVERSITY OF
MICHIGAN

Acknowledgements

The microarray work presented in this chapter was produced in a collaborative effort with the Functional Core Genomics Laboratories (FCGL) at UCSF. I designed all experiments, collected and genotyped all embryos, and harvested, produced, and analyzed all RNA used in these experiments. Rebecca Barbeau, a research technician in the FCGL, performed the hybridization and her and me together gridded the arrays in the GenePix program for data acquisition. Agnes Paquet, a resident statistician for the FCGL, assisted me with statistical analysis of the array data. The FCGL is directed by Dr. David Erle and co-directed by Dr. Andrea Barzak. I want to thank them all for their time, assistance, and discussions throughout this project.

Abstract

The primary function of the integrin $\beta 8$ subunit in the central nervous system (CNS) is regulation of vascular morphogenesis during embryogenesis. How it mediates this function is unknown. Although some molecules have been identified *in vitro*, to interact with the $\alpha v\beta 8$ integrin, there is little *in vivo* evidence to support their role in a signaling pathway involving $\alpha v\beta 8$ integrin and vascular development of the brain. Here, we utilized a microarray strategy to investigate, on a genome-wide scale, genes which may function together with $\alpha v\beta 8$ integrin during vascular development of the brain. Specifically, we compared E12.5 forebrains from control and *itg $\beta 8$* mutants generated by crossing the conditional (floxed) *itg $\beta 8$* mice to *nescr $\epsilon 8$* transgenic mice. We previously determined that these mutants have a similar time of onset of cerebral hemorrhage compared to *itg $\beta 8$* -null animals and were thus ideal for this study. However, using this strategy, we did not identify any genes that were differentially expressed in mutant and control forebrains. We discuss the limitations of this strategy as well as some potential signaling molecules through which the $\alpha v\beta 8$ integrin may regulate vascular development within the CNS.

Introduction

The integrin family of extracellular matrix molecules functions by transmitting biochemical signals across the plasma membrane of the cell. This transfer of information can occur in either direction. The molecules that interact with many integrins have been well characterized and some stereotypical pathways through which integrins function have been assembled (Giancotti and Ruoslahti, 1999; Zamir and Geiger, 2001). In particular, molecules such as focal adhesion kinase (FAK), paxillin, and α -actinin provide a link from the cytoplasmic tail of the integrin β subunit to the actin cytoskeleton and other signaling pathway which permits integrins to regulate cell adhesion, motility, and gene expression.

Most integrins bind an extracellular ligand within the extracellular matrix. It is not clear, however, that all integrins bind the same intracellular signaling molecules during their many and various functions. The integrin $\alpha\beta 8$ is the prime example of this fact. Most integrin β subunits contain two consensus sequences within their cytoplasmic tails: the FAK binding LLxxxHDRRE sequence and the NPxY domain known to function in talin binding and integrin activation (Liu et al., 2000). These polypeptide sequences are absent in the cytoplasmic tail of the integrin $\beta 8$ subunit. Recently, the cytoplasmic tail of the integrin $\beta 8$ subunit was shown to bind a protein called Band 4.1B in a yeast-two hybrid screen (McCarty et al., 2005a). Since it seems unlikely that the cytoplasmic tail of the integrin $\beta 8$ subunit can bind and be activated by talin, it is possible that Band 4.1B performs this function for the $\alpha\beta 8$ integrin. The other possibility is that Band 4.1B associates with the cytoplasmic tail of the integrin $\beta 8$ subunit upon binding of its extracellular ligand functioning as the primary signaling molecule in an $\alpha\beta 8$ integrin

intracellular signaling pathway. However, the functional consequence of this interaction remains to be determined. Moreover, it has been established that this protein is not necessary for normal development (Yi et al., 2005).

Perhaps the intracellular signaling molecules with which the integrin $\alpha\beta8$ interacts would be better understood if the extracellular ligands the integrin binds *in vivo* were clearly identified. *In vitro*, $\alpha\beta8$ binds vitronectin, laminin, collagen IV, fibronectin, and the latency associated peptide of TGF- β 1 (LAP- β 1) (Nishimura et al., 1994; Venstrom and Reichardt, 1995; Mu et al., 2002). However, none of these molecules appear to function in vascular development of the brain (see chapter 1) which is the primary function of the $\alpha\beta8$ integrin (McCarty et al., 2005b; Proctor et al., 2005).

Loss of *itg β 8* from neuroepithelial cells using the *nescre8* line causes the onset of cerebral hemorrhage at E12.5 [see Chapter 2 and (Proctor et al., 2005)]. This is the same time at which hemorrhage first occurs in *itg β 8* null mutants (Zhu et al., 2002) making this the ideal time point to analyze gene expression in these mutants. To gain a better understanding of the pathways in which the integrin $\alpha\beta8$ functions, we chose the high throughput, genome-wide, strategy of DNA microarray analysis (Allison et al., 2006). Using this strategy, we compared E12.5 *nescre8 itg β 8* mutant forebrains with E12.5 control forebrains to find genes that are differentially expressed and those that implicate potential pathways in which integrins containing the $\beta8$ subunit may function.

Materials and Methods

PCR genotyping of mice. Female *itg β 8^{lox/lox}* mice were crossed to male *itg β 8^{null/+};cre/+* mice to generate *itg β 8^{lox/null};cre/+* mutant progeny as well as heterozygous and wild-type littermate progeny. All progeny were genotyped by standard PCR analysis using DNA

from tail tissue. Primers specific for each allele were used to identify progeny and are as follows: *itgβ8* wild-type (250bp) and floxed-allele (370bp) (5'-GAGATGCAAGAGTGTTTACC-3') and (5'-CACTTTAGTATGCTAATGATGG-3'); *itgβ8* null-allele (450bp) (5'-AGAGGCCACTTGTGTAGCGCCAAG-3') and (5'-GGAGGCATACAGTCTAAATTGT-3'); *cre* (400bp) (5'-CTGGCAATTTCCGGCTATACGTAACAGGGTG-3') and (5'-GCCTGCATTACCGGTCGATGCAAC-3').

Mouse lines. The *itgβ8^{flx/flx}* mice were produced according to procedures covered in detail in chapter 1 [see also (Proctor et al., 2005)]; the *itgβ8^{null/+}* mice (Zhu et al., 2002); the *nescre8* mice (Petersen et al., 2002) and the *R26R* mice (Soriano, 1999) have been described previously. The *β-actin-cre* were generously provided by G. Martin at UCSF and have been previously described (Lewandoski, 1997). Embryo staging and analysis were performed by timed matings with noon on the plug date defined as E0.5. Mice were cared for according to animal protocols approved by the UCSF Committee on Animal Research.

Morphological and histological analysis. Whole animals, or brains, were submerged in 4% paraformaldehyde in PBS overnight at 4°C followed by submersion in 30% sucrose at 4°C until saturated and then frozen in Tissue Tek OCT (Miles, Elkart, IN) for cutting 20 μm sections using a cryostat. Embryos used for immunohistochemistry were decapitated and the heads were then fixed in 4% paraformaldehyde in PBS 1-2 hours, cryoprotected in 30% sucrose, embedded in OCT and cut on the cryostat (20 μm sections). For LacZ staining, whole embryos or P0 brains were fixed for two hours in 0.2% glutaraldehyde 4°C, washed in PBS containing 0.02% NP-40 for 15 minutes, and stained with a freshly

made X-gal (5-bromo-4-chloro-3-indolyl- β -D-galactopyronoside) solution according to the standard protocol. These embryos or P0 brains were subsequently fixed in 4% paraformaldehyde in PBS overnight, cryoprotected in 30% sucrose, embedded in OCT and cut on the cryostat (15 μ m sections). All sections were counterstained with Nuclear Fast Red according to a standard protocol and then photographed using a CCD camera mounted on a dissecting microscope.

Immunohistochemistry. Primary antibodies were used as follows: β -galactosidase (1:5000, ICN Biochemicals, Costa Mesa, CA). OCT embedded frozen sections were placed in 5% goat serum, 5% BSA, and 0.3% Triton X-100 for 2 hours at room temperature. Sections were incubated with primary antibodies overnight at 4°C followed by fluorescent labeling with mouse or rabbit Alexa 488 (1:250, Invitrogen, Eugene, OR) or Texas Red (1:500, Invitrogen) in blocking buffer. For the isolectin B4 staining: paraformaldehyde-fixed sections were blocked as above for primary antibodies followed by permeablization in PBS containing 1% Triton X-100, 1mM CaCl₂, 1mM MgCl₂, 0.1mM MnCl₂. These sections were then incubated with biotin-conjugated isolectin B4 (20ng/ μ L, Sigma L-2140) overnight at 4°C in permeablization solution. After 5 washes in PBS, sections were incubated with streptavidin-conjugated Alexa 594 (1:500, Molecular Probes) in blocking buffer. Sections were counterstained with the nuclear marker TO-PRO-3 (1:4000, Molecular Probes). All sections were analyzed using a Zeiss LSM 5 Pascal confocal microscope.

Collection, purification, and analysis of RNA. Total RNA for Northern blots was obtained from control and mutant *itg β 8 nescr ϵ 8* postnatal day zero (P0) forebrains using the RNA-Bee Isolation of RNA Kit (TEL-TEST, Friendswood, TX). A 700 bp fragment

from the 3' untranslated region of *itgβ8* was used as a probe. A 500 bp fragment of *GAPDH* (glyceraldehydes-3-phosphate dehydrogenase) gene was used as a probe as a control for RNA loading. For RT-PCR, total RNA was obtained from control and mutant *itgβ8 β-actin-cre* postnatal day zero (P0) brains using the RNA-Bee Isolation of RNA Kit (TEL-TEST). Using a standard poly(dT) oligo primer, we performed a standard reverse transcription reaction and used the resulting cDNA in a standard PCR reaction using the following primers: (wild-type (510bp) and mutant (260bp) (5'-

AATATGACTCTCACAGACGG- 3'); (5'-TGTCTGTGCATGTTGTAACG- 3'). For microarray analysis, nine control and nine mutant *itgβ8 nescre8* E12.5 forebrains were collected and as much of the meningeal layer removed as possible. These forebrains were then placed in RNA Later (Qiagen) at -20°C during genotyping. Total RNA was obtained from nine control and nine mutant forebrains using the Qiagen RNeasy Mini Kit (Valencia, CA). Total RNA quality was assessed using a Pico Chip on an Agilent 2100 Bioanalyzer courtesy of Dr. David Erle (Director of the Functional Core Genomics Laboratories, UCSF).

Target RNA Amplification for Spotted Oligonucleotide Arrays. Sample preparation, labeling, and array hybridizations were performed according to standard protocols from the UCSF Shared Microarray Core Facilities (<http://arrays.ucsf.edu/protocols>). RNA amplifications were performed using the Amino-Allyl MessageAmp II aRNA Kit (Ambion, Austin, TX) according to the manufacturer's protocol. One μg of total RNA was used for one-round amplification experiments. Amplified RNA (aRNA) quality was assessed using a Pico Chip on an Agilent 2100 Bioanalyzer. 7.5 μg of aRNA was used per sample for each array. The amplified RNA s were coupled to N-hydroxysuccinimidyl

esters of Cy3 or Cy5 dyes (CyScribe, Amersham Biosciences) for 1 h in the dark. The labeled aRNAs were purified and concentrated using Zymo RNA cleanup columns (Zymo, Orange, CA). Note: Dye swaps were incorporated into the experimental design to accommodate for any dye bias that may have been introduced during the coupling reactions. aRNA was then fragmented to 50-300 base pairs with Ambion fragmentation buffer for 15 minutes at 70°C (cat #8740, Ambion, Austin, TX).

MEEBO Array Hybridization, Scanning, and Image Analysis. Mouse Exonic Evidence Based Oligonucleotide (MEEBO) microarrays were printed and obtained from the UCSF Shared Microarray Facility at UCSF. The MEEBO set is comprised of more than 38,000 70-mer oligonucleotides that have been designed to represent constitutively expressed transcripts for nearly every gene in the mouse genome (<http://www.arrays.ucsf.edu/meebo.html>). Additionally, the set contains splice variants for over 3,000 genes and a comprehensive set of controls. Nine MEEBO arrays were used to process nine paired mutant/control samples of labeled aRNA. Prior to hybridization, excess oligonucleotide was removed from the arrays by gently shaking them for 10 minutes in 0.2% SDS. Arrays were then washed 5 times with distilled, filtered water and dried for 5 minutes at 600 rpm in a centrifuge. A solution of 0.1% SDS, 5X SSC and 1% BSA was applied to the arrays for 1-2 hours at 42°C to block nonspecific binding. Arrays were then washed 5 times with distilled, filtered water and dried for 5 minutes at 600 rpm in a centrifuge. Labeled aRNAs were added to Ambion's Hybridization buffer (cat #8861), denatured for 5 minutes at 95°C, and applied to the arrays using a cover slip (LifterSlip, Erie Scientific, Portsmouth, NH). Arrays were placed in a SciGene Hybex hybridization chamber (Scigene, Sunnyvale, CA) at 55°C for

48 hours. After hybridization, arrays were washed successively with 1X SSC at 55C for 3 minutes , and then 0.03% SDS, 0.2X SSC, and 0.05X SSC for 3 minutes at room temperature and dried for 5 minutes at 600 rpm in a centrifuge. Arrays were scanned using an Axon 4000B laser scanner (Molecular Devices Corp., Union City, CA). During this process, one array broke and was eliminated from the analysis. Image analyses were performed using the software package GenePix 6.1 (Molecular Devices Corp). Quality analysis of the hybridizations was performed using the Bioconductor software package *arrayQuality* [see <http://www.bioconductor.org> and (Gentleman et al., 2004; Yang and Paquet, 2005)]. The analysis showed that two of the remaining arrays were of poor quality and were therefore eliminated from subsequent analysis. We also used various exploratory tools to ensure that there was no outlier array in the dataset. Thus, the remaining six MEEBO arrays were used to generate the dataset. This dataset was normalized using robust locally weighted regression (*loess*) to correct for intensity, spatial and other dye biases (Cleveland, 1979; Yang et al., 2002). This procedure was performed within each print-tip group and was carried out using the Bioconductor software package *marray* [see <http://www.bioconductor.org> and (Gentleman et al., 2004; Yang and Paquet, 2005)]. In the context of microarray experiments, *loess* normalization captures the non-linear dependence of the intensity log-ratio $M = \log_2(\text{Cy5}) - \log_2(\text{Cy3}) = \log_2(\text{Cy5}/\text{Cy3})$ on the overall intensity $A = (\log_2(\text{Cy5}) + \log_2(\text{Cy3}))/2$. No background correction was performed. We performed analysis of differential expression using a linear model. Model fitting was performed using the *limma* R library from the Bioconductor Project (Smyth, 2004). We examined p-values for differentially expressed

gene declaration. P-values were adjusted for family-wise Type I error rates (the rate of false positives) using the Bonferroni adjustment.

Results

Expression analysis of *cre* in the *nescre8* line

The *nescre8* transgenic mouse line expresses *cre* under control of the entire *nestin* promoter/enhancer beginning at E8.5 (Petersen et al., 2002). To understand its recombination pattern in more detail, we crossed this *cre* line to the *R26R* ROSA reporter strain carrying a floxed stop allele of *lacZ* (Soriano, 1999). At P0, *cre* activity was very strong and widespread in the brain (Fig. 3-1A). Since the *nescre8* transgenic mouse line is reported to express *cre* early during development (Petersen et al., 2002), we looked, using confocal microscopy, at E11.0 embryo progeny from the *nescre8/R26R* cross. β -galactosidase staining was strong within the neuroepithelium and little mosaicism was observed (Fig. 3-1C).

Analysis of *itg β 8* mRNA produced in the *itg β 8 nescre8* mutants

Cre mediated deletion of exon 4 of *itg β 8* results in a translational frame shift that generates a premature stop codon [see chapter 2 and Proctor et al., 2005)]. As a result, *itg β 8* mRNA is destabilized by the mRNA surveillance mechanism that degrades mRNA containing untranslated exons (Mendell et al., 2004). To determine if mutant *itg β 8* mRNA was in fact degraded, we performed RT-PCR of Exon 4 using mRNA obtained from *itg β 8 *β*actin-cre* P0 mutants (Fig. 3-2A). Although some mutant product was amplified, it was reduced compared to the control wild-type band indicating the mutant product is being actively degraded in the cell. We also performed a Northern blot analysis of RNA collected from an *itg β 8 nescre8* P0 mutant forebrain and a littermate

control forebrain using an *itgβ8* 3'UTR probe. As expected, there was some *itgβ8* message remaining in these mutants. This remaining message most likely came from cell types, such as those within the meninges, which were not recombined by this cre line. Indeed, others have reported similar findings when using cre mediated recombination of conditional alleles [for studies in the CNS of integrins and related molecules refer to (Graus-Porta et al., 2001; Petersen et al., 2002; Beggs et al., 2003; McCarty et al., 2005b)]. Therefore, we predict that there are no functional $\alpha\beta8$ heterodimers expressed by mutant cells in *itgβ8* conditional mutants.

Analysis of RNA collected from E12.5 forebrains of *itgβ8 nescre8* mutants for use as a probe for microarray chip screening

Hemorrhages in the *itgβ8 nescre8* mutants appeared by day E12.5 (see Chapter 2), the same time at which *itgβ8* null animals develop intracerebral hemorrhage. For this reason, we chose to use this cre line to generate mutant mRNA to utilize as a probe for looking for genes that may function in a pathway with integrin $\beta8$. Female *itgβ8^{lox/lox}* mice were crossed to male *itgβ8^{null/+};nescre8/+* mice to generate *itgβ8^{lox/null};nescre8/+* mutant progeny as well as heterozygous and wild-type littermate progeny. Forebrains from E12.5 control and mutant mice were collected and as much of the meninges removed as possible before lysing the tissue to collect RNA from nine mutant animals and nine control animals (Table 3-1). All total RNA collected had a minimum ratio of 260 nm/280 nm UV absorbance of 1.8 indicating these RNA's were of prime quality (Table 3-1). This total RNA was amplified in a single reaction per sample to generate a large quantity of amplified RNA that was also of very high quality (Table 3-1). Using an Agilent 2100 Bioanalyzer, we confirmed the quality of the total and amplified RNA by

electrophoresis. All total RNA's had sharp 18S and 28S peaks with no observable fragmentation between them (Fig. 3-3B, C). All amplified RNA's had an average length of approximately 2 kilobases (Fig. 3-3E, F).

Gene expression analysis of E12.5 *itgβ8 nescre8* mutant and control forebrains using MEEBO microarrays

In order to identify genes that were differentially expressed in E12.5 *itgβ8 nescre8* mutant and control forebrains, we exposed Mouse Exonic Evidence Based Oligonucleotide (MEEBO) microarrays (Fig. 3-4A) to amplified RNA from both sample sets. The MEEBO chips are an unpublished set of microarrays printed by spotting 70-mer oligonucleotides for every gene in the mouse genome, as well as other sequences of interest such as expressed sequence tags (ESTs) from cDNAs identified by Riken, on glass slides. Spotted long oligonucleotide arrays have historically provided similar quality results, both quantitatively and qualitatively, compared to the widely known Affymetrix GeneChips at a reduced cost making them an attractive alternative for functional genomic analyses [the published spotted oligo-arrays compared human samples (Barczak et al., 2003)]. The individual plots of fold change versus average signal intensity showed that most of the genes on the arrays were not differentially expressed, but that there were some genes with low signal intensity which may be differentially expressed (Fig. 3-4C). However, this is of some concern since this means that these genes have a diminished signal, and are thus difficult to detect with precision using microarray technology.

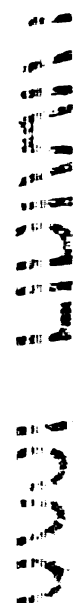
The differential expression signal also seemed somewhat inconsistent across the arrays so we looked at genes that gave consistent signal according to dye color and had a

p value < 0.05 (Bonferroni corrected). Although we could detect no bias for the Cy5 channel, there was an obvious bias for the Cy3 channel regardless of whether Cy3 was used to label the control or mutant sample (Fig. 3-5A). To confirm that there was in fact a Cy3 channel bias in this experiment, we hybridized one sample against itself (Fig. 3-5B). As expected, there was a cluster of genes that were more strongly labeled in the Cy3 channel than the Cy5 channel thus confirming the Cy3 channel bias in our experiment. However, this bias was limited to genes with very low signal intensity so we repeated our analysis by only looking at genes with median signal intensity greater than 9 (median A > 9 on log₂ scale). Using this approach, we did not identify any candidate genes that were differentially expressed in the *itgβ8 nescre8* mutant mRNA population versus the control mRNA population (Fig. 3-5C). While this was very surprising, it is possible that since the primary cell type with a phenotype in these mutants is the endothelial cells, the gene expression changes occurring in these cells could have been diluted out since these cells represent a relatively small proportion of all the cell types in the neuroepithelium at this time point. However, since we previously showed that *itgβ8* is required in neuroepithelial cells, and not endothelial cells, for proper vascular development of the brain (Chapter 2 and Proctor et al., 2005), we anticipated that loss of *itgβ8* from the neuroepithelium would have measurable effects on gene expression within the neuroepithelium. It remains possible though, that even within the neuroepithelium, *itgβ8* might only be required within a subset of those cells and the gene expression changes that occurred within those select cells that actually lost *itgβ8* were simply diluted out in the total RNA collected from the population as a whole.

Discussion

This study was designed as a high-throughput experiment to uncover genes that may function in conjunction with the $\alpha v\beta 8$ integrin in vascular development of the brain. We used Mouse Exonic Evidence Based Oligonucleotide (MEEBO) microarrays spotted with 70-mer oligonucleotides, representing every gene in the mouse genome, to compare mRNA collected from *itg β 8 nescr ϵ 8* mutants and control forebrains at embryonic day 12.5 (Table 3-1; Fig. 3-3). This transgenic line drives *cre* expression very robustly and recombines the neuroepithelium (Fig. 3-1) beginning at E8.5 (Petersen et al., 2002). We previously determined that E12.5 was the time at which these mutants first develop cerebral hemorrhage [see Chapter 2 and (Proctor et al., 2005)] which is the same time at which as *itg β 8* null animals develop cerebral hemorrhage (Zhu et al., 2002). Therefore, we were confident that the *itg β 8* gene was being removed from neuroepithelial cells using the *nescr ϵ 8* mouse line and collected RNA from mutant and control forebrains at 12.5 days post conception. Although we detected some *itg β 8* transcript by Northern blot (Fig. 3-2), we believe this transcript comes from cell types, such as those of the meninges that were not recombined by this *cre* line.

Using this microarray strategy we did not identify any genes that were up or down-regulated in *itg β 8 nescr ϵ 8* mutant forebrains compared to controls (Fig. 3-5). This may be a reflection of the fact that a majority of genes assayed in this study showed low overall signal intensity. One of the limitations of this approach is that genes with low signal intensity are difficult to detect with precision using microarray technology. Thus, while some genes may have subtle, yet significant, changes in gene expression, these changes will likely be undetected using this approach. Secondly, since the MEEBO arrays utilize a two color hybridization strategy to determine differences in gene



expression, it is critical that the two fluorescent dyes are not inherently brighter than one another. The dyes used in this experiment did not meet this requirement for genes with low signal intensity (Fig. 3-5). In fact, the Cy3 channel was significantly brighter than the Cy5 channel near the lower range of signal intensity. This resulted in an inaccurate measure of gene expression across arrays. Thus, future experiments with these MEEBO arrays will require dyes that behave more identically so that gene expression changes can be measured with greater precision and accuracy.

The *itgβ8* subunit is required within the neuroepithelium for proper vascular development of the brain (see Chapter 2 and Proctor et al., 2005). We expected that loss of *itgβ8* from the neuroepithelium would have measurable effects on gene expression within the neuroepithelium. However, the primary cell type within the neuroepithelium that appeared aberrant in mutants lacking *itgβ8* from the neuroepithelium was astroglia (see Chapter 2 and Proctor et al., 2005). If in fact these cells are the only cells in which *itgβ8* is required for proper vascular development of the CNS, it is possible that any gene expression changes that occurred within these cells in *itgβ8 nescre8* mutants were diluted out in the total RNA collected from the neuroepithelium as a whole. If this hypothesis is correct, it will be important in future array experiments to enrich the population of cells collected from the control and *itgβ8* mutants with this specific population of cells. Once reagents are generated that will enable specific labeling of *itgβ8* expressing cells, this can be achieved using common methods for cell sorting. The other cell type with a phenotype in *itgβ8* mutants is the endothelial cells (Zhu et al., 2002; Proctor et al., 2005). Therefore, we expected to see gene expression changes occurring in these cells in addition to the gene expression changes expected within the neuroepithelium. However,

these cells represent a relatively small proportion of all the cell types in the neuroepithelium at this time point. Therefore, it may also be the case for these cells that gene expression changes that occurred in the *itgβ8 nescre8* mutants were diluted out within the population of total RNA collected from the entire neuroepithelium. Thus, it will also be important in future array experiments to analyze these cells separately from the rest of the neuroepithelium. This can easily be achieved by driving GFP expression in all endothelial cells using a *tie2-GFP* reporter line. This will enable FACS sorting of brain endothelial cells from the neuroepithelial cells and will allow gene expression changes occurring specifically in these cells to be measured.

CNS vascular development and the integrin $\alpha\beta 8$

Despite the lack of information gained from this experiment regarding the potential pathways in which $\alpha\beta 8$ may function to regulate vascular development of the brain, there are candidate molecules that have been proposed to function in a pathway with $\alpha\beta 8$. TGF- β and its associated receptors are known to play important roles in the regulation of migration and proliferation of endothelial cells during angiogenesis (Goumans et al., 2003; Lebrin et al., 2005). The integrin $\alpha\beta 8$ has been shown to bind the RGD containing latency-associated peptide of TGF- $\beta 1$ (LAP- $\beta 1$) in cultured human epithelial airway cells and cultured human astrocytes (Mu et al., 2002; Cambier et al., 2005). LAP- $\beta 1$ is a component of the TGF- β large latent complex (LLC), which is a secreted molecule found within the extracellular matrix. The LLC prevents TGF- $\beta 1$ from interacting with its receptors until it is liberated or “activated” by cleavage from the LLC and LAP by specific enzymes within the ECM (Annes et al., 2003; Todorovic et al., 2005). In the airway epithelium, $\alpha\beta 8$ binds LAP- $\beta 1$ which is subsequently cleaved by

the matrix metalloprotease, MT1-MMP, to activate or liberate, free TGF- β 1 (Mu et al., 2002). Interestingly, α v β 8 mediated activation of TGF- β 1 leads to an inhibition of airway epithelial cell proliferation *in vitro*. The evidence presented above suggests a model in the brain in which α v β 8 binds LAP- β 1 within the basal lamina between glial cells and endothelial cells, and through interaction with a MMP, liberates soluble TGF- β 1. TGF- β 1 could then interact cell non-autonomously with neighboring endothelial cells to activate pathways that would inhibit their proliferation and/or migration. This is an interesting model since a hallmark feature of loss of *itg β 8* from neuroepithelial cells is hyperproliferative endothelial cells (Zhu et al., 2002; Proctor et al., 2005). In addition, in co-culture with human astrocytes, immortalized mouse endothelial cells up-regulate the anti-angiogenic genes plasminogen activator inhibitor-1 (*PAI-1*) and thrombospondin-1 (*TSP-1*) (Cambier et al., 2005). These observations provide a potential pathway, centered on TGF- β 1, for α v β 8 mediated regulation of endothelial cell proliferation and migration.

Another gene of interest is *neuropilin-1* (*nrp-1*). Deletion of *nrp-1* results in defective yolk sac and cerebral vessel development and early embryonic death (Kawasaki et al., 1999). Additionally, *nrp-1* mutants display aberrant endothelial cell clusters (Gerhardt et al., 2004) similar to those observed in the *itg β 8* null and neuroepithelial specific *itg β 8* mutants (Zhu et al., 2002; Proctor et al., 2005). Neuropilin-1 is a known receptor for the VEGF₁₆₅ isoform of VEGF-A (Breier et al., 1992; Soker et al., 1998), and the VEGF₁₆₅ binding site on neuropilin-1 is necessary for proper capillary development in the embryonic mouse brain (Gu et al., 2003). Moreover, it is well known that increased capillary permeability and endothelial cell hyperproliferation are known effects of augmented VEGF expression (Cheng et al., 1997; Sundberg et al., 2001; Gora-Kupilas

and Josko, 2005). Through possible direct contact, or indirect communication via an accessory ECM molecule, with neuropilin-1 expressed on endothelial cells, $\alpha v\beta 8$ expressed on glial cells may down regulate expression or secretion of specific isoforms of VEGF, such as VEGF₁₆₅, from those glial cells. Thus through coordinated communication with neuropilin-1, $\alpha v\beta 8$ could regulate vascular morphogenesis by inhibiting pathways that promote endothelial cell proliferation.

The gene *krit1* may also be an interesting candidate molecule to investigate in future studies. Mutations in this gene lead to a human disease known as cerebral cavernous malformations (CCM) (Lagerge-le Couteulx et al., 1999; Gunel et al., 2002). CCM patients develop CNS hemorrhage characterized by tortuous blood vessels devoid of surrounding brain parenchyma (Marchuk et al., 2003). Krit1 has a C-terminal FERM domain, which is thought to interact with the actin cytoskeleton (Marchuk et al., 2003). In addition, Krit1 has an ankyrin repeat domain, which is known to mediate protein-protein interaction (Sedgwick et al., 1999). Interestingly, Krit1 also contains an NPxY motif in the N-terminal domain of the protein which is known to interact with the integrin cytoplasmic domain-associated protein alpha (ICAP-1 α) which has been shown to bind the integrin $\beta 1$ subunit cytoplasmic tail (Zhang et al., 2001; Zawistowski et al., 2002). ICAP-1 α is known to associate with the Rho GTPases Cdc42 and Rac1 and regulate integrin mediated cell adhesion (Degani et al., 2002). It is tempting to think that Krit1 may be an intracellular binding partner for the integrin $\beta 8$ subunit and that together these proteins function in a pathway to regulate vascular morphogenesis of the brain. Perhaps, $\alpha v\beta 8$ may function through Krit1 to regulate astroglial adhesion to the extracellular matrix near endothelial cells where close association of these cell types is required for

proper vessel development. An alternative hypothesis is that the $\alpha\beta8$ -Krit1 interaction is required for secretion of ECM components or growth factors that influence endothelial cell proliferation and morphogenesis. It will be interesting to determine whether a physical interaction between $\alpha\beta8$ and Krit1 can be identified.

Lastly, it is worth mentioning two other molecules which may function with the $\alpha\beta8$ integrin to regulate vascular development of the brain. The protein called Band 4.1B was recently shown to bind the cytoplasmic tail of the integrin $\beta8$ subunit (McCarty et al., 2005a). While the functional consequence of this interaction is yet to be determined, it is possible that Band 4.1B functions as a down-stream signaling component in an $\alpha\beta8$ mediated signaling pathway. Alternatively, it may function to activate this integrin and facilitate $\alpha\beta8$ mediated adhesion to the extracellular matrix between astroglial processes and the endothelial cells within the neuroepithelium. This possibility is less likely since $\alpha\beta8$ integrin is thought to be constitutively active (Januzzi et al., 2004). The second molecule is the Rho GDP dissociation inhibitor-1 (Rho GDI), which was identified in kidney mesangial cells to bind the cytoplasmic tail of the integrin $\beta8$ subunit (S. Lakhe-Reddy and J.R. Schelling, submitted to Journal of Biological Chemistry). It was proposed that the interaction between Rho GDI and the cytoplasmic tail of the integrin $\beta8$ subunit permitted activation of the small G-protein Rac1 by a guanine exchange factor since the Rho GDI would be bound and unable to inhibit Rac1 activation. While it is unclear how this mechanism may function to regulate endothelial cell proliferation within the neuroepithelium, these molecules are candidates worthy of further investigation.

Verifying pathways in which $\alpha\beta8$ functions

The genes discussed above are, at this point, candidate molecules that may function in conjunction with the integrin $\alpha v\beta 8$ to regulate vascular development of the brain. It is now necessary to determine whether these genes are up or down-regulated in the *itg $\beta 8$ nescre8* mutants by performing real-time quantitative PCR or at least Northern blot analysis of the mRNA collected from these animals' forebrains. Secondly, Western blot analysis of the proteins these genes encode should be used to determine if the any observed change in gene expression level results in a physical change in the amount of protein expressed in mutant cells to gain a more thorough understanding of the *itg $\beta 8$* phenotype. In addition, each of these genes should be localized within the forebrain with respect to integrin $\beta 8$ expression either by immunolabeling or *in situ* hybridization. The former will be a challenge until a trustworthy antibody for the integrin $\beta 8$ subunit is generated. Note: A discussion of the current antibodies generated against the integrin $\beta 8$ subunit can be found in the Appendix.

From the perspective of identifying potential pathways in which $\alpha v\beta 8$ integrin functions, this study did not provide the information we had hoped. However, it does demonstrate the need, when using these genome-wide approaches, to specify the most relevant biological samples so that specific questions can be addressed. Thus, in future it will be necessary to perform this microarray analysis separately on neuroepithelial cells that express *itg $\beta 8$* , and the endothelial cells it regulates, in separate experiments.

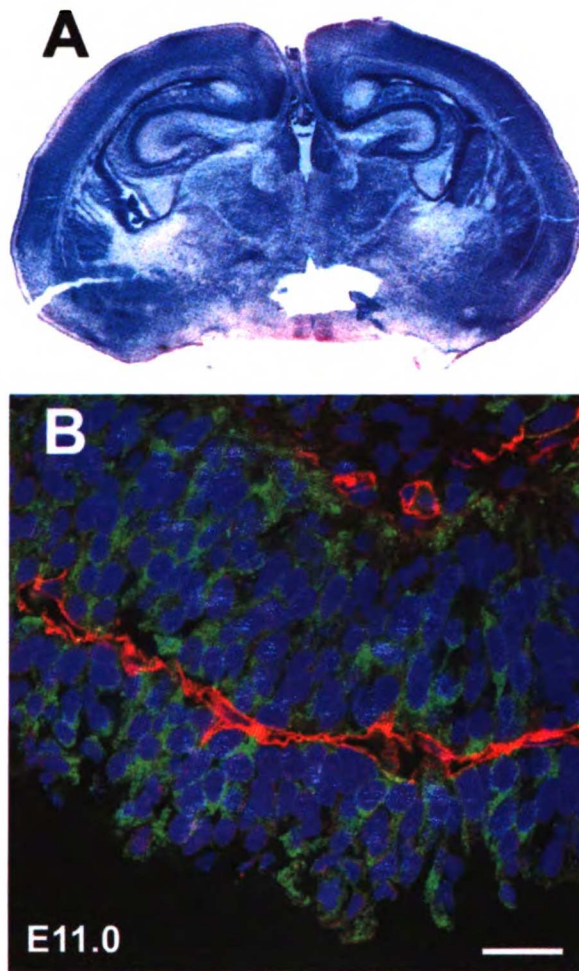


Figure 3-1. Analysis of the *nescre8* transgenic line using the *R26R* reporter line.

A, LacZ stained coronal section from a P0 cortex obtained from a cross between a *nescre8* positive animal and the *R26R* reporter line. Recombination is strong throughout the cortex, hippocampus, and thalamus. **C**, β-Galactosidase (*βGal*) expression analysis of E11.0 embryo cortex prior to the onset of hemorrhage in the *itgβ8 nescre8* mutant. Note that βGal (green) immunolabeling is limited to cells within the future cortical plate. Endothelial cells were immunolabeled with isolectin B4 (red) and were not recombined by this cre line. Cell nuclei were counterstained with TO-PRO-3 (blue). Scale bar: B, 20 μm.

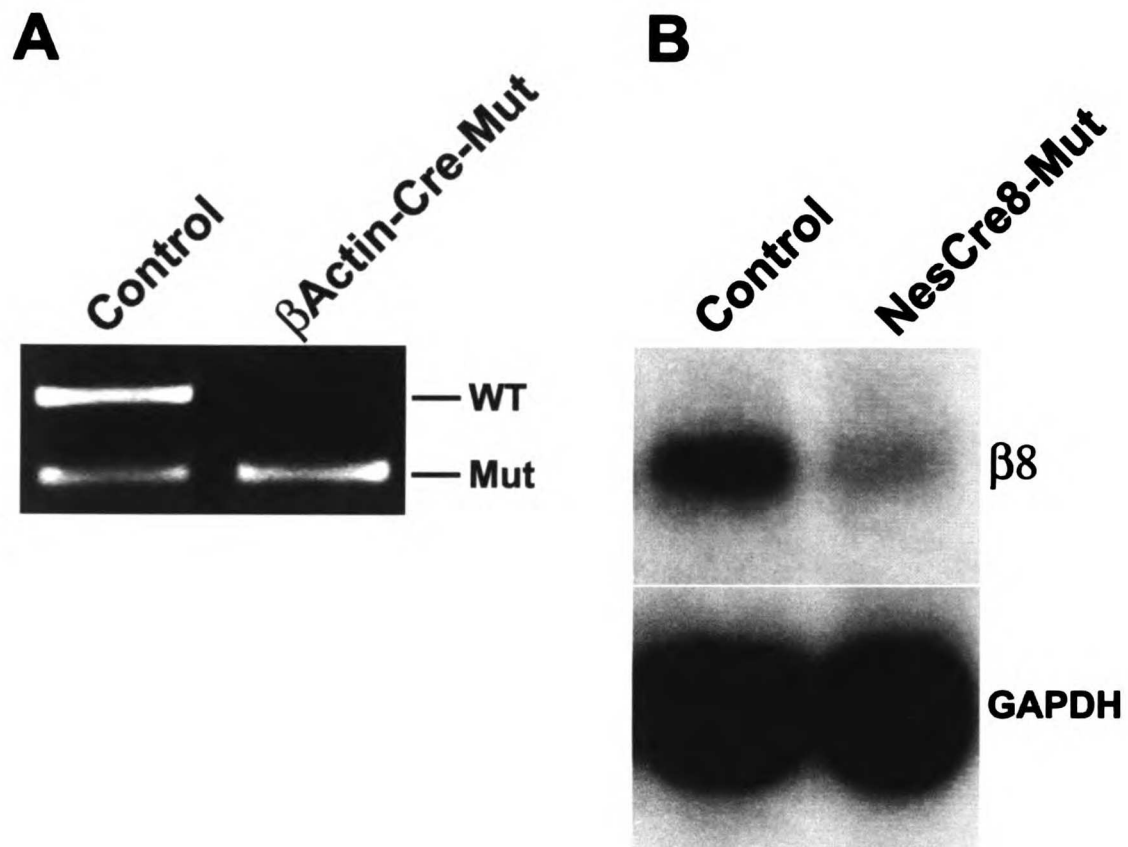


Figure 3-2. RT-PCR and Northern blot analysis of RNA in *itg β 8* mutants.

Figure 3-2. RT-PCR and Northern blot analysis of RNA from *itgβ8* mutants.

A, RT-PCR was performed with primers within exons 3 and 5 to ascertain the presence or absence of exon 4 transcript from the *itgβ8* gene in the P0 *itgβ8^{lox/mull}; β-actin cre/+* mutant. A mutant band was amplified, but note the weight of the mutant band is approximately half the weight of the wild-type band, in the control lane, indicating this mutant RNA transcript is being actively degraded in the cell. *B*, Northern blot analysis of RNA acquired from the forebrain of a P0 *itgβ8^{lox/mull}; nescre8/+* mutant and *itgβ8^{lox/+}; nescre8/+* heterozygote littermate control. For northern blot analysis a probe designed within the 3' UTR was used to detect *itgβ8* transcript while a *GAPDH* probe was used as a load control. Note that a small amount of *itgβ8* transcript was detected which may reflect a subset of cells, such as the meninges, that were not recombined by this cre line.

Table 3-1. Quantification of RNA collected and amplified from E12.5 *itgβ8 nescre8* mutants and control forebrains.

Sample ID M=Mutant C=Control	Total RNA					Amplified RNA				
	mg tissue	ng/μl	260/280	μl	total μg	ng/μl	260/280	260/230	total μl	total μg
M2	16.4	864	2.1	25	21.6	658	1.97	1.53	136.5	89.8
M9	11.3	995	1.8	25	24.9	628.9	1.95	1.79	136.5	85.8
C4	9.4	590	2	25	14.8	716.8	1.95	1.6	136.5	97.8
C5	10.6	918	2.1	25	22.9	617.8	1.95	1.66	136.5	84.3
C3	13.5	1121	1.8	25	28.0	725.1	1.92	1.69	136.5	99.0
M4	15.2	1053	2	25	26.3	843.3	1.92	1.62	136.5	115.1
M6	10.8	1060	2	25	26.5	931.8	1.92	1.81	136.5	127.2
C7	13	939	1.8	25	23.5	800.3	1.92	1.68	136.5	109.2
M11	12.5	946	1.9	25	23.6	568.8	1.89	1.54	136.5	77.6
C13	14.9	1100	2.2	25	27.5	786.9	1.92	1.74	136.5	107.4
M14	9	911	2.3	25	22.8	766	1.93	1.73	136.5	104.6
C15	10.2	988	2.1	25	24.7	742.9	1.92	1.53	136.5	101.4
C16	15.1	1121	2.2	25	28.0	787.5	1.93	1.46	136.5	107.5
C17	12.9	1082	2.2	25	27.0	884.5	1.93	1.52	136.5	120.7
M19	13.2	1085	2.1	25	27.1	872.7	1.92	1.59	136.5	119.1
C20	14	873	1.9	25	21.8	665	1.94	1.29	136.5	90.8
M22	12.7	979	2.7	25	24.5	722.6	1.93	1.45	136.5	98.6
M24	10.8	842	2	25	21.0	639.2	1.93	1.52	136.5	87.2

E12.5 embryo forebrains were collected and weighed from a cross between a female *itgβ8^{lox/lox}* animal and an *itgβ8^{null/+}*; *nescre8/+* animal. After genotyping, each forebrain was given a letter (M for mutant or C for control) and a number code. Three litters were collected and processed in three batches (color coded in red, blue, and black). The weight of each forebrain, the concentration of the total RNA collected from that tissue, the 260 nm/280 nm ratio, and the total mass of RNA collected are listed. One microgram of each sample was amplified in a single round amplification reaction to produce amplified RNA for each sample. The concentration of the amplified RNA produced, the 260 nm/280nm ratio, the 260 nm/230 nm ratio, and the total mass of amplified RNA produced are listed.

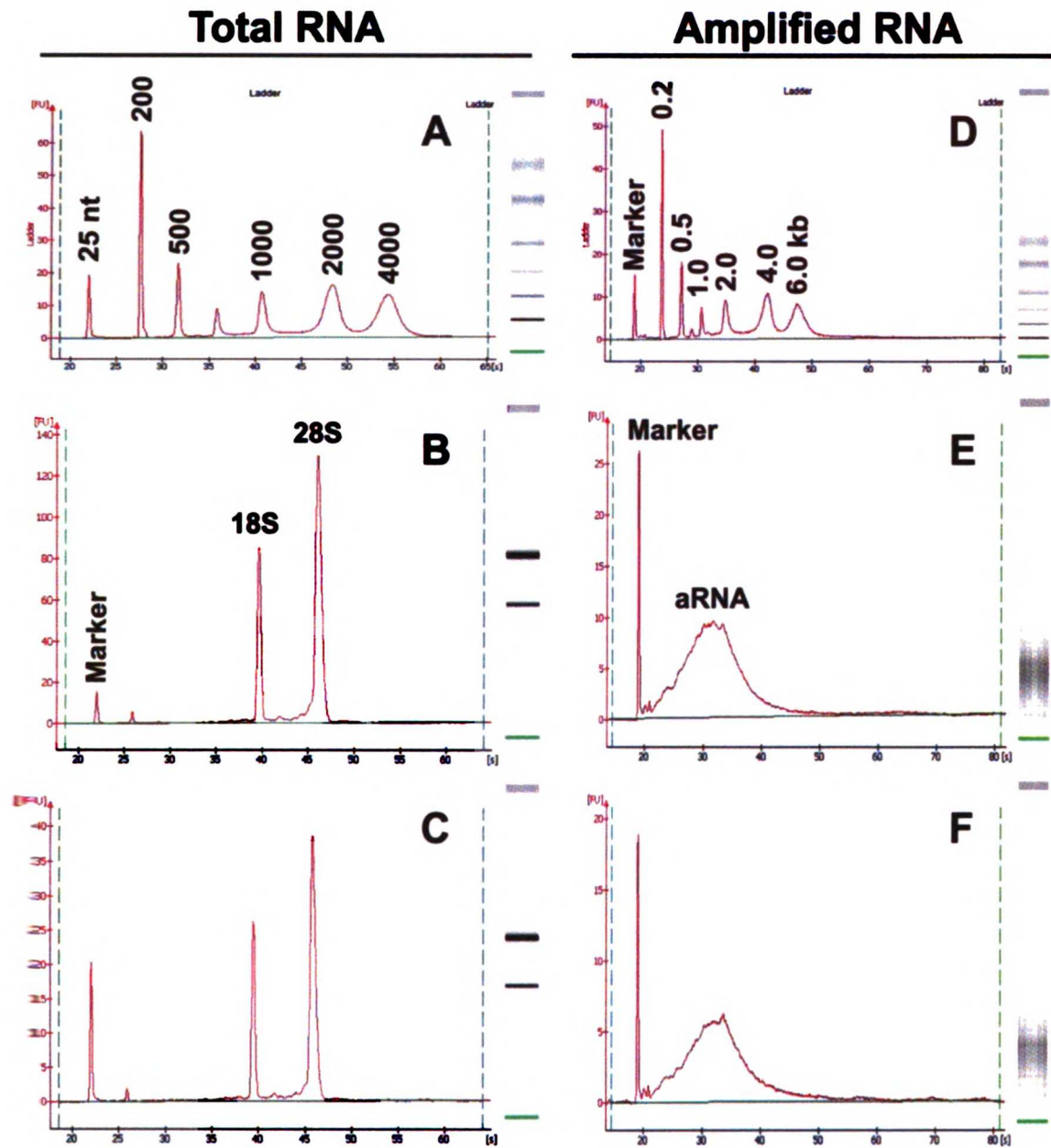
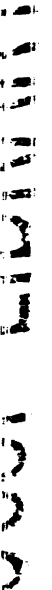


Figure 3-3. Quality analysis of total RNA and amplified RNA from E12.5 *itgβ8* *nescre8* mutants and control forebrains.

Figure 3-3. Quality analysis of total RNA and amplified RNA from E12.5 *itgβ8 nescre8* mutants and control forebrains.

An Agilent Technologies 2100 Bioanalyzer was used to analyze all samples. Typical traces and gel lanes are shown for both control and mutant total and amplified RNA. *A*, RNA ladder used for total RNA. *B*, Trace of total RNA collected from control animal 13. Notice the lack of fragmentation peaks between the very sharp and clean 18S and 28S ribosomal RNA peaks. *C*, Trace of total RNA collected from mutant animal 11. Notice the lack of fragmentation peaks between the very sharp and clean 18S and 28S ribosomal RNA peaks. *D*, RNA ladder used for amplified RNA. *E*, Trace of amplified RNA collected from control animal 16. Notice that most of the amplified RNA is between 1.0 and 4.0kb in length. *F*, Trace of amplified RNA collected from mutant animal 19. Notice that most of the amplified RNA is between 1.0 and 4.0kb in length.



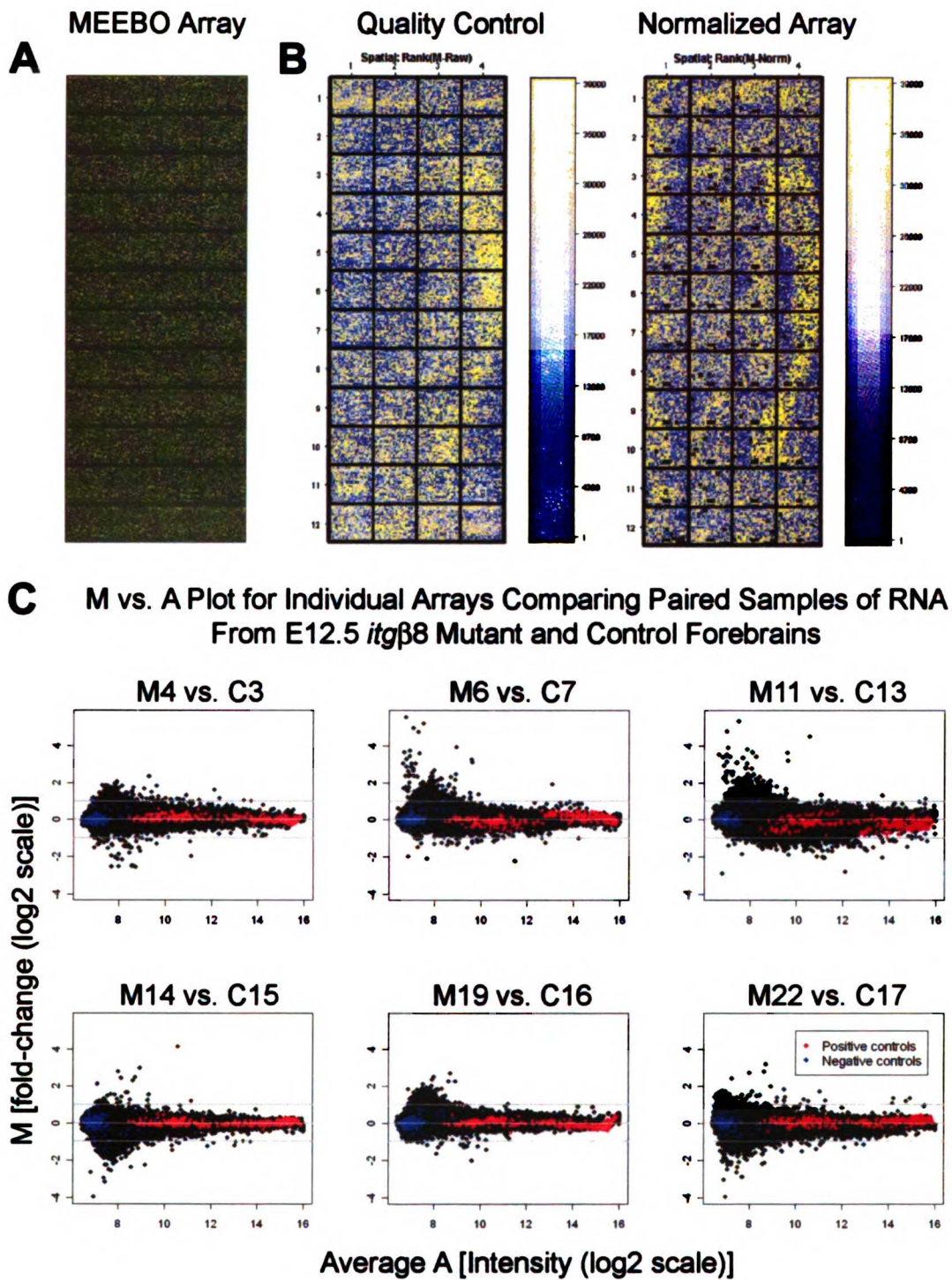
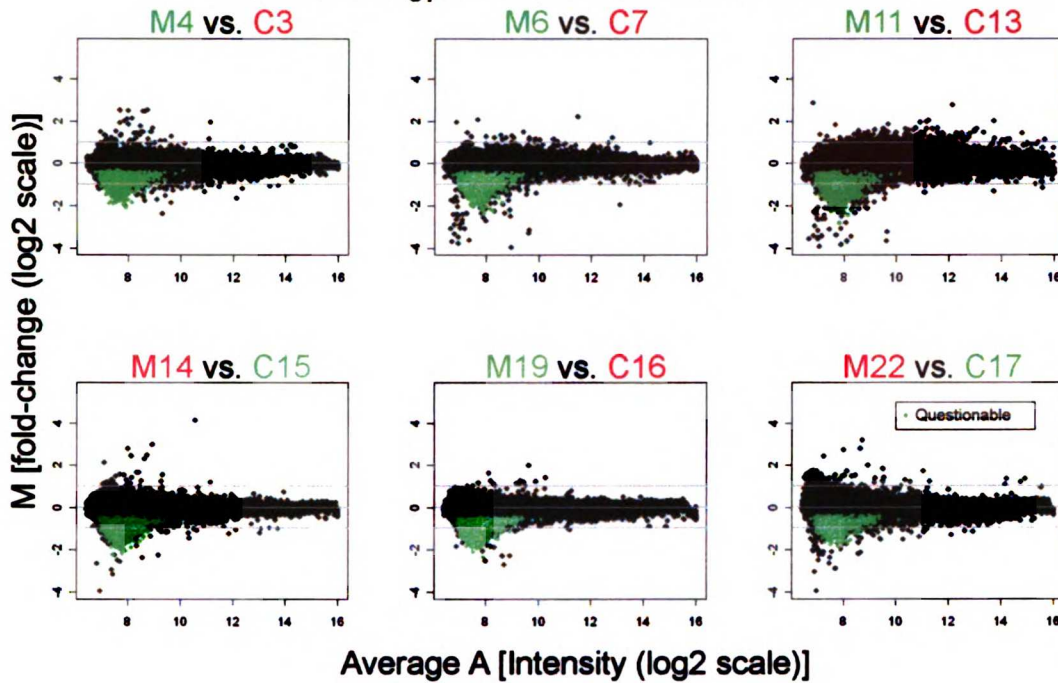


Figure 3-4. Gene expression analysis of E12.5 *itgβ8 nescre8* mutant and control forebrains using MEEBO microarrays.

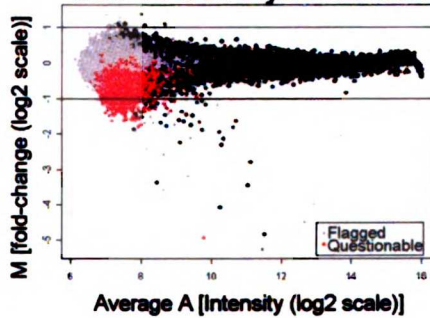
Figure 3-4. Gene expression analysis of E12.5 *itgβ8 nescre8* mutant and control forebrains using MEEBO microarrays.

A, Scanned image of one of the six MEEBO microarrays used in this experiment. *B*, “Quality Control” is a spatial plot of raw *M* (fold change) values (no background subtraction). Each spot is ranked according to its *M* value. We used a blue to yellow color scale, where blue represents the higher rank and yellow represents the lower one. Missing spots are represented as white squares. This is a quick way to visually detect uneven hybridization and missing spots. “Normalized Array” is a spatial plot of *M* values after loess normalization is used. Each spot is ranked according to its *M* value. We used a blue to yellow color scale, where blue represents the higher rank and yellow represents the lower one. Missing spots are represented as white squares. In addition, flagged spots (dim and/or uneven spots) are highlighted by a black square. This type of graphical representation helps verify that normalization removed any spatial effects. *C*, Scatter plot of *M* values (log-ratio of mutant versus control) and median log intensity (median *A* values) for each of the six individual arrays used in this experiment. The within-array controls are shown in red and blue. Also, the mutant sample ID and the control sample ID hybridized to each chip are shown above each scatter plot. Notice the large proportion of genes with median *A* < 9 in all sample comparisons.

A M vs. A Plot for Individual Arrays Comparing Paired Samples of RNA From E12.5 *itgβ8* Mutant and Control Forebrains



B Self vs Self Hybridization



C Combined M vs. A Plot for E12.5 *itgβ8* Mutant vs. Control

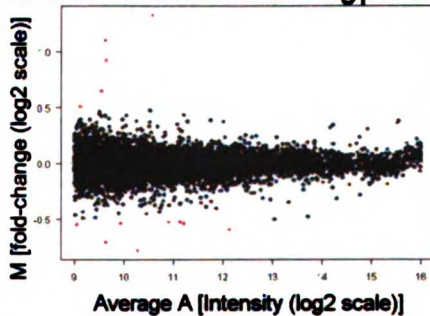


Figure 3-5. Secondary analysis of gene expression in E12.5 *itgβ8 nescre8* mutant and control forebrains using MEEBO microarrays.

Figure 3-5. Secondary analysis of gene expression in E12.5 *itgβ8 nescre8* mutant and control forebrains using MEEBO microarrays.

The differential expression signal seemed inconsistent across the six MEEBO arrays, and it appeared that most of these genes had very low signal intensity (median $A < 9$). To check for dye bias, we looked at genes that were potentially differentially expressed (p value < 0.05 after adjusting using the Bonferroni correction) and correlated them to dye color (labeled “Questionable” in the following plots). *A*, Scatter plot of M values (log-ratio of mutant versus control) and median log intensity (median A values) for the six individual arrays used in this experiment. Negative M values signify that the spot was green and positive M values signify the spot was red. The mutant sample ID and the control sample ID hybridized to each chip is shown above each scatter plot as well as the dye color used to label each sample (green = Cy3; red = Cy5). Note that irrespective of sample genotype (control or mutant) questionable genes consistently correlated with the Cy3 label. *B*, Scatter plot of M values (log-ratio of mutant versus control) and median log intensity (median A values) for a mutant sample hybridized to itself. All genes should label equally with both dyes since the same sample was labeled with both dye colors and hybridized to the same array. However, note that there is an obvious dye bias for the Cy3 label at low signal intensities ($A < 9$) since a group of questionable genes is evident with negative M values. *C*, Scatter plot of M values (log-ratio of mutant versus control) and median log intensity (median A values > 9) for all of the six arrays used in this experiment combined after properly accommodating for dye swaps. Note that after eliminating low signal intensity spots ($A < 9$), and therefore eliminating spots with dye

Chapter 4

Integrin $\beta 8$ is Required in the Adult Mouse for Proper Locomotion, Urinary Function, and Cortical Astrocyte Localization

1
2
3
4
5
6
7
8
9
10
11
12
13
14
15
16
17
18
19
20
21
22
23
24
25
26
27
28
29
30
31
32
33
34
35
36
37
38
39
40
41
42
43
44
45
46
47
48
49
50
51
52
53
54
55
56
57
58
59
60
61
62
63
64
65
66
67
68
69
70
71
72
73
74
75
76
77
78
79
80
81
82
83
84
85
86
87
88
89
90
91
92
93
94
95
96
97
98
99
100

Acknowledgements

I want to thank William Walantus for teaching me the delicate technique of perfusion. I also want to thank Keling Zang for making numerous trips to the mouse facility to help me footprint all the mutants presented in this chapter.

Abstract

In the previous chapter, I demonstrated that *itgβ8* is required in neuroepithelial glial cells for proper vascular development of the brain. Additionally, I demonstrated that adult animals lacking *itgβ8* in the central nervous system (CNS) do not have cerebral hemorrhage and thus must repair the vascular malformations that occur during development. In the current chapter, I utilized a similar targeted deletion strategy to remove *itgβ8* from select populations of cells within the brain to determine if there is any requirement in the adult CNS for *itgβ8*. Ablating *itgβ8* from migrating neurons in the cortex or oligodendrocytes and motor neurons did not result in any identifiable phenotype. However, targeted deletion of *itgβ8* from the neuroepithelium resulted in mutant animals that begin to display abnormal gait in their hind limbs approximately six to twelve weeks after birth. These mutants also develop severe urinary dysfunction which may ultimately contribute to their premature death. Although morphological cortical abnormalities were not observed in these mutants, the brains of *itgβ8* neuroepithelial cell mutants have an abnormal distribution of astrocytes indicating that the $\alpha\beta8$ integrin may play a role in proper cortical astrocyte localization in the adult animal.

Introduction

The integrin $\alpha\beta8$ is required for proper capillary development within the central nervous system (CNS) (Bader et al., 1998; McCarty et al., 2002; Zhu et al., 2002). In addition to its primary function during vascular morphogenesis in the embryonic brain, there is evidence to suggest that $\alpha\beta8$ may also play important roles in the adult nervous system. The integrin $\alpha\beta8$ may function as a regulator of glial migration and differentiation in the CNS. First, it was demonstrated that high expression levels of the integrin $\beta8$ subunit is correlated with oligodendrocyte differentiation in the presence of axons (Milner et al., 1997a). Other evidence suggests that it plays a direct role in astrocyte migration *in vitro* (Milner et al., 1999). Secondly, both the $\alpha\upsilon$ and $\beta8$ integrin subunits have been localized to neurons and glial processes in the adult rodent nervous system (Nishimura et al., 1998; Pinkstaff et al., 1999). In the peripheral nervous system (PNS) there is evidence that $\alpha\upsilon\beta8$ is expressed by Schwann cells during their coordinated migration along growing axons (Milner et al., 1997b). It has also been proposed to be a receptor for fibrin, a derivative of fibrinogen, which is produced at sites of Schwann cell injury *in vitro* (Chernousov and Carey, 2003).

Since both the integrin $\beta8$ (*itg $\beta8$*) and integrin $\alpha\upsilon$ (*itg $\alpha\upsilon$*) conventional mutants die just after birth, the study of postnatal functions for these two genes has not been possible until recently. This past year, a conditional mutant of *itg $\alpha\upsilon$* was shown to have defective hind limb coordination and urinary dysfunction as a result of loss of *itg $\alpha\upsilon$* from all neuroepithelial cells in the CNS and PNS (McCarty et al., 2005). In the discussion of Chapter 2 (Proctor et al., 2005), I noted that we also observed hind limb coordination defects in adult mutants lacking *itg $\beta8$* in cells derived from the neuroepithelium. In this

chapter I explore this phenotype in more detail and, using several different cre lines, determine that *itgβ8* may be required in the PNS, rather than the CNS, for normal hind limb gait and urinary tract function.

Materials and Methods

PCR genotyping of mice. Female *itgβ8^{lox/lox}* mice were crossed to male *itgβ8^{null/+};cre/+* mice to generate *itgβ8^{lox/null};cre/+* mutant progeny as well as heterozygous and wild-type littermate progeny. All progeny were genotyped by standard PCR analysis using DNA from tail tissue. Primers specific for each allele were used to identify progeny and are as follows: *itgβ8* wild-type (250bp) and floxed-allele (370bp) (5'-GAGATGCAAGAGTGTTTACC-3') and (5'-CACTTTAGTATGCTAATGATGG-3'); *itgβ8* null-allele (450bp) (5'-AGAGGCCACTTGTGTAGCGCCAAG-3') and (5'-GGAGGCATACAGTCTAAATTGT-3'); cre (400bp) (5'-CTGGCAATTTCGGCTATACGTAACAGGGTG-3') and (5'-GCCTGCATTACCGGTCGATGCAAC-3').

Mouse lines. The *itgβ8^{lox/lox}* mice were produced according to procedures covered in detail in chapter 2 [see also (Proctor et al., 2005)]. The *itgβ8^{null/+}* mice (Zhu et al., 2002), the *nestin-cre* mice (Tronche et al., 1999), the *nescre8* mice (Petersen et al., 2002), and the *nex-cre* (Beggs et al., 2003; Brockschneider et al., 2004; Proctor et al., 2005) have been described previously. The *olig1-cre* mice were a kind gift of Dr. David Rowitch (Harvard University, Cambridge MA), and have been described previously (Lu et al., 2002). Mice were cared for according to animal protocols approved by the UCSF Committee on Animal Research.

Morphological and histological analysis. Adult mice were anesthetized with 2.5% avertin in 0.9% NaCl using 15 μ l per gram mouse weight and perfused with 50 mL of 4% paraformaldehyde (PFA) in PBS followed by 20 mL of 15% sucrose in PBS, which was followed by perfusion with 20 mL of 30% sucrose in PBS. This tissue was frozen directly in 30% sucrose for cutting 40 μ m sections using a sliding microtome. Nissl stain was used according to standard procedures. NeuroTrace 530 red fluorescent Nissl stain (Invitrogen, Eugene, OR) was used according the manufacturers protocol. For the Evan's Blue Dye experiment, before mice were perfused with PFA, they were perfused with 20 mL 2.5% Evan's Blue dye [(E2129) Sigma, St. Louis, MO].

Immunohistochemistry. Primary antibodies were used as follows: GFAP polyclonal (pAb) (1:250, Dako, High Wycombe, UK), platelet-endothelial cell adhesion molecule (PECAM) (CD31) monoclonal (mAb) (1:150, Pharmingen, San Diego, CA). Free floating sections stored in PBS were mounted on Superfrost Plus microscope slides (Erie Scientific Co., Portsmouth, NH) and allowed to dry overnight. The slides were then placed in 5% goat serum, 5% BSA, and 0.3% Triton X-100 (Sigma) for 2 hours at room temperature. Sections were incubated with primary antibodies overnight at 4°C followed by fluorescent labeling with anti-mouse or rabbit Alexa 488 (1:250, Invitrogen) or Cy5 (1:500, Invitrogen) secondary IgG antibodies in blocking buffer. All sections were analyzed using a Zeiss LSM 5 Pascal confocal microscope.

Results

Adult *itg β 8 nestin-cre* and *itg β 8 nescre8* mutants display abnormal gait, urinary dysfunction, and shortened lifespan

Since *itgβ8* null animals die before or shortly after birth, we utilized the conditional *itgβ8* floxed allele to look at phenotypes in adult mutants. Using four different *cre* lines, we made several lines of adult *itgβ8* mutants and examined them weekly for any behavioral abnormalities throughout their life time. Table 4-1 summarizes the findings for the four different *cre* lines used in this study. Of particular interest is the shortened average lifespan of the *itgβ8 nestin-cre* mutants and the *itgβ8 nescre8* mutants of approximately twenty-two weeks and thirteen weeks, respectively. In addition to shorted lifespan, both of these mutants developed an abnormal gait in hind limbs on average nine and six weeks after birth, respectively (Table 4-1; Fig. 4-1B, C). Some animals dragged one or the other hind leg while walking and some animals toe-walked, keeping their backs arched elevating their torso off of the bottom of the cage. All of the mutant animals generated using these two *cre* lines developed severe urinary dysfunction as well (Table 4-1). In males, the penis became permanently distended, potentially indicating that fluid was unable to exit the urethra. Support for this hypothesis comes from the observation, upon dissection, that the bladders of these animals were massively enlarged and filled with urine. The impaired ability to urinate most likely resulted in a debilitating amount of pain that may have adversely affected their gait. Additionally, this urinary dysfunction lead to infection and most likely contributed to the premature death of these mutants.

Expression analysis of *cre* in the *nescre8* line

Although the phenotypes of the *itgβ8 nestin-cre* mutants and *itgβ8 nescre8* mutants were largely identical, we wanted to understand why the *itgβ8 nescre8* mutants have an earlier time of onset of the hind limb phenotype and a shorter lifespan compared

to the *itgβ8 nestin-cre* mutants. The *nescr8* transgenic line uses both the neural and muscle enhancer elements of the *nestin* promoter to drive *cre* (Petersen et al., 2002). To understand its recombination pattern in more detail, we crossed the *nescr8* line to the *R26R* reporter strain carrying a floxed stop allele of *lacZ* (Soriano, 1999). At P0, *cre* activity was very strong and widespread in the brain (see Fig. 3-1A in Chapter 3) and spinal cord (Fig. 4-2A). It was also very strong in the dorsal root ganglion (Fig. 4-2B). Most muscle was also stained strongly for LacZ although the heart and lungs seemed largely unstained in this assay (Fig. 4-2B). The *nestin* neural enhancer element, which drives *cre* expression in both the *nestin-cre* and *nescr8* lines (Tronche et al., 1999; Petersen et al., 2002), is expressed in both neuroepithelial cells within CNS and neurons and Schwann cells within the PNS (Zimmerman et al., 1994). Expression of *cre* in the CNS has been studied in both *cre* lines (Tronche et al., 1999; Graus-Porta et al., 2001; Petersen et al., 2002). The main difference appears to be the time of onset of *cre* expression. The *nestin-cre* line drives *cre* expression as early as E10.5 (Graus-Porta et al., 2001) whereas the *nescr8* line drives *cre* expression beginning two days earlier at E8.5 (Petersen et al., 2002). In the PNS, both *cre* lines have been shown to recombine dorsal root ganglia [*nescr8* current study; *nestin-cre* (Schwander et al., 2004)]. Thus, in addition to their time of onset, the primary difference between these *cre* lines is the recombination of muscle in the *nescr8* line [current study and (Petersen et al., 2002)]. These differences are a reflection of the fact that only the neural enhancer element is used to drive *cre* expression in the *nestin-cre* line (Tronche et al., 1999) whereas the entire *nestin* promoter is used to drive *cre* in the *nescr8* line (Petersen et al., 2002).

It is possible, then, that the earlier time of onset of the hind limb locomotion deficit, the urinary dysfunction, and the shorter lifespan observed in the *itgβ8 nescre8* mutants compared to the *itgβ8 nestin-cre* mutants may be due to earlier loss of *itgβ8* from neuroepithelial cells within the CNS and PNS in these mutants. In addition, since weak expression of *itgβ8* has been identified in skeletal muscle (Moyle et al., 1991), loss of *itgβ8* from the muscle in *itgβ8 nescre8* mutants may have contributed to the earlier onset of these phenotypes.

Loss of *itgβ8* from post-mitotic neurons, oligodendrocytes, or motor neurons does not result in behavioral abnormalities or shortened lifespan

To test the hypothesis that *itgβ8* is required in the adult CNS for normal function of the hind legs and urinary tract, we crossed the *itgβ8* floxed allele to two other cre lines to remove *itgβ8* more specifically from populations of cells within the CNS. First, *itgβ8* was ablated from all post-mitotic cortical neurons using *nex-cre* (Beggs et al., 2003; Brockschneider et al., 2004). The *cre* cDNA was inserted, using a knock-in strategy, into the *nex* locus ensuring *nex* cell-specific expression of *cre* (Brockschneider et al., 2004). This gene encodes a basic helix-loop-helix transcription factor and its promoter was used to drive *cre* expression primarily in pyramidal, post-mitotic migrating neurons in the future cortical plate by E11 resulting in robust expression throughout the forebrain by E12.5 (S. Goebbels and K. Nave, unpublished observations). In addition, *nex-cre* expression exhibits little to no mosaicism *in vivo* as determined by *R26R* and *eGFP* reporter analysis [K.A. Nave personal communication and (Wu et al., 2005)]. Mutant animals generated using *nex-cre* did not develop any noticeable defect in hind limb coordination (Fig. 4-1D) or urinary function, and had a normal lifespan compared to

control animals (Table 4-1). Thus, *itgβ8* does not seem to be required in post-mitotic cortical neurons for proper hind limb locomotor activity and urinary function.

Second, *itgβ8* was removed from oligodendrocytes and motor neurons using the *olig1-cre* line (Lu et al., 2002). Expression of *cre* driven by the *olig1* promoter begins at E8.5 (Wu et al., 2006). Robust expression of *cre* in motor neuron precursors occurs by E10.5 and in oligodendrocyte precursors by E12.5 (Lu et al., 2002; Wu et al., 2006). This *cre*-line was used to drive expression of diphtheria toxin in motor neurons and oligodendrocytes which resulted in nearly complete loss of motor neurons and complete loss of oligodendrocytes (Wu et al., 2006) indicating that the *olig1-cre* line may be slightly mosaic in motor neurons. Mutant animals generated using the *olig1-cre* line did not develop any noticeable defect in hind limb coordination (Fig. 4-1E) or urinary function, and had a normal lifespan compared to control animals (Table 4-1).

The cause of the hind limb coordination phenotype observed in the adult *itgβ8 nestin-cre* mutants and *itgβ8 nescre8* mutants could be due to loss of *itgβ8* from either the central nervous system or peripheral nervous system. Sagittal sections of adult *itgβ8 nestin-cre* mutant brains were examined six to ten weeks after birth by Nissl stain (Fig. 4-3 and coronal sections in Chapter 2). Similar to control animals, this mutant showed no sign of cortical or thalamic hemorrhage nor did there appear to be any gross morphological abnormalities in these areas of the brain (Fig. 4-3B). The spinal cord was stained with a fluorescent Nissl, but no gross morphological defects were observed in adult *itgβ8 nestin-cre* mutants (Fig. 4-3D).

Taken together, these data suggest that *itgβ8* is most likely not required post-mitotic neurons, oligodendrocytes, or motor neurons of the CNS for normal gait and

bladder control. While a detailed analysis remains to be completed, it seems plausible that the hind limb coordination, the urinary dysfunction, and the premature death observed in the *nestin-cre* and *nescre8 itgβ8* mutants are a consequence of loss of *itgβ8* from peripheral nerves, or Schwann cells that ensheath those nerves, which innervate those respective areas.

Adult *itgβ8 nestin-cre* mutants display abnormally localized cortical astrocytes

Neonatal *itgβ8 nestin-cre* mutants had abnormally organized astroglial processes [see Chapter 2 and (Proctor et al., 2005)]. To determine whether adult *itgβ8 nestin-cre* mutants had abnormal mature cortical astrocytes, coronal sections of mutant and control brains were stained with GFAP, a well known marker for astrocytes. Compared to control animals, astrocytes in the cortices of mutant animals were broadly dispersed (Fig. 4-4B, D, F; n=2). Additionally, astrocytes in control animals seemed to be localized around blood vessels (Fig. 4-4A) whereas in the mutant the astrocytes were not. This apparent astrocytosis in the adult *itgβ8 nestin-cre* mutants could be a result of persistent leakage of the blood vessels since hemorrhage occurred during embryogenesis. To test this hypothesis, adult animals were perfused with Evan's Blue dye, a small molecule commonly used to determine if the blood-brain barrier is intact. Using confocal microscopy, no excess dye was found in *itgβ8 nestin-cre* mutant brains compared to control brains (Fig. 4-4B-F). It is possible then, that integrin β8 may play a direct role in localization of astrocytes within the adult central nervous system.

Discussion

Using a floxed allele of *itgβ8*, we examined the functions of integrins containing the β8 subunit in the adult CNS and PNS. Targeted deletion of *itgβ8* from all central and

peripheral neuroepithelial cells causes three distinct phenotypes. First, mutant animals develop an abnormal gait six to twelve weeks after birth. Second, mutant animals develop severe urinary dysfunction that may ultimately contribute to their premature death. Lastly, these mutants have abnormally localized astrocytes throughout the brain indicating that integrins containing the $\beta 8$ subunit may function to properly localize these cells in adult cortices. Despite the phenotypes observed when *itg $\beta 8$* is removed from all neuroepithelial precursors, no phenotype was observed in animals in which *itg $\beta 8$* was ablated from post-mitotic cortical neurons, oligodendrocytes or motor neurons. This later result suggests that loss of *itg $\beta 8$* from peripheral neurons and glia, and not central motor neurons or oligodendrocytes, results in abnormal hind limb coordination and urinary dysfunction.

The integrin $\beta 8$ subunit and the adult nervous system

In the adult CNS, integrins play important roles in synapse formation and function (Chavis and Westbrook, 2001; Milner and Campbell, 2002; Wildering et al., 2002). Since the integrin $\beta 8$ subunit has been localized to neuronal synapses and dendrites in the adult rodent CNS (Nishimura et al., 1998) it seemed likely that it would have important functions in the adult brain. However, when *itg $\beta 8$* was removed from post-mitotic cortical neurons no behavioral phenotype was observed. Similarly, no behavioral phenotypes were observed in mutants from which *itg $\beta 8$* had been removed from oligodendrocytes or motor neurons of the CNS. When *itg $\beta 8$* was removed from neuroepithelial cells in both the CNS and PNS, however, mutant animals developed an abnormal gait (Fig. 4-1), urinary dysfunction, abnormally localized cortical astrocytes (Fig. 4-4), and died prematurely (Table 4-1). It is interesting that cortical astrocytes in

this mutant are broadly distributed throughout the cortex since $\alpha\text{v}\beta\text{8}$ is thought to function during astrocyte migration (Milner et al., 1999). Perhaps, rather than functioning during migration, $\alpha\text{v}\beta\text{8}$ functions to target astrocytes to appropriate locations within the CNS. The other possibility is that these are reactive astrocytes responding to persistent leakage of the vasculature in the brains of these mutants. However, when perfused with Evan's Blue dye, no defect in BBB permeability was observed (Fig. 4-4). However, to thoroughly eliminate this possibility, other markers for reactive astrocytes such as vimentin, will need to be assayed in these mutants.

Since no abnormalities resulted from ablation of *itg β8* from CNS cortical neurons, oligodendrocytes, or motor neurons it seems likely that the abnormalities observed in the *itg β8 nestin-cre* and *nescre8* mutants were a result of loss of *itg β8* from neurons and glia in the peripheral nervous system. In the PNS there is evidence that integrins regulate glial cell proliferation, migration, differentiation, and myelination (Previtali et al., 2001). Specifically the beta subunits, such as integrin β1 , are necessary for the proper myelination of dorsal root ganglion neurons by Schwann cells (Feltri et al., 2002). In the case of the integrin $\alpha\text{v}\beta\text{8}$, Schwann cells express the integrin during the migration that occurs with growing axons (Milner et al., 1997b). Perhaps loss of $\alpha\text{v}\beta\text{8}$ from Schwann cells in the PNS results in axons that are unable to appropriately conduct electrical signals to muscles that control bladder function and hind limb coordination. Further analysis of these cells in these mutants will be required to test this possibility.

Comparison of *itg β8 nestin-cre* mutants to conditional *itgav nestin-cre* mutants

Since neither the *itgav* or *itg β8* null animals survive long after birth, use of the floxed *itg β8* allele has enabled investigation of the postnatal functions of β8 . To date,

both floxed alleles of *itgβ8* and *itgav* have been crossed to *nestin-cre* to investigate potential roles for these integrin subunits in the adult animal [present study and (McCarty et al., 2005)]. Both mutants derived from the *nestin-cre* cross developed abnormal gait in the hind limbs six to twelve weeks after birth. Similarly, both mutants develop severe urinary dysfunction that lead to infection and early death of these animals. Lastly, both mutants also have broadly distributed astrocytes throughout the cortex. In their recent study of *itgav* in the adult nervous system, McCarty et al., (2005) attributed the hind limb defect to motor neuron degeneration and demyelination in the spinal cord and cerebellum. While our study of *itgβ8* did not test this directly, the evidence presented here argues against their hypothesis since removal of *itgβ8* from motor neurons and oligodendrocytes using *olig1-cre* did not result in hind limb or other deficits of any kind. Rather, this data suggests the possibility that removal of *itgβ8* from PNS sensory ganglia using *nestin-cre* is more likely the cause of the abnormal gait and urinary dysfunction observed in these mutants. Support for this hypothesis comes from our observation that some of these mutants toe-walk and elevate their torso, preventing their bellies from contacting the bottom of the cage. This suggests that these animals are enduring significant amounts of pain associated with the enlarged bladder and urinary dysfunction. Thus, it is possible that the gait defect observed in these mutants is a secondary consequence of severe pain resulting from the inability of these animals to voluntarily urinate. Therefore, *itgβ8* may be particularly important in the parasympathetic and/or sympathetic nerves that innervate the pelvic ganglion which controls the muscles of the bladder.

Integrin $\alpha v \beta 8$ regulation of astrocyte localization

The phenotypes of the *itgβ8* and *itgav nestin-cre* mutants are essentially identical. In the central nervous system, neither mutant appears to have any cortical layering defect, but both animals have an abnormal number and abnormally localized GFAP positive cortical astrocytes. Several extracellular matrix molecules have been proposed as ligands for $\alpha\text{v}\beta 8$ (please refer to Chapter 1 for a complete discussion of these molecules), but only vitronectin and TGF- β 1 are known to promote migration and adhesion, respectively, via this integrin *in vitro* (Nishimura et al., 1994; Mu et al., 2002). While vitronectin deficient mice have no known phenotype (Zheng et al., 1995), TGF- β 1 deficient mice have smaller cerebral cortices associated with increased neuronal death and concomitant microgliosis (Brionne et al., 2003). While microglial activation was not assayed in either the *itgav* or *itgβ8 nestin-cre* mutants, the microgliosis observed in the TGF- β 1 deficient mice is distinct from the astrocytosis observed in *itgβ8* and *itgav nestin-cre* mutants. Microglial cells are F4/80-positive, but GFAP-negative cells that infiltrate areas of degenerating cells within the brain. When the authors looked at GFAP positive astrocytes, they saw no increase in number or abnormal distribution of these cells in TGF- β 1 deficient mutants (Brionne et al., 2003). Together, these data suggest that $\alpha\text{v}\beta 8$ is required for proper astrocyte distribution and/or localization *in vivo* and that the cortical astrocytosis observed in the *itgβ8* and *itgav nestin-cre* mutants is most likely not a result of deficient signaling through TGF- β 1.

Summary

The current study defines a role for *itgβ8* in the adult nervous system. While this study raises more questions than it answers about the cellular and molecular mechanisms that underlie its role in the adult nervous system, it does underscore the importance of

itgβ8 beyond proper vascular development of the brain. It demonstrates that *itgβ8* is required for the healthy function of nervous system throughout the life of the animal and that it is ultimately required for normal lifespan in mammals. Our data indicate that the primary defect in these animals, in terms of the defective motor coordination and bladder function, is not within the central nervous system, but in the ganglia of the peripheral nervous system. This contradicts the results and hypotheses put forth for the *itgav nestin-cre* mutants (McCarty et al., 2005). Sorting out where the primary defect lies in these adult mutants will be critical to understanding the role of the integrin $\alpha\beta8$ in the adult animal. First, it will be important to understand which of the peripheral ganglia and which motor neurons express *itgβ8*. This experiment will be particularly difficult until a reliable antibody that recognizes the $\beta8$ subunit is made and optimized for immunohistochemistry. Next it will be important to understand the biochemical and morphological changes that occur within the ganglia and motor neurons as a result of loss of *itgβ8*. Hopefully, by gaining a better understanding of the distribution of the $\alpha\beta8$ integrin within both the peripheral nervous system and central nervous system, we will gain a more thorough understanding of how this integrin functions in regulating motor coordination, proper bladder function and cortical astrocyte localization.

Cre Line used to generate <i>itgβ8</i> mutants	Number of Animals in study (n)	Average Age of Hind limb Phenotype Onset (Weeks)	Average Life Span (Weeks)	Phenotype UDI=Urinary Dysfunction and Infection
Nestin-Cre	5	9	22	UDI-Dragging Hind Limbs
NesCre8	5	6	13	UDI-Dragging Hind Limbs
NEX-Cre	5	N/A	>55	None
Olig-1 Cre	5	N/A	>55	None
Control	7	N/A	>55	None

Table 4-1. Age of onset of phenotypes identified during adulthood and lifespan of conditional *itgβ8* mutants generated using various cre lines.

itgβ8 was deleted from mutant animals using *nestin-cre*, *nescre8*, *nex-cre*, or *olig1-cre* and allowed to survive as long as possible. Animals with *itgβ8* deleted from cells expressing *nestin-cre* or *nescre8* displayed multiple phenotypes. All of these mutants developed hind limb coordination and movement problems. They would toe-walk and/or drag their hind limbs. Additionally, all *nestin-cre* and *nescre8* developed dysfunctional bladder control and eventually died due, most likely, to severe bladder infections. These phenotypes began appearing on average after approximately nine weeks in the *itgβ8 nestin-cre* mutants and after, on average, only six weeks in the *itgβ8 nescre8* mutants. Dissection, after the death of these mutants, revealed bladders in these mutants that were massively enlarged and filled with an abnormally large volume of urine compared to control littermates. The *itgβ8 nestin-cre* mutants and the *itgβ8 nescre8* mutants lived approximately twenty-two and thirteen weeks, respectively. By contrast, mutant animals lacking *itgβ8* due to deletion by *olig1-cre* or *nex-cre* did not display these abnormal phenotypes or any other discernable phenotype. They had a normal lifespan compared to controls.

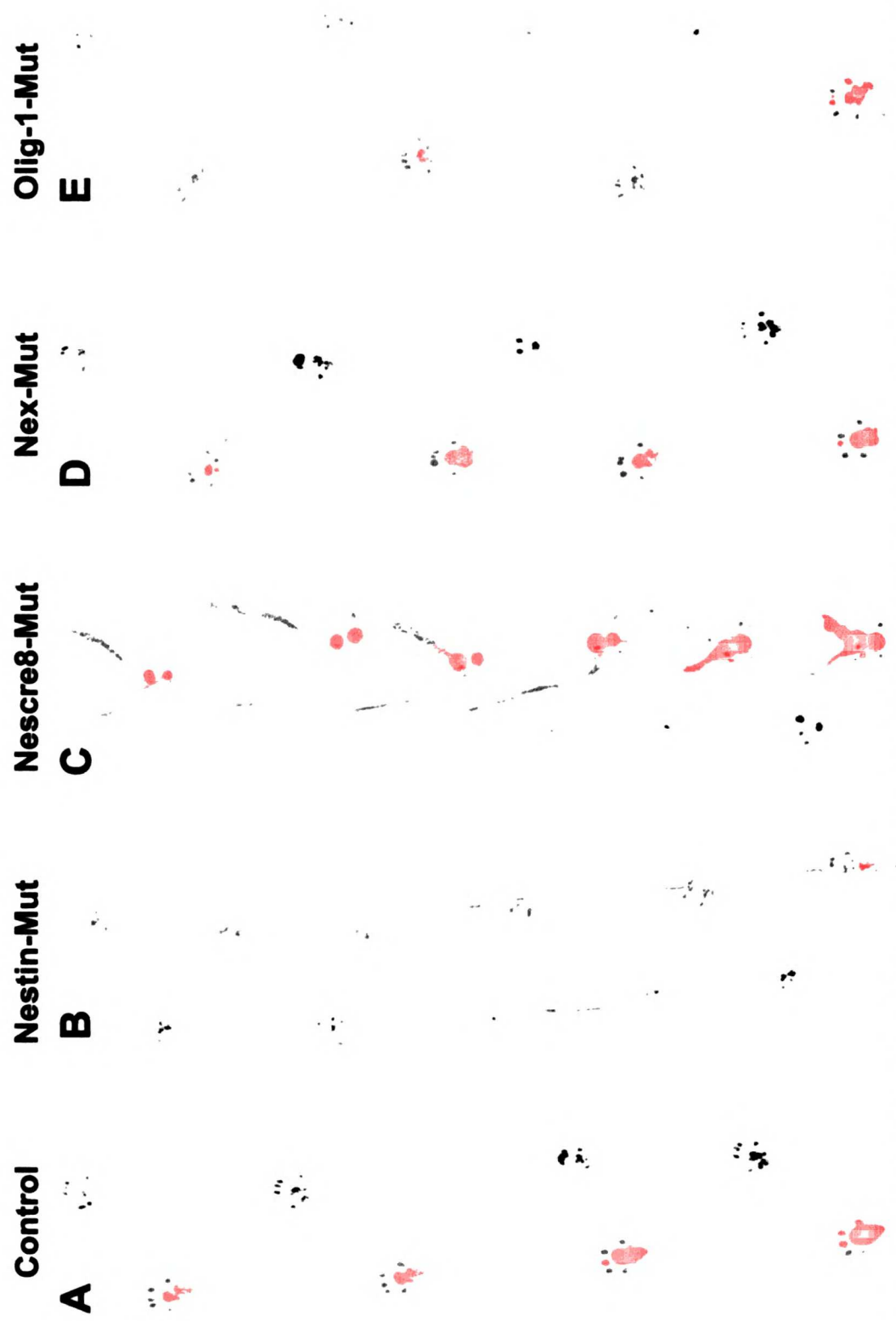


Figure 4-1. Adult *itgβ8 nestin-cre* mutants and the *itgβ8 nescr8* mutants display abnormal hindlimb coordination during locomotor activity.

Figure 4-1. Adult *itgβ8 nestin-cre* mutants and the *itgβ8 nescre8* mutants display abnormal hind limb coordination during locomotor activity.

The hind feet of adult animals (at least 10 weeks of age) were dipped in either red or black ink and each animal was placed in a tube that was dark at one end. The bottom of the tube contained white Whatman paper that the animal was required to walk across to reach the dark end of the tube. Once at the dark end of the tube the paper was removed and photographed. *A*, footprints from a control animal. *B*, footprints from a *nestin-cre* mutant. Notice the obvious dragging of the right hind limb. *C*, footprints from a *nescre8* mutant. Notice the obvious dragging of the right hind limb and toe-walking of the left hind foot. *D*, footprints from a *nex-cre* mutant. *E*, footprints from an *olig1-cre* mutant. Note the normal gaits in *D* and *E*.

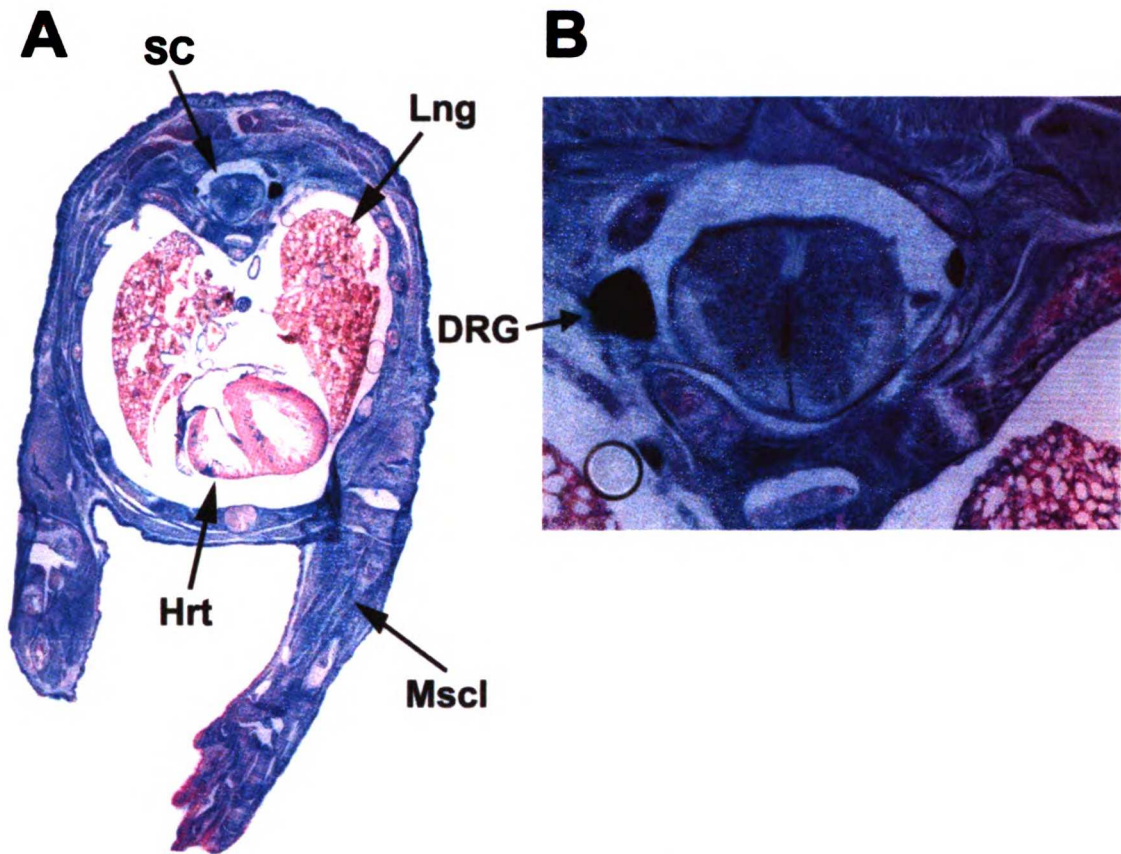


Figure 4-2. *R26R* reporter analysis of the *nescre8* transgenic mouse line.

A, LacZ stained cross section of a P0 animal at the level of the heart and lungs.

Cre mediated recombination at P0 is not limited to the brain. Muscle is also strongly recombined. *B*, Expanded view of the area around the spinal cord in *A*

to demonstrate LacZ staining in the dorsal root ganglion. SC, spinal cord;

Lng, lung; Hrt, heart; Mscl, muscle; DRG, dorsal root ganglion.

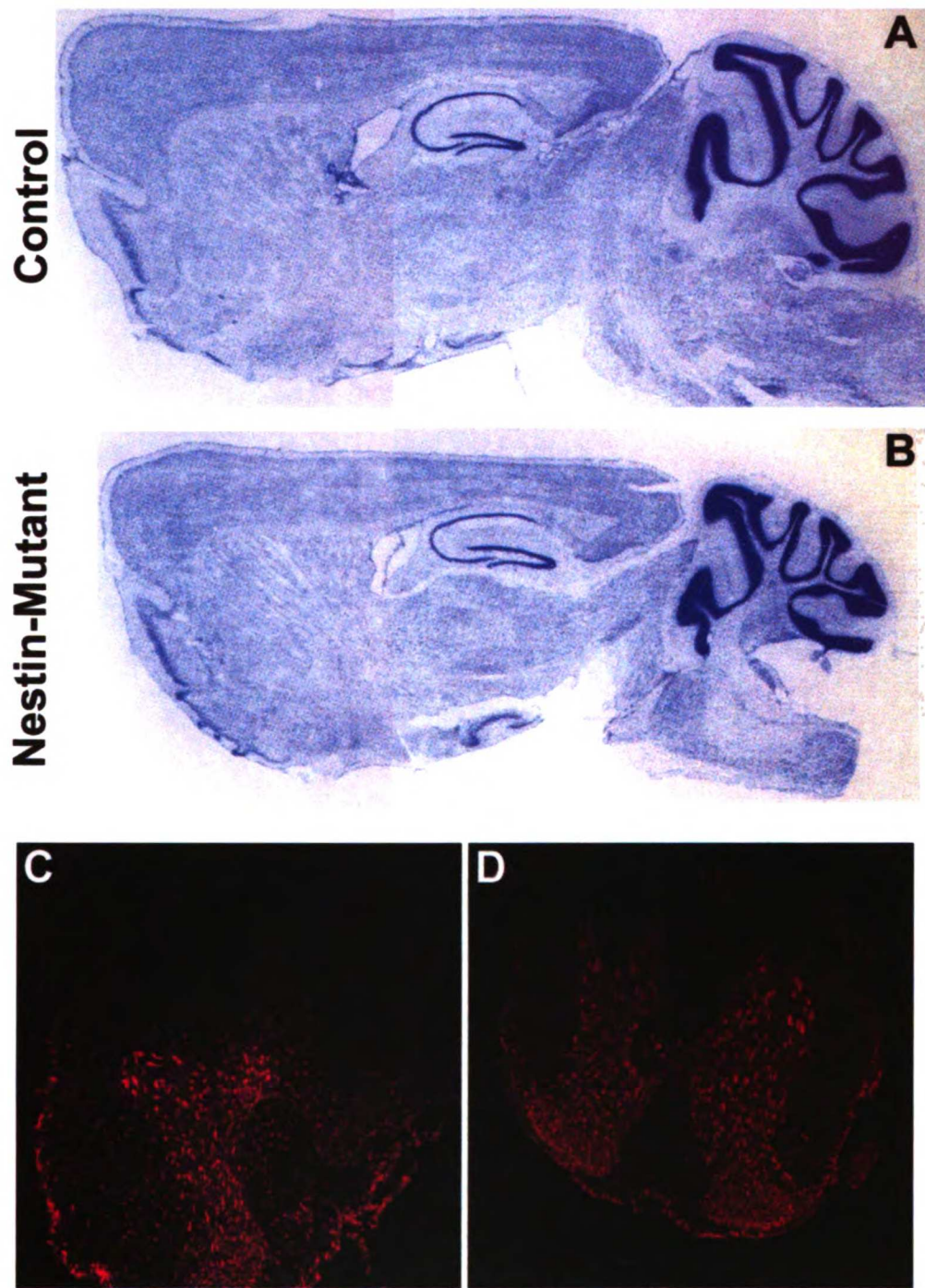


Figure 4-3. Adult *itgβ8 nestin-cre* mutants show no sign of brain hemorrhage.

Figure 4-3. Adult *itgβ8 nestin-cre* mutants show no sign of brain hemorrhage.

A, six-week old control *B*, six-week old *nestin-cre* targeted mutant saggital sections stained with Nissl. Note lack of hemorrhage or other obvious defect in the cortex, thalamus, cerebellum, or brainstem. *C*, six-week old control *D*, six-week old *nestin-cre* targeted mutant coronal spinal cord sections. Note the lack of any obvious morphological abnormality.

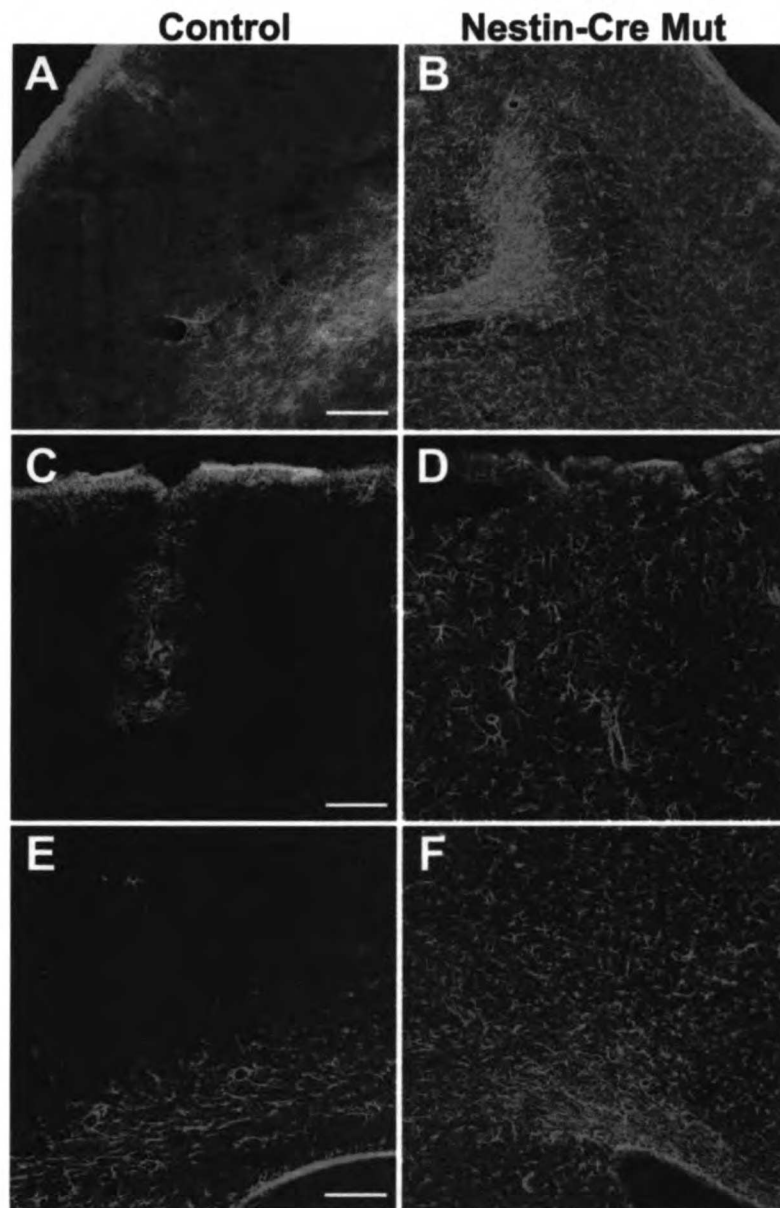


Figure 4-4. Adult *itgβ8 nestin-cre* mutants have abnormally organized cortical astrocytes, but do not have leaky blood vessels.

Figure 4-4. Adult *itgβ8 nestin-cre* mutants have abnormally organized cortical astrocytes, but do not have leaky blood vessels.

Anti-GFAP and PECAM immunostaining of glia and endothelial cells and, respectively, in adult coronal sections of dorsal forebrains. *A*, control cortical section in an area near the pial surface with astrocytes stained with GFAP (green). Notice the restriction of astrocytes to the thalamo-cortical tract and blood vessels near the pial surface. *B*, *nestin-cre* mutant section in an area near the pial surface with astrocytes stained with GFAP. Notice the broad distribution of these cells throughout the cortex. *C*, control cortical section in an area near the pial surface showing the close association of astrocytes [labeled with GFAP(green)]with blood vessels [labeled with PECAM (blue)]; *D*, *nestin-cre* mutant. Notice the astrocytes do not seem to be organized around blood vessels as in control. Rather, they are broadly dispersed. *E*, control cortical area near the lateral ventricle. Notice that astrocytes are limited to the thalamo-cortical tract. *F*, *nestin-cre* targeted mutant. Notice the widespread presence of astrocytes. Brains in C-F were perfused with Evan's Blue dye which appears red in fluorescent analysis. Notice the lack of red staining in either the control or *nestin-cre* mutant sections indicating an intact vascular system in these adult animals. Scale bar: A, E, 50 μm; C, 100 μm.

Chapter 5

Discussion, Final Summary, and Future Perspectives

Discussion

Integrins are a family of extracellular adhesion molecules that function during the most fundamental cell-biological processes. They mediate stable adhesion of cells to their substrate by providing a physical link between the extracellular matrix (ECM) and the cytoskeleton (Hynes, 1992). Integrins also act as signaling receptors that relay information about the substrate to the interior of the cell, which the cell can interpret as growth, motility, differentiation, or survival signals (Giancotti and Ruoslahti, 1999; Miranti and Brugge, 2002). Lastly, integrins contribute to most, if not all, of the morphogenetic events that shape a developing multicellular organism (Gumbiner, 1996; Bokel and Brown, 2002). It is no surprise, then, that integrins are present and conserved in all metazoans (Hynes and Zhao, 2000). It should also be as no surprise that mutations in many of the integrin genes result in embryonic or perinatal lethality (De Arcangelis and Georges-Labouesse, 2000; Bouvard et al., 2001).

Only integrins containing either the αv or the $\beta 8$ subunits have been shown to be required for vascular development of the murine placenta, yolk sac, and central nervous system (Bader et al., 1998; McCarty et al., 2002; Zhu et al., 2002). What's more, loss of the integrin $\beta 8$ subunit results in hyperproliferative endothelial cells and hemorrhage within the cerebral cortices of the brain. This endothelial cell phenotype indicated that $\alpha v\beta 8$ may be expressed directly on endothelial cells, but *in situ* analysis suggested it is only expressed on neuroepithelial cells (Zhu et al., 2002). While it is known that the $\alpha v\beta 8$ integrin can putatively bind ligands containing an Arginine-Glycine-Aspartate (RGD) tri-peptide motif *in vitro* (Nishimura et al., 1994), which ligand it is binding in the during brain development is unclear. Moreover, the integrin $\beta 8$ subunit's cytoplasmic

domain shares little homology with other known β subunits (Moyle et al., 1991), leaving many to wonder whether integrins containing the $\beta 8$ subunit functions using canonical integrin signaling pathways.

It was with these questions and insights in mind that I began my thesis. Specifically, I wanted to know three things: 1) In which cell(s) of the CNS is the *integrin $\beta 8$* (*itg $\beta 8$*) subunit required for normal vascular development of the brain? 2) What ligand(s) does $\alpha v\beta 8$ bind in the brain and which pathway(s) does $\alpha v\beta 8$ activate during CNS vascular development? 3) Does the $\alpha v\beta 8$ integrin have any function in the adult animal? Before I summarize and discuss my progress toward answering these questions, I would like to review what we currently know about vascular development of the central nervous system.

CNS Vascular Development

In the mouse, a perineural vascular plexus (PNVP) forms within the meningeal layer surrounding the neural tube between E8.5 and E10.5 (Nakao et al., 1988). Capillary sprouts from the PNVP penetrate the external limiting membrane of the neuroectoderm between E9.5 and E10.5 and grow radially (perpendicular to the pial surface) toward the ventricle (Bar, 1983; Marin-Padilla, 1985; Ruhrberg et al., 2002). During this migration, a specialized cell called the tip cell, guides the elongating capillary along radial glial processes toward the subventricular zone (Gerhardt et al., 2003; Gerhardt et al., 2004). When these radially penetrating vessels reach the subventricular zone of the neuroepithelium, they branch laterally and fuse together forming a primary capillary plexus (Bar, 1983; Ruhrberg et al., 2002). This subventricular zone plexus of capillaries connected by radial vessels to the pia-meningial circulation forms the basic vascular

framework of the central nervous system. This basic plexus is modified throughout development to accommodate the rapidly growing CNS. The increase in surface area of the cerebral cortex induces additional sprouts from the PNVP to penetrate and grow into the neuroepithelium (Bar, 1983). Furthermore, as the volume of the brain increases, the radial vessels elongate and branch laterally to expand the original plexus formed within the subventricular zone (Bar, 1983; Yu et al., 1994; Gerhardt et al., 2004). Branching occurs when opposed radial vessels send out filopodial extensions that make contact and fuse (Gerhardt et al., 2003; Gerhardt et al., 2004). These lateral branches form within the individual layers of the cortex as they emerge from the cortical plate (Yu et al., 1994) creating a very regular vascular plexus that extends from the pial surface to the ventricle. Thus, the inside-out pattern of capillary development ensures that the proliferative areas of the CNS are properly perfused with trophic factors and essential nutrients.

Vascular endothelial cells line the luminal space of all blood vessels and compartmentalize the systemic circulation of blood flow. Most blood vessel inter-endothelial cell junctions are highly permeable and non-selectively allow diffusion of ions, peptides, and macromolecules into the organs through which they transverse. However, the CNS is unique in that a distinctive structure, known as the blood-brain-barrier (BBB) is formed to protect the brain microenvironment from molecules and ions present in the blood stream and to prevent potent hormones, growth factors, and other molecules from exiting the CNS and affecting peripheral tissues [reviewed in (Abbott and Romero, 1996; Engelhardt, 2003)]. During CNS development, the inter-endothelial cell junctions become more extensive, interconnected (Kniesel et al., 1996), and the outer leaflets of adjacent membranes within the junctional contacts fuse (Schulze and Firth,

1992). As endothelial cells invade the neuroectoderm, they come into close contact with neuroepithelial cells, radial glia, and astrocytes (Marin-Padilla, 1985; Bass et al., 1992). Interaction with these cells as well as recruitment of pericytes, which are vascular support cells, is required for proper development of the BBB (Lindahl et al., 1997; Bauer and Bauer, 2000). In fact, the mature BBB is composed of a complex cellular system of highly specialized (differentiated) endothelial cells in close association with a large number of pericytes and astrocytic endfeet [reviewed in (Engelhardt, 2003; Nedergaard et al., 2003)].

Many molecules have been characterized during the processes of angiogenesis and BBB formation. Vascular endothelial growth factor (VEGF) is critical to the initial steps in capillary plexus formation. Tip cells of the invading endothelium enter epithelial tissues by detecting a gradient of VEGF expressed and secreted within the epithelia (Leung et al., 1989; Ruhrberg et al., 2002; Gerhardt et al., 2003). To accomplish this, endothelial cells express the VEGFR-1 and VEGFR-2 receptors which can bind all three isoforms of VEGF-A (VEGF₁₂₁, VEGF₁₆₅, VEGF₁₈₉ in humans and VEGF₁₂₀, VEGF₁₆₄, VEGF₁₈₈ in mice). In addition, they also express neuropilin (Nrp) which specifically binds the VEGF₁₆₅ isoform (Soker et al., 1998). The gradient of VEGF within epithelial tissues is produced through the differing affinities of these isoforms for the ECM. VEGF₁₂₁ is freely diffusible and thus acts over long ranges. VEGF₁₆₅ has an intermediate affinity for the ECM and therefore an intermediate diffusion profile while VEGF₁₈₉ is fully bound to the ECM and acts only over a short range (Ruhrberg et al., 2002; Gerhardt et al., 2003). VEGF has functions in addition to tip cell guidance. The stalk cells that are immediately behind the tip cell proliferate as the tip cell navigates to its target (Gerhardt

et al., 2003). Thus, while VEGF appears to be a guidance cue for the tip cell, it functions primarily as a proliferative cue for these stalk cells (Gerhardt et al., 2003). Lastly, while VEGF seems to have a primarily attractive role during endothelial cell guidance, molecules within the ephrin (Eph) family function as repulsive cues for endothelial cells (Oike et al., 2002) and regulate arterial and venous fate decisions made by endothelial cells throughout development (Wang et al., 1998; Adams et al., 1999; Wang et al., 2004).

In addition to the molecules that function during endothelial cell guidance, there are several other molecules that play important roles during angiogenesis. Several excellent reviews have been written on the subject, [please see (Engelhardt, 2003; Carmeliet and Tessier-Lavigne, 2005; Coultas et al., 2005; Eichmann et al., 2005)], but I would like to mention a few that play critical roles in the processes described above.

After the primary plexus is formed, the angiopoietins, their Tie receptor tyrosine kinases as well as members of the Notch signaling pathway are important for vessel remodeling and differentiation (Krebs et al., 2000; Thurston, 2003). Transforming growth factor β (TGF- β) has many functions that include inhibition and stimulation of endothelial cell motility and proliferation (Goumans et al., 2002; Goumans et al., 2003) and control pericyte and smooth-muscle cell proliferation and differentiation (Betsholtz et al., 2005; Lebrin et al., 2005). The platelet derived growth factor B (PDGF-B) and its receptor is known to be required for recruitment of pericytes (Lindahl et al., 1997; Lindblom et al., 2003) and the proteins claudin-3 and claudin-5 are responsible for establishing the tight junctions between brain endothelial cells (Furuse et al., 1999; Morita et al., 1999) that are primarily responsible for the barrier function of the BBB. Lastly, the integrin family of

adhesion receptors plays very specific roles throughout the process of angiogenesis that I will discuss below.

Integrins are potent regulators of angiogenesis in several different contexts. Loss of the integrin $\alpha 5\beta 1$, a fibronectin receptor, causes severe vascular abnormalities and various mesodermal defects resulting in early embryonic lethality in mice (Yang et al., 1993). Two collagen receptors, $\alpha 1\beta 1$ $\alpha 2\beta 1$, are known to promote tumor angiogenesis (Senger et al., 1997). In tumor and retinal assays *in vitro*, inhibitors of $\alpha v\beta 3$ and $\alpha v\beta 5$ integrins expressed on endothelial cells inhibit angiogenesis (Brooks et al., 1994; Friedlander et al., 1995; Friedlander et al., 1996). However, loss of these two integrins *in vivo* has been shown to actually enhance angiogenesis (Reynolds et al., 2002) prompting some to hypothesize that αv integrins are in fact negative regulators of angiogenesis (Hynes, 2002). Interestingly, no vascular defects were observed in *itg\beta 3/itg\beta 5* double knockout mice, *itg\beta 6* mutants (Huang et al., 1996; McCarty et al., 2002) or mice lacking *itg\beta 1* in neuroepithelial cells (Graus-Porta et al., 2001). However, this hypothesis may be particularly true for the $\alpha v\beta 8$ integrin. Loss of either the αv or $\beta 8$ subunits results in abnormal proper capillary development within the CNS, placenta, and yolk sac (Bader et al., 1998; McCarty et al., 2002; Zhu et al., 2002). In fact, in the absence of αv or $\beta 8$, endothelial cells of the central nervous system become hyperproliferative and massive cerebral hemorrhages develop during early embryogenesis which may contribute to the neonatal death of these mutant animals (McCarty et al., 2002; Zhu et al., 2002). However, unlike $\alpha v\beta 3$ and $\alpha v\beta 5$ which are expressed exclusively on endothelial cells, $\alpha v\beta 8$ does not appear to be expressed on endothelial cells (Pinkstaff et al., 1999; Zhu et al., 2002). Therefore, it is possible that via a cell non-cell autonomous mechanism, $\alpha v\beta 8$

expressed on neuroepithelial cells negatively regulates endothelial cell proliferation and morphogenesis during vascular development of the brain.

Summary of Chapters

To define the cell types in which the *itgβ8* is required for normal vascular development of the brain, we generated a floxed allele of *itgβ8* (Chapter 2). We demonstrated that targeted deletion of *itgβ8* from the embryonic neuroepithelium causes abnormal vascular development resulting in cerebral hemorrhage. Importantly, we also showed that ablation of *itgβ8* from embryonic endothelial cells does not result in abnormal development of brain vasculature. To more specifically define the neuroepithelial cell type in which *itgβ8* is required for normal vascular development of the brain, we removed *itgβ8* from post-mitotic cortical neurons. However, no cerebral hemorrhages were observed in these mutants. Therefore, we deduced that expression of integrins containing the β8 subunit is required on non-neuronal cells within the neuroepithelium for proper blood vessel development in the CNS. Neuroepithelial derived astroglia lacking *itgβ8* are disorganized, particularly in relation to the vasculature within the forebrain. Thus, we concluded that *itgβ8* is most likely required in glia for normal vascular development of the brain. These findings complement earlier work on *itgβ8* null mice, and further defined the cell types that must express β8 within the CNS to promote normal vascular development during embryogenesis. In addition, we observed no hemorrhages in adult animals lacking *itgβ8* in cells generated within the neuroepithelium. This result indicated to us that *itgβ8* is not required postnatally for proper cerebral blood vessel function.

In Chapter 3, we performed a genome-wide microarray analysis of E12.5 mutant forebrains lacking *itgβ8* in the neuroepithelium in order to understand the signaling molecules through which the integrin $\alpha\beta8$ may control vascular morphogenesis in the CNS. Unfortunately, using this assay we did not identify any genes that were differentially expressed in the *itgβ8* mutants compared to controls. We discuss, however, current evidence that implicates several molecules to function in a pathway with the $\alpha\beta8$ integrin. First, there is evidence to suggest a model in the brain in which $\alpha\beta8$ binds LAP- $\beta1$ within the basal lamina between glial cells and endothelial cells, and through interaction with a MMP, liberates soluble TGF- $\beta1$. TGF- $\beta1$ could then interact cell non-autonomously with neighboring endothelial cells to activate pathways that would inhibit their proliferation and/or migration. This is an interesting model since a hallmark feature of loss of *itgβ8* from neuroepithelial cells is hyperproliferative endothelial cells (Zhu et al., 2002; Proctor et al., 2005). In addition, in co-culture with human astrocytes, immortalized mouse endothelial cells up-regulate the anti-angiogenic genes plasminogen activator inhibitor-1 (*PAI-1*) and thrombospondin-1 (*TSP-1*) (Cambier et al., 2005). These observations provide a potential pathway, centered around TGF- $\beta1$, for $\alpha\beta8$ mediated regulation of endothelial cell proliferation and migration.

A second model suggests that through possible communication with neuropilin-1, a receptor for VEGF₁₆₅, expressed on endothelial cells, $\alpha\beta8$ expressed on glial cells may down regulate expression or secretion of specific isoforms of VEGF, such as VEGF₁₆₅ (a molecule known to regulate endothelial cell proliferation), from those glial cells. Thus through coordinated communication with neuropilin-1, $\alpha\beta8$ could regulate vascular morphogenesis by inhibiting pathways that promote endothelial cell proliferation. A

third molecule, Krit1, is known to function in integrin associated pathways and mutations in this gene lead to a human disease known as cerebral cavernous malformations (CCM) (Laberge-le Couteulx et al., 1999; Gunel et al., 2002; Marchuk et al., 2003). CCM patients develop CNS hemorrhage characterized by tortuous blood vessels devoid of surrounding brain parenchyma (Marchuk et al., 2003) similar to those observed in $\text{itg}\beta 8$ mutants (Zhu et al., 2002; Proctor et al., 2005).

Lastly, two other molecules may function with the $\alpha\text{v}\beta 8$ integrin to regulate vascular development of the brain. One protein, called Band 4.1B, was recently shown to bind the cytoplasmic tail of the integrin $\beta 8$ subunit (McCarty et al., 2005a). While the functional consequence of this interaction is yet to be determined, it is possible that Band 4.1B functions as a down-stream signaling component in an $\alpha\text{v}\beta 8$ mediated signaling pathway. Alternatively, it may function to activate this integrin and facilitate $\alpha\text{v}\beta 8$ mediated adhesion to the extracellular matrix between astroglial processes and the endothelial cells within the neuroepithelium. This possibility is less likely since $\alpha\text{v}\beta 8$ integrin is thought to be constitutively active (Januzzi et al., 2004). Moreover, this protein is not required for normal development (Yi et al., 2005). The second molecule is the Rho GDP dissociation inhibitor-1 (Rho GDI), which was identified in kidney mesangial cells to bind the cytoplasmic tail of the integrin $\beta 8$ subunit (S. Lakhe-Reddy and J.R. Schelling, submitted to Journal of Biological Chemistry). It was proposed that the interaction between Rho GDI and the cytoplasmic tail of the integrin $\beta 8$ subunit permitted activation of the small G-protein Rac1 by a guanine exchange factor since the Rho GDI would be bound and unable to inhibit Rac1 activation. However, it is unclear how this mechanism may function to regulate endothelial cell proliferation within the

neuroepithelium. Further experiments will be required to test whether these candidates are up or down-regulated in the *itgβ8* mutants.

In the adult CNS, integrins play important roles in synapse formation and function (Chavis and Westbrook, 2001; Milner and Campbell, 2002; Wildering et al., 2002).

Since the integrin β8 subunit has been localized to neuronal synapses and dendrites in the adult rodent CNS (Nishimura et al., 1998) it seemed likely that it would have important functions in the adult brain. In Chapter 4, we used our floxed allele of *itgβ8* to examine the functions of integrins containing the β8 subunit in the adult CNS and PNS. Targeted deletion of *itgβ8* from all central and peripheral neuroepithelial cells results in dramatically reduced lifespan and three distinct phenotypes. First, mutant animals develop an abnormal gait six to twelve weeks after birth. Second, mutant animals develop severe urinary dysfunction that ultimately results in severe infection. While the urinary dysfunction, per se, may not have caused the premature death of these mutants, the resulting infection may have contributed to their shorted lifespan. Lastly, these mutants have abnormally localized astrocytes throughout the brain indicating that integrins containing the β8 subunit may function to properly localize these cells in adult cortices. Despite the phenotypes observed when *itgβ8* is removed from all neuroepithelial precursors, no phenotype was observed in animals in which *itgβ8* was ablated from post-mitotic cortical neurons, oligodendrocytes or motor neurons. This later result suggests that loss of *itgβ8* from peripheral neurons, and not central motor neurons or oligodendrocytes, results in abnormal hind limb coordination and urinary dysfunction.

Future Perspectives

The experiments and studies presented here bring up some important questions that will need to be addressed in future experiments. While our study of *itgβ8* during development has defined the cell type responsible for the endothelial cell abnormalities observed in the *itgβ8* null animals, they did not address the temporal aspect during which vascular development of the brain becomes aberrant in these mutants. It will be important to use confocal or perhaps two-photon microscopy to visualize the precise aspects of the endothelial cell defects in real time. Does $\alpha v\beta 8$ function during the initial invasion of the neuroectoderm? Does $\alpha v\beta 8$ function in vessel branch formation? Does $\alpha v\beta 8$ function during establishment of the blood brain barrier? Understanding the temporal dynamics of precisely when endothelial cell behavior deviates from those of control mice would help us understand the true mechanism of $\alpha v\beta 8$ function in the neuroepithelium. Secondly, while we did not identify any genes which might function together with $\alpha v\beta 8$ integrin in a pathway to regulate vascular development of the brain using our microarray approach, it did demonstrate the need, when using these genome-wide approaches, to specify the most relevant biological samples so that specific questions can be addressed. Thus, in future it will be necessary to perform this microarray analysis separately on neuroepithelial cells that express *itgβ8* and the endothelial cells it regulates in separate experiments. In addition, there are several candidate genes (ie *nrp-1*, *tgf-β*, etc. as described above in the summary of Chapter 3) which can be investigated immediately by real-time quantitative PCR analysis of mRNA collected from specific populations of neuroepithelial or endothelial cells in control and mutant animals' forebrains to determine if there are any changes their expression as a result of loss of *itgβ8*. Lastly, it is now important to gain a better understanding of the

adult phenotypes we have reported here. Our data indicate that the primary defect, in terms of the defective motor coordination and bladder function, in these mutant animals is not within the central nervous system, but in the ganglia of the peripheral nervous system. This contradicts the results and hypotheses put forth for the *itgav nestin-cre* mutants (McCarty et al., 2005). Sorting out where the primary defect lies in these adult mutants will be critical to understanding the role of the integrin $\alpha v \beta 8$ in the adult animal. First, it will be important to understand which of the peripheral ganglia and which motor neurons express *itg $\beta 8$* . This experiment will be particularly difficult until a reliable antibody that recognizes the $\beta 8$ subunit is made and optimized for immunohistochemistry. Next it will be important to understand the biochemical and morphological changes that occur within the ganglia and motor neurons as a result of loss of *itg $\beta 8$* . Most importantly, it is essential now to identify the ligand(s) for $\alpha v \beta 8$ in the different contexts in which it functions. Only then will we have a full understanding of the mechanism by which $\alpha v \beta 8$ functions in vascular development of the brain and motor coordination and astrocyte localization in adult animals. Perhaps we will also gain a better understanding of the reasons this integrin evolved so differently than the other members of this family of cell adhesion molecules.

REFERENCES

- Abbott NJ (2002) Astrocyte-endothelial interactions and blood-brain barrier permeability. *J Anat* 200:629-638.
- Abbott NJ, Romero IA (1996) Transporting therapeutics across the blood-brain barrier. *Mol Med Today* 2:106-113.
- Adair BD, Xiong JP, Maddock C, Goodman SL, Arnaout MA, Yeager M (2005) Three-dimensional EM structure of the ectodomain of integrin $\{\alpha\}V\{\beta\}3$ in a complex with fibronectin. *J Cell Biol* 168:1109-1118.
- Adams RH, Wilkinson GA, Weiss C, Diella F, Gale NW, Deutsch U, Risau W, Klein R (1999) Roles of ephrinB ligands and EphB receptors in cardiovascular development: demarcation of arterial/venous domains, vascular morphogenesis, and sprouting angiogenesis. *Genes Dev* 13:295-306.
- Allison DB, Cui X, Page GP, Sabripour M (2006) Microarray data analysis: from disarray to consolidation and consensus. *Nat Rev Genet* 7:55-65.
- Annes JP, Munger JS, Rifkin DB (2003) Making sense of latent TGFbeta activation. *J Cell Sci* 116:217-224.
- Arnaout MA, Mahalingam B, Xiong JP (2005) Integrin structure, allostery, and bidirectional signaling. *Annu Rev Cell Dev Biol* 21:381-410.
- Bader BL, Rayburn H, Crowley D, Hynes RO (1998) Extensive vasculogenesis, angiogenesis, and organogenesis precede lethality in mice lacking all alpha v integrins. *Cell* 95:507-519.
- Bar T (1983) Patterns of vascularization in the developing cerebral cortex. *Ciba Found Symp* 100:20-36.

- Barczak A, Rodriguez MW, Hanspers K, Koth LL, Tai YC, Bolstad BM, Speed TP, Erle DJ (2003) Spotted long oligonucleotide arrays for human gene expression analysis. *Genome Res* 13:1775-1785.
- Bass T, Singer G, Slusser J, Liuzzi FJ (1992) Radial glial interaction with cerebral germinal matrix capillaries in the fetal baboon. *Exp Neurol* 118:126-132.
- Bauer HC, Bauer H (2000) Neural induction of the blood-brain barrier: still an enigma. *Cell Mol Neurobiol* 20:13-28.
- Beggs HE, Schahin-Reed D, Zang K, Goebbels S, Nave KA, Gorski J, Jones KR, Sretavan D, Reichardt LF (2003) FAK deficiency in cells contributing to the basal lamina results in cortical abnormalities resembling congenital muscular dystrophies. *Neuron* 40:501-514.
- Belot N, Rorive S, Doyen I, Lefranc F, Bruyneel E, Dedecker R, Micik S, Brotchi J, Decaestecker C, Salmon I, Kiss R, Camby I (2001) Molecular characterization of cell substratum attachments in human glial tumors relates to prognostic features. *Glia* 36:375-390.
- Betsholtz C, Lindblom P, Gerhardt H (2005) Role of pericytes in vascular morphogenesis. *Exs*:115-125.
- Bokel C, Brown NH (2002) Integrins in development: moving on, responding to, and sticking to the extracellular matrix. *Dev Cell* 3:311-321.
- Bouvard D, Brakebusch C, Gustafsson E, Aszodi A, Bengtsson T, Berna A, Fassler R (2001) Functional consequences of integrin gene mutations in mice. *Circ Res* 89:211-223.

- Braren R, Hu H, Kim YH, Beggs HE, Reichardt LF, Wang R (2006) Endothelial FAK is essential for vascular network stability, cell survival, and lamellipodial formation. *J Cell Biol* 172:151-162.
- Breier G, Albrecht U, Sterrer S, Risau W (1992) Expression of vascular endothelial growth factor during embryonic angiogenesis and endothelial cell differentiation. *Development* 114:521-532.
- Brionne TC, Tesseur I, Masliah E, Wyss-Coray T (2003) Loss of TGF-beta 1 leads to increased neuronal cell death and microgliosis in mouse brain. *Neuron* 40:1133-1145.
- Brockschneider D, Lappe-Siefke C, Goebbels S, Boesl MR, Nave KA, Riethmacher D (2004) Cell depletion due to diphtheria toxin fragment A after Cre-mediated recombination. *Mol Cell Biol* 24:7636-7642.
- Brooks PC, Montgomery AM, Rosenfeld M, Reisfeld RA, Hu T, Klier G, Chersesh DA (1994) Integrin alpha v beta 3 antagonists promote tumor regression by inducing apoptosis of angiogenic blood vessels. *Cell* 79:1157-1164.
- Burrige K, Chrzanowska-Wodnicka M (1996) Focal adhesions, contractility, and signaling. *Annu Rev Cell Dev Biol* 12:463-518.
- Calderwood DA (2004) Integrin activation. *J Cell Sci* 117:657-666.
- Cambier S, Mu DZ, O'Connell D, Boylen K, Travis W, Liu WH, Broaddus VC, Nishimura SL (2000) A role for the integrin alphavbeta8 in the negative regulation of epithelial cell growth. *Cancer Res* 60:7084-7093.
- Cambier S, Gline S, Mu D, Collins R, Araya J, Dolganov G, Einheber S, Boudreau N, Nishimura SL (2005) Integrin alpha(v)beta8-mediated activation of transforming

- growth factor-beta by perivascular astrocytes: an angiogenic control switch. *Am J Pathol* 166:1883-1894.
- Carmeliet P, Tessier-Lavigne M (2005) Common mechanisms of nerve and blood vessel wiring. *Nature* 436:193-200.
- Chavis P, Westbrook G (2001) Integrins mediate functional pre- and postsynaptic maturation at a hippocampal synapse. *Nature* 411:317-321.
- Cheng SY, Nagane M, Huang HS, Cavenee WK (1997) Intracerebral tumor-associated hemorrhage caused by overexpression of the vascular endothelial growth factor isoforms VEGF121 and VEGF165 but not VEGF189. *Proc Natl Acad Sci U S A* 94:12081-12087.
- Chernousov MA, Carey DJ (2003) α V β 8 integrin is a Schwann cell receptor for fibrin. *Exp Cell Res* 291:514-524.
- Cleveland WS (1979) Robust locally weighted regression and smoothing scatterplots. *JASA* 74:829-836.
- Coultas L, Chawengsaksophak K, Rossant J (2005) Endothelial cells and VEGF in vascular development. *Nature* 438:937-945.
- De Arcangelis A, Georges-Labouesse E (2000) Integrin and ECM functions: roles in vertebrate development. *Trends Genet* 16:389-395.
- Degani S, Balzac F, Brancaccio M, Guazzone S, Retta SF, Silengo L, Eva A, Tarone G (2002) The integrin cytoplasmic domain-associated protein ICAP-1 binds and regulates Rho family GTPases during cell spreading. *J Cell Biol* 156:377-387.
- Denier C, Gasc JM, Chapon F, Domenga V, Lescoat C, Joutel A, Tournier-Lasserre E (2002) *Krit1*/cerebral cavernous malformation 1 mRNA is preferentially

- expressed in neurons and epithelial cells in embryo and adult. *Mech Dev* 117:363-367.
- Dickson MC, Martin JS, Cousins FM, Kulkarni AB, Karlsson S, Akhurst RJ (1995) Defective haematopoiesis and vasculogenesis in transforming growth factor-beta 1 knock out mice. *Development* 121:1845-1854.
- Doetsch F (2003) The glial identity of neural stem cells. *Nat Neurosci* 6:1127-1134.
- Eichmann A, Le Noble F, Autiero M, Carmeliet P (2005) Guidance of vascular and neural network formation. *Curr Opin Neurobiol* 15:108-115.
- Eliceiri BP (2001) Integrin and growth factor receptor crosstalk. *Circ Res* 89:1104-1110.
- Engelhardt B (2003) Development of the blood-brain barrier. *Cell Tissue Res* 314:119-129.
- Fjellbirkeland L, Cambier S, Broaddus VC, Hill A, Brunetta P, Dolganov G, Jablons D, Nishimura SL (2003) Integrin alphavbeta8-mediated activation of transforming growth factor-beta inhibits human airway epithelial proliferation in intact bronchial tissue. *Am J Pathol* 163:533-542.
- Flanders KC, Ludecke G, Engels S, Cissel DS, Roberts AB, Kondaiiah P, Lafyatis R, Sporn MB, Unsicker K (1991) Localization and actions of transforming growth factor-beta s in the embryonic nervous system. *Development* 113:183-191.
- Friedlander M, Brooks PC, Shaffer RW, Kincaid CM, Varner JA, Cheresch DA (1995) Definition of two angiogenic pathways by distinct alpha v integrins. *Science* 270:1500-1502.

- Friedlander M, Theesfeld CL, Sugita M, Fruttiger M, Thomas MA, Chang S, Cheresh DA (1996) Involvement of integrins alpha v beta 3 and alpha v beta 5 in ocular neovascular diseases. *Proc Natl Acad Sci U S A* 93:9764-9769.
- Furuse M, Sasaki H, Tsukita S (1999) Manner of interaction of heterogeneous claudin species within and between tight junction strands. *J Cell Biol* 147:891-903.
- Gentleman RC, Carey VJ, Bates DM, Bolstad B, Dettling M, Dudoit S, Ellis B, Gautier L, Ge Y, Gentry J, Hornik K, Hothorn T, Huber W, Iacus S, Irizarry R, Leisch F, Li C, Maechler M, Rossini AJ, Sawitzki G, Smith C, Smyth G, Tierney L, Yang JY, Zhang J (2004) Bioconductor: open software development for computational biology and bioinformatics. *Genome Biol* 5:R80.
- Gerhardt H, Ruhrberg C, Abramsson A, Fujisawa H, Shima D, Betsholtz C (2004) Neuropilin-1 is required for endothelial tip cell guidance in the developing central nervous system. *Dev Dyn* 231:503-509.
- Gerhardt H, Golding M, Fruttiger M, Ruhrberg C, Lundkvist A, Abramsson A, Jeltsch M, Mitchell C, Alitalo K, Shima D, Betsholtz C (2003) VEGF guides angiogenic sprouting utilizing endothelial tip cell filopodia. *J Cell Biol* 161:1163-1177.
- Giancotti FG, Ruoslahti E (1999) Integrin signaling. *Science* 285:1028-1032.
- Gora-Kupilas K, Josko J (2005) The neuroprotective function of vascular endothelial growth factor (VEGF). *Folia Neuropathol* 43:31-39.
- Goumans MJ, Lebrin F, Valdimarsdottir G (2003) Controlling the angiogenic switch: a balance between two distinct TGF- β receptor signaling pathways. *Trends Cardiovasc Med* 13:301-307.

- Goumans MJ, Valdimarsdottir G, Itoh S, Rosendahl A, Sideras P, ten Dijke P (2002) Balancing the activation state of the endothelium via two distinct TGF-beta type I receptors. *Embo J* 21:1743-1753.
- Graus-Porta D, Blaess S, Senften M, Littlewood-Evans A, Damsky C, Huang Z, Orban P, Klein R, Schittny JC, Muller U (2001) Beta1-class integrins regulate the development of laminae and folia in the cerebral and cerebellar cortex. *Neuron* 31:367-379.
- Green LJ, Mould AP, Humphries MJ (1998) The integrin beta subunit. *Int J Biochem Cell Biol* 30:179-184.
- Gu C, Rodriguez ER, Reimert DV, Shu T, Fritsch B, Richards LJ, Kolodkin AL, Ginty DD (2003) Neuropilin-1 conveys semaphorin and VEGF signaling during neural and cardiovascular development. *Dev Cell* 5:45-57.
- Gumbiner BM (1996) Cell adhesion: the molecular basis of tissue architecture and morphogenesis. *Cell* 84:345-357.
- Gunel M, Laurans MS, Shin D, DiLuna ML, Voorhees J, Choate K, Nelson-Williams C, Lifton RP (2002) KRIT1, a gene mutated in cerebral cavernous malformation, encodes a microtubule-associated protein. *Proc Natl Acad Sci U S A* 99:10677-10682.
- Hanada R, Teranishi H, Pearson JT, Kurokawa M, Hosoda H, Fukushima N, Fukue Y, Serino R, Fujihara H, Ueta Y, Ikawa M, Okabe M, Murakami N, Shirai M, Yoshimatsu H, Kangawa K, Kojima M (2004) Neuromedin U has a novel anorexigenic effect independent of the leptin signaling pathway. *Nat Med* 10:1067-1073.

- Harlow EL, D. (1988) *Antibodies: A Laboratory Manual*. Cold Spring Harbor: Cold Spring Harbor Laboratory.
- Hemler ME (1998) Integrin associated proteins. *Curr Opin Cell Biol* 10:578-585.
- Hirsch E, Gullberg D, Balzac F, Altruda F, Silengo L, Tarone G (1994) Alpha v integrin subunit is predominantly located in nervous tissue and skeletal muscle during mouse development. *Dev Dyn* 201:108-120.
- Huang XZ, Wu JF, Cass D, Erle DJ, Corry D, Young SG, Farese RV, Jr., Sheppard D (1996) Inactivation of the integrin beta 6 subunit gene reveals a role of epithelial integrins in regulating inflammation in the lung and skin. *J Cell Biol* 133:921-928.
- Huttenlocher A, Ginsberg MH, Horwitz AF (1996) Modulation of cell migration by integrin-mediated cytoskeletal linkages and ligand-binding affinity. *J Cell Biol* 134:1551-1562.
- Hynes RO (1992) Integrins: versatility, modulation, and signaling in cell adhesion. *Cell* 69:11-25.
- Hynes RO (2002a) Integrins: bidirectional, allosteric signaling machines. *Cell* 110:673-687.
- Hynes RO (2002b) A reevaluation of integrins as regulators of angiogenesis. *Nat Med* 8:918-921.
- Hynes RO, Zhao Q (2000) The evolution of cell adhesion. *J Cell Biol* 150:F89-96.
- Jackson T, Clark S, Berryman S, Burman A, Cambier S, Mu D, Nishimura S, King AM (2004) Integrin alphavbeta8 functions as a receptor for foot-and-mouth disease virus: role of the beta-chain cytodomain in integrin-mediated infection. *J Virol* 78:4533-4540.

- Jannuzi AL, Bunch TA, West RF, Brower DL (2004) Identification of integrin beta subunit mutations that alter heterodimer function in situ. *Mol Biol Cell* 15:3829-3840.
- Jarad G, Wang B, Khan S, DeVore J, Miao H, Wu K, Nishimura SL, Wible BA, Konieczkowski M, Sedor JR, Schelling JR (2002) Fas activation induces renal tubular epithelial cell beta 8 integrin expression and function in the absence of apoptosis. *J Biol Chem* 277:47826-47833.
- Kaartinen V, Voncken JW, Shuler C, Warburton D, Bu D, Heisterkamp N, Groffen J (1995) Abnormal lung development and cleft palate in mice lacking TGF-beta 3 indicates defects of epithelial-mesenchymal interaction. *Nat Genet* 11:415-421.
- Kacem K, Lacombe P, Seylaz J, Bonvento G (1998) Structural organization of the perivascular astrocyte endfeet and their relationship with the endothelial glucose transporter: a confocal microscopy study. *Glia* 23:1-10.
- Kashiwagi H, Schwartz MA, Eigenthaler M, Davis KA, Ginsberg MH, Shattil SJ (1997) Affinity modulation of platelet integrin alphaIIb beta3 by beta3-endonexin, a selective binding partner of the beta3 integrin cytoplasmic tail. *J Cell Biol* 137:1433-1443.
- Kawasaki T, Kitsukawa T, Bekku Y, Matsuda Y, Sanbo M, Yagi T, Fujisawa H (1999) A requirement for neuropilin-1 in embryonic vessel formation. *Development* 126:4895-4902.
- Keller RS, Shai SY, Babbitt CJ, Pham CG, Solaro RJ, Valencik ML, Loftus JC, Ross RS (2001) Disruption of integrin function in the murine myocardium leads to

perinatal lethality, fibrosis, and abnormal cardiac performance. *Am J Pathol* 158:1079-1090.

Kniesel U, Risau W, Wolburg H (1996) Development of blood-brain barrier tight junctions in the rat cortex. *Brain Res Dev Brain Res* 96:229-240.

Kolanus W, Nagel W, Schiller B, Zeitlmann L, Godar S, Stockinger H, Seed B (1996) Alpha L beta 2 integrin/LFA-1 binding to ICAM-1 induced by cytohesin-1, a cytoplasmic regulatory molecule. *Cell* 86:233-242.

Krebs LT, Xue Y, Norton CR, Shutter JR, Maguire M, Sundberg JP, Gallahan D, Closson V, Kitajewski J, Callahan R, Smith GH, Stark KL, Gridley T (2000) Notch signaling is essential for vascular morphogenesis in mice. *Genes Dev* 14:1343-1352.

Laberge-le Couteulx S, Jung HH, Labauge P, Houtteville JP, Lescoat C, Cecillon M, Marechal E, Joutel A, Bach JF, Tournier-Lasserre E (1999) Truncating mutations in CCM1, encoding KRIT1, cause hereditary cavernous angiomas. *Nat Genet* 23:189-193.

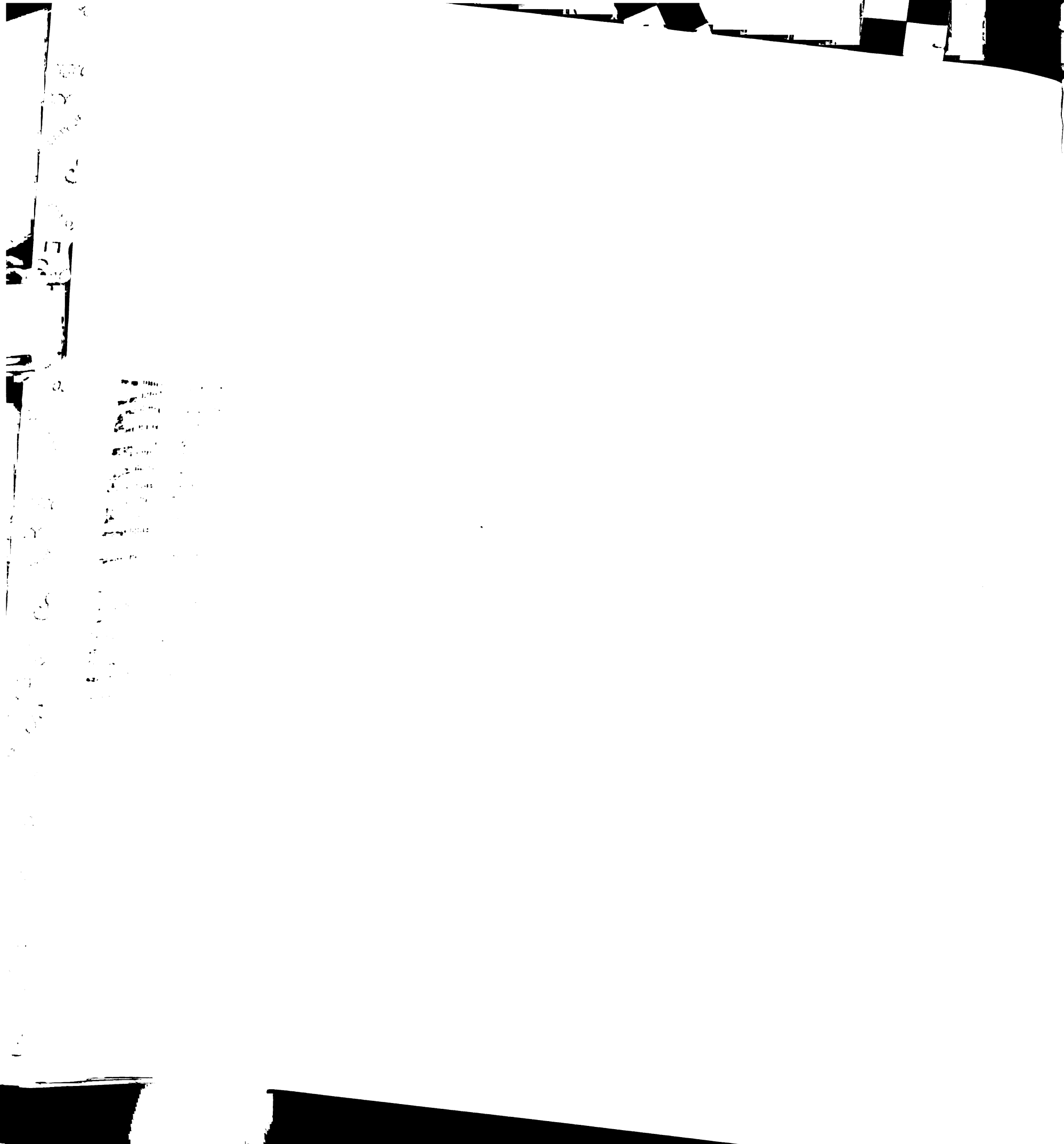
Lebrin F, Deckers M, Bertolino P, Ten Dijke P (2005) TGF-beta receptor function in the endothelium. *Cardiovasc Res* 65:599-608.

Leung DW, Cachianes G, Kuang WJ, Goeddel DV, Ferrara N (1989) Vascular endothelial growth factor is a secreted angiogenic mitogen. *Science* 246:1306-1309.

Lewandoski M, Meyers, E. N. and Martin, G. R. (1997) Analysis of Fgf8 gene function in vertebrate development. *Cold Spring Harbor Symp Quant Biol* 62:159-168.

- Li S, Edgar D, Fassler R, Wadsworth W, Yurchenco PD (2003) The role of laminin in embryonic cell polarization and tissue organization. *Dev Cell* 4:613-624.
- Lindahl P, Johansson BR, Leveen P, Betsholtz C (1997) Pericyte loss and microaneurysm formation in PDGF-B-deficient mice. *Science* 277:242-245.
- Lindblom P, Gerhardt H, Liebner S, Abramsson A, Enge M, Hellstrom M, Backstrom G, Fredriksson S, Landegren U, Nystrom HC, Bergstrom G, Dejana E, Ostman A, Lindahl P, Betsholtz C (2003) Endothelial PDGF-B retention is required for proper investment of pericytes in the microvessel wall. *Genes Dev* 17:1835-1840.
- Liu S, Calderwood DA, Ginsberg MH (2000) Integrin cytoplasmic domain-binding proteins. *J Cell Sci* 113 (Pt 20):3563-3571.
- Lu C, Takagi J, Springer TA (2001) Association of the membrane proximal regions of the alpha and beta subunit cytoplasmic domains constrains an integrin in the inactive state. *J Biol Chem* 276:14642-14648.
- Lu CF, Springer TA (1997) The alpha subunit cytoplasmic domain regulates the assembly and adhesiveness of integrin lymphocyte function-associated antigen-1. *J Immunol* 159:268-278.
- Lu QR, Sun T, Zhu Z, Ma N, Garcia M, Stiles CD, Rowitch DH (2002) Common developmental requirement for Olig function indicates a motor neuron/oligodendrocyte connection. *Cell* 109:75-86.
- Marchuk DA, Srinivasan S, Squire TL, Zawistowski JS (2003) Vascular morphogenesis: tales of two syndromes. *Hum Mol Genet* 12 Spec No 1:R97-112.
- Marin-Padilla M (1985) Early vascularization of the embryonic cerebral cortex: Golgi and electron microscopic studies. *J Comp Neurol* 241:237-249.

- Martin-Bermudo MD, Dunin-Borkowski OM, Brown NH (1998) Modulation of integrin activity is vital for morphogenesis. *J Cell Biol* 141:1073-1081.
- Mathias P, Galleno M, Nemerow GR (1998) Interactions of soluble recombinant integrin α v β 5 with human adenoviruses. *J Virol* 72:8669-8675.
- McCarty JH, Cook AA, Hynes RO (2005a) An interaction between α v β 8 integrin and Band 4.1B via a highly conserved region of the Band 4.1 C-terminal domain. *Proc Natl Acad Sci U S A* 102:13479-13483.
- McCarty JH, Lacy-Hulbert A, Charest A, Bronson RT, Crowley D, Housman D, Savill J, Roes J, Hynes RO (2005b) Selective ablation of α v integrins in the central nervous system leads to cerebral hemorrhage, seizures, axonal degeneration and premature death. *Development* 132:165-176.
- McCarty JH, Monahan-Earley RA, Brown LF, Keller M, Gerhardt H, Rubin K, Shani M, Dvorak HF, Wolburg H, Bader BL, Dvorak AM, Hynes RO (2002) Defective associations between blood vessels and brain parenchyma lead to cerebral hemorrhage in mice lacking α v integrins. *Mol Cell Biol* 22:7667-7677.
- McDowall A, Inwald D, Leitinger B, Jones A, Liesner R, Klein N, Hogg N (2003) A novel form of integrin dysfunction involving β 1, β 2, and β 3 integrins. *J Clin Invest* 111:51-60.
- Mendell JT, Sharifi NA, Meyers JL, Martinez-Murillo F, Dietz HC (2004) Nonsense surveillance regulates expression of diverse classes of mammalian transcripts and mutes genomic noise. *Nat Genet* 36:1073-1078.
- Milner R, Campbell IL (2002) The integrin family of cell adhesion molecules has multiple functions within the CNS. *J Neurosci Res* 69:286-291.



- Milner R, Frost E, Nishimura S, Delcommenne M, Streuli C, Pytela R, Ffrench-Constant C (1997a) Expression of alpha vbeta3 and alpha vbeta8 integrins during oligodendrocyte precursor differentiation in the presence and absence of axons. *Glia* 21:350-360.
- Milner R, Huang X, Wu J, Nishimura S, Pytela R, Sheppard D, ffrench-Constant C (1999) Distinct roles for astrocyte alphavbeta5 and alphavbeta8 integrins in adhesion and migration. *J Cell Sci* 112 (Pt 23):4271-4279.
- Milner R, Wilby M, Nishimura S, Boylen K, Edwards G, Fawcett J, Streuli C, Pytela R, ffrench-Constant C (1997b) Division of labor of Schwann cell integrins during migration on peripheral nerve extracellular matrix ligands. *Dev Biol* 185:215-228.
- Miner JH, Cunningham J, Sanes JR (1998) Roles for laminin in embryogenesis: exencephaly, syndactyly, and placentopathy in mice lacking the laminin alpha5 chain. *J Cell Biol* 143:1713-1723.
- Miranti CK, Brugge JS (2002) Sensing the environment: a historical perspective on integrin signal transduction. *Nat Cell Biol* 4:E83-90.
- Misson JP, Edwards MA, Yamamoto M, Caviness VS, Jr. (1988) Identification of radial glial cells within the developing murine central nervous system: studies based upon a new immunohistochemical marker. *Brain Res Dev Brain Res* 44:95-108.
- Morita K, Sasaki H, Furuse M, Tsukita S (1999) Endothelial claudin: claudin-5/TMVCF constitutes tight junction strands in endothelial cells. *J Cell Biol* 147:185-194.
- Moyle M, Napier MA, McLean JW (1991) Cloning and expression of a divergent integrin subunit beta 8. *J Biol Chem* 266:19650-19658.

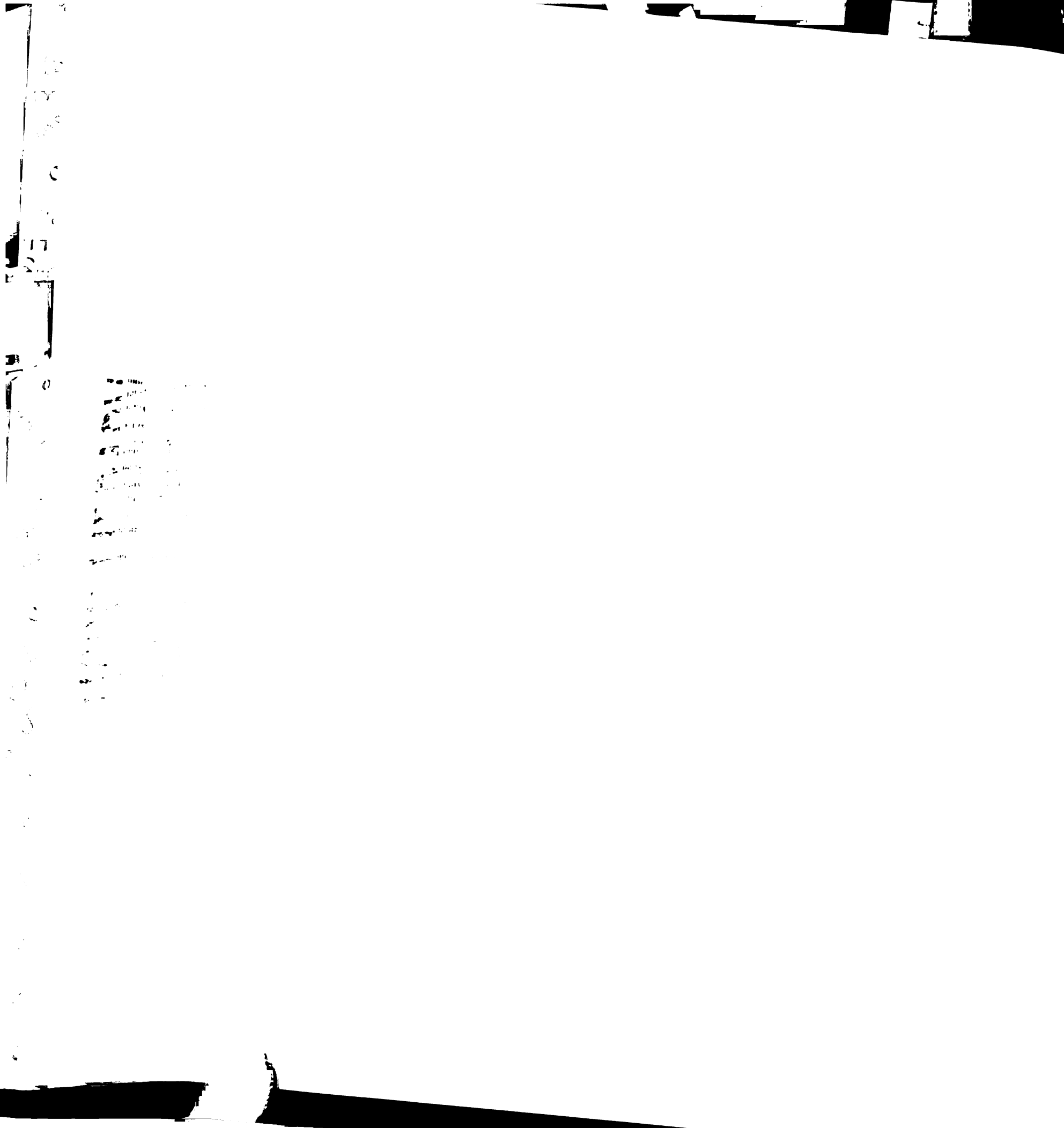
- Mu D, Cambier S, Fjellbirkeland L, Baron JL, Munger JS, Kawakatsu H, Sheppard D, Broaddus VC, Nishimura SL (2002) The integrin alpha(v)beta8 mediates epithelial homeostasis through MT1-MMP-dependent activation of TGF-beta1. *J Cell Biol* 157:493-507.
- Nakao T, Ishizawa A, Ogawa R (1988) Observations of vascularization in the spinal cord of mouse embryos, with special reference to development of boundary membranes and perivascular spaces. *Anat Rec* 221:663-677.
- Nedergaard M, Ransom B, Goldman SA (2003) New roles for astrocytes: redefining the functional architecture of the brain. *Trends Neurosci* 26:523-530.
- Nishimura SL, Sheppard D, Pytela R (1994) Integrin alpha v beta 8. Interaction with vitronectin and functional divergence of the beta 8 cytoplasmic domain. *J Biol Chem* 269:28708-28715.
- Nishimura SL, Boylen KP, Einheber S, Milner TA, Ramos DM, Pytela R (1998) Synaptic and glial localization of the integrin alphavbeta8 in mouse and rat brain. *Brain Res* 791:271-282.
- Oike Y, Ito Y, Hamada K, Zhang XQ, Miyata K, Arai F, Inada T, Araki K, Nakagata N, Takeya M, Kisanuki YY, Yanagisawa M, Gale NW, Suda T (2002) Regulation of vasculogenesis and angiogenesis by EphB/ephrin-B2 signaling between endothelial cells and surrounding mesenchymal cells. *Blood* 100:1326-1333.
- O'Toole TE, Katagiri Y, Faull RJ, Peter K, Tamura R, Quaranta V, Loftus JC, Shattil SJ, Ginsberg MH (1994) Integrin cytoplasmic domains mediate inside-out signal transduction. *J Cell Biol* 124:1047-1059.



- Palecek SP, Loftus JC, Ginsberg MH, Lauffenburger DA, Horwitz AF (1997) Integrin-ligand binding properties govern cell migration speed through cell-substratum adhesiveness. *Nature* 385:537-540.
- Park JA, Choi KS, Kim SY, Kim KW (2003) Coordinated interaction of the vascular and nervous systems: from molecule- to cell-based approaches. *Biochem Biophys Res Commun* 311:247-253.
- Pasterkamp RJ, Peschon JJ, Spriggs MK, Kolodkin AL (2003) Semaphorin 7A promotes axon outgrowth through integrins and MAPKs. *Nature* 424:398-405.
- Petersen PH, Zou K, Hwang JK, Jan YN, Zhong W (2002) Progenitor cell maintenance requires numb and numbl like during mouse neurogenesis. *Nature* 419:929-934.
- Pinkstaff JK, Detterich J, Lynch G, Gall C (1999) Integrin subunit gene expression is regionally differentiated in adult brain. *J Neurosci* 19:1541-1556.
- Poschl E, Schlotzer-Schrehardt U, Brachvogel B, Saito K, Ninomiya Y, Mayer U (2004) Collagen IV is essential for basement membrane stability but dispensable for initiation of its assembly during early development. *Development* 131:1619-1628.
- Previtali SC, Feltri ML, Archelos JJ, Quattrini A, Wrabetz L, Hartung HP (2001) Role of integrins in the peripheral nervous system. *Prog Neurobiol* 64:35-49.
- Proctor JM, Zang K, Wang D, Wang R, Reichardt LF (2005) Vascular development of the brain requires beta8 integrin expression in the neuroepithelium. *J Neurosci* 25:9940-9948.
- Proetzl G, Pawlowski SA, Wiles MV, Yin M, Boivin GP, Howles PN, Ding J, Ferguson MW, Doetschman T (1995) Transforming growth factor-beta 3 is required for secondary palate fusion. *Nat Genet* 11:409-414.

- Reynolds LE, Wyder L, Lively JC, Taverna D, Robinson SD, Huang X, Sheppard D, Hynes RO, Hodivala-Dilke KM (2002) Enhanced pathological angiogenesis in mice lacking beta3 integrin or beta3 and beta5 integrins. *Nat Med* 8:27-34.
- Riemenschneider MJ, Mueller W, Betensky RA, Mohapatra G, Louis DN (2005) In situ analysis of integrin and growth factor receptor signaling pathways in human glioblastomas suggests overlapping relationships with focal adhesion kinase activation. *Am J Pathol* 167:1379-1387.
- Rodriguez CI, Buchholz F, Galloway J, Sequerra R, Kasper J, Ayala R, Stewart AF, Dymecki SM (2000) High-efficiency deleter mice show that FLPe is an alternative to Cre-loxP. *Nat Genet* 25:139-140.
- Ruhrberg C, Gerhardt H, Golding M, Watson R, Ioannidou S, Fujisawa H, Betsholtz C, Shima DT (2002) Spatially restricted patterning cues provided by heparin-binding VEGF-A control blood vessel branching morphogenesis. *Genes Dev* 16:2684-2698.
- Rupp PA, Little CD (2001) Integrins in vascular development. *Circ Res* 89:566-572.
- Sadakata T, Mizoguchi A, Sato Y, Katoh-Semba R, Fukuda M, Mikoshiba K, Furuichi T (2004) The secretory granule-associated protein CAPS2 regulates neurotrophin release and cell survival. *J Neurosci* 24:43-52.
- Schulze C, Firth JA (1992) Interendothelial junctions during blood-brain barrier development in the rat: morphological changes at the level of individual tight junctional contacts. *Brain Res Dev Brain Res* 69:85-95.

- Schwander M, Shirasaki R, Pfaff SL, Muller U (2004) Beta1 integrins in muscle, but not in motor neurons, are required for skeletal muscle innervation. *J Neurosci* 24:8181-8191.
- Sedgwick SG, Smerdon SJ (1999) The ankyrin repeat: a diversity of interactions on a common structural framework. *Trends Biochem Sci* 24:311-316.
- Senger DR, Claffey KP, Benes JE, Perruzzi CA, Sergiou AP, Detmar M (1997) Angiogenesis promoted by vascular endothelial growth factor: regulation through alpha1beta1 and alpha2beta1 integrins. *Proc Natl Acad Sci U S A* 94:13612-13617.
- Serini G, Valdembri D, Zanivan S, Morterra G, Burkhardt C, Caccavari F, Zammataro L, Primo L, Tamagnone L, Logan M, Tessier-Lavigne M, Taniguchi M, Puschel AW, Bussolino F (2003) Class 3 semaphorins control vascular morphogenesis by inhibiting integrin function. *Nature* 424:391-397.
- Serru V, Le Naour F, Billard M, Azorsa DO, Lanza F, Boucheix C, Rubinstein E (1999) Selective tetraspan-integrin complexes (CD81/alpha4beta1, CD151/alpha3beta1, CD151/alpha6beta1) under conditions disrupting tetraspan interactions. *Biochem J* 340 (Pt 1):103-111.
- Shull MM, Ormsby I, Kier AB, Pawlowski S, Diebold RJ, Yin M, Allen R, Sidman C, Proetzel G, Calvin D, et al. (1992) Targeted disruption of the mouse transforming growth factor-beta 1 gene results in multifocal inflammatory disease. *Nature* 359:693-699.



- Sieg DJ, Hauck CR, Ilic D, Klingbeil CK, Schaefer E, Damsky CH, Schlaepfer DD (2000) FAK integrates growth-factor and integrin signals to promote cell migration. *Nat Cell Biol* 2:249-256.
- Simard M, Arcuino G, Takano T, Liu QS, Nedergaard M (2003) Signaling at the gliovascular interface. *J Neurosci* 23:9254-9262.
- Smyth GK (2004) Linear models and empirical Bayes methods for assessing differential expression in microarray experiments. *Statistical Applications in Genetics and Molecular Biology* 3.
- Soker S, Takashima S, Miao HQ, Neufeld G, Klagsbrun M (1998) Neuropilin-1 is expressed by endothelial and tumor cells as an isoform-specific receptor for vascular endothelial growth factor. *Cell* 92:735-745.
- Soldi R, Mitola S, Strasly M, Defilippi P, Tarone G, Bussolino F (1999) Role of alphavbeta3 integrin in the activation of vascular endothelial growth factor receptor-2. *Embo J* 18:882-892.
- Soriano P (1999) Generalized lacZ expression with the ROSA26 Cre reporter strain. *Nat Genet* 21:70-71.
- Springer TA, Wang JH (2004) The three-dimensional structure of integrins and their ligands, and conformational regulation of cell adhesion. *Adv Protein Chem* 68:29-63.
- Stapp MA (1999) Alpha9 and beta8 integrin expression correlates with the merger of the developing mouse eyelids. *Dev Dyn* 214:216-228.
- Sterk LM, Geuijen CA, Oomen LC, Calafat J, Janssen H, Sonnenberg A (2000) The tetraspan molecule CD151, a novel constituent of hemidesmosomes, associates

with the integrin $\alpha 6 \beta 4$ and may regulate the spatial organization of hemidesmosomes. *J Cell Biol* 149:969-982.

Stupack DG, Cheresh DA (2004) Integrins and angiogenesis. *Curr Top Dev Biol* 64:207-238.

Sundberg C, Nagy JA, Brown LF, Feng D, Eckelhoefer IA, Manseau EJ, Dvorak AM, Dvorak HF (2001) Glomeruloid microvascular proliferation follows adenoviral vascular permeability factor/vascular endothelial growth factor-164 gene delivery. *Am J Pathol* 158:1145-1160.

Tadokoro S, Shattil SJ, Eto K, Tai V, Liddington RC, de Pereda JM, Ginsberg MH, Calderwood DA (2003) Talin binding to integrin beta tails: a final common step in integrin activation. *Science* 302:103-106.

Takagi J, Erickson HP, Springer TA (2001) C-terminal opening mimics 'inside-out' activation of integrin $\alpha 5 \beta 1$. *Nat Struct Biol* 8:412-416.

Takagi J, Petre BM, Walz T, Springer TA (2002) Global conformational rearrangements in integrin extracellular domains in outside-in and inside-out signaling. *Cell* 110:599-511.

Thurston G (2003) Role of Angiopoietins and Tie receptor tyrosine kinases in angiogenesis and lymphangiogenesis. *Cell Tissue Res* 314:61-68.

Todorovic V, Jurukovski V, Chen Y, Fontana L, Dabovic B, Rifkin DB (2005) Latent TGF- β binding proteins. *Int J Biochem Cell Biol* 37:38-41.

Tronche F, Kellendonk C, Kretz O, Gass P, Anlag K, Orban PC, Bock R, Klein R, Schutz G (1999) Disruption of the glucocorticoid receptor gene in the nervous system results in reduced anxiety. *Nat Genet* 23:99-103.

Tsuboi S (2002) Calcium integrin-binding protein activates platelet integrin alpha IIb beta 3. *J Biol Chem* 277:1919-1923.

Tuckwell DS, Humphries MJ (1997) A structure prediction for the ligand-binding region of the integrin beta subunit: evidence for the presence of a von Willebrand factor A domain. *FEBS Lett* 400:297-303.

Unsicker K, Flanders KC, Cissel DS, Lafyatis R, Sporn MB (1991) Transforming growth factor beta isoforms in the adult rat central and peripheral nervous system. *Neuroscience* 44:613-625.

Venstrom K, Reichardt L (1995) Beta 8 integrins mediate interactions of chick sensory neurons with laminin-1, collagen IV, and fibronectin. *Mol Biol Cell* 6:419-431.

Wang HU, Chen ZF, Anderson DJ (1998) Molecular distinction and angiogenic interaction between embryonic arteries and veins revealed by ephrin-B2 and its receptor Eph-B4. *Cell* 93:741-753.

Wang Z, Cohen K, Shao Y, Mole P, Dombkowski D, Scadden DT (2004) Ephrin receptor, EphB4, regulates ES cell differentiation of primitive mammalian hemangioblasts, blood, cardiomyocytes, and blood vessels. *Blood* 103:100-109.

Wary KK, Mainiero F, Isakoff SJ, Marcantonio EE, Giancotti FG (1996) The adaptor protein Shc couples a class of integrins to the control of cell cycle progression. *Cell* 87:733-743.

Wildering WC, Hermann PM, Bulloch AG (2002) Rapid neuromodulatory actions of integrin ligands. *J Neurosci* 22:2419-2426.

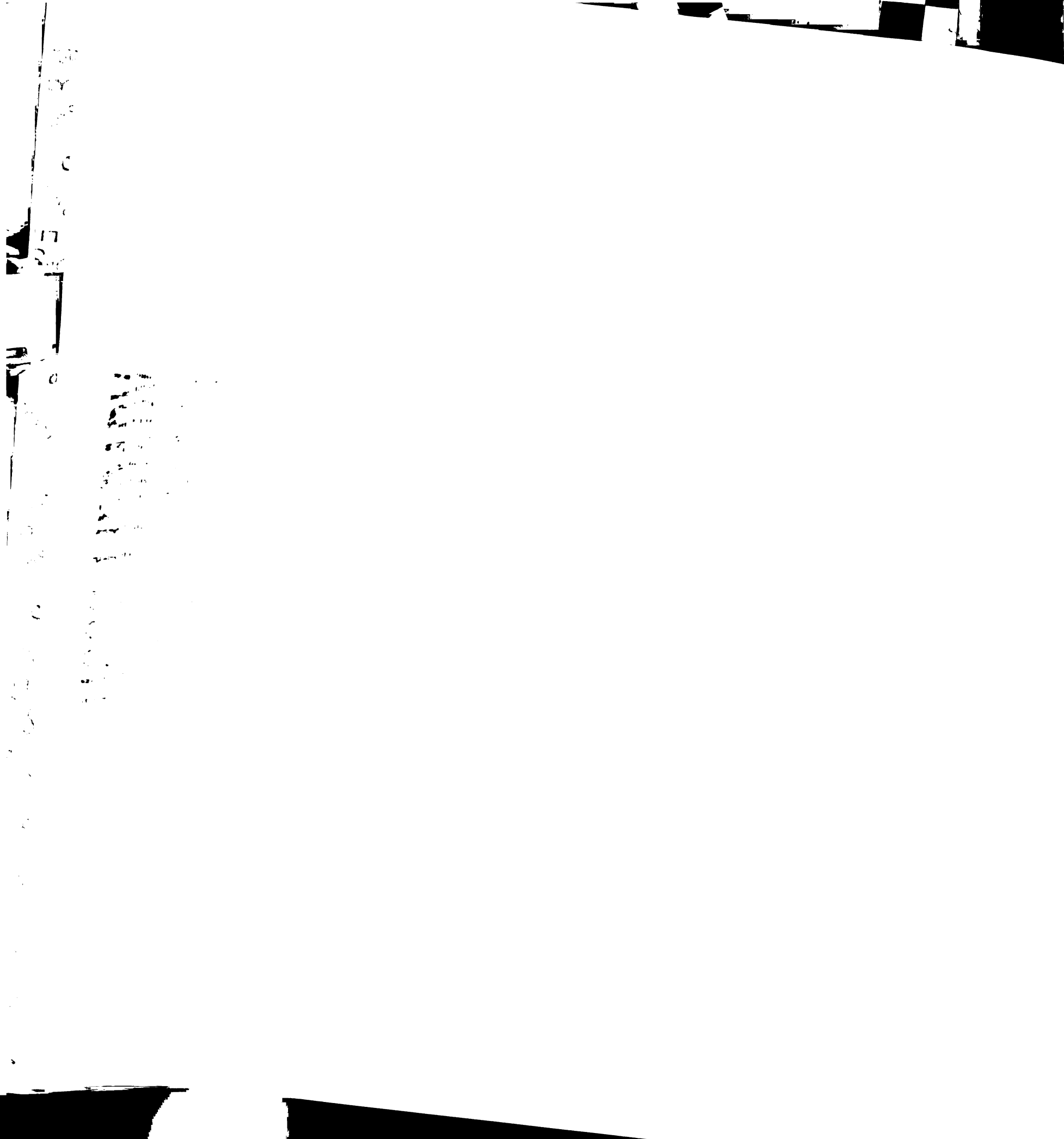
Woodside DG, Liu S, Ginsberg MH (2001) Integrin activation. *Thromb Haemost* 86:316-323.

111
112
113
114
115
116
117
118
119
120
121
122
123
124
125
126
127
128
129
130
131
132
133
134
135
136
137
138
139
140
141
142
143
144
145
146
147
148
149
150
151
152
153
154
155
156
157
158
159
160
161
162
163
164
165
166
167
168
169
170
171
172
173
174
175
176
177
178
179
180
181
182
183
184
185
186
187
188
189
190
191
192
193
194
195
196
197
198
199
200

111
112
113
114
115
116
117
118
119
120
121
122
123
124
125
126
127
128
129
130
131
132
133
134
135
136
137
138
139
140
141
142
143
144
145
146
147
148
149
150
151
152
153
154
155
156
157
158
159
160
161
162
163
164
165
166
167
168
169
170
171
172
173
174
175
176
177
178
179
180
181
182
183
184
185
186
187
188
189
190
191
192
193
194
195
196
197
198
199
200

- Wu C, Keivens VM, O'Toole TE, McDonald JA, Ginsberg MH (1995) Integrin activation and cytoskeletal interaction are essential for the assembly of a fibronectin matrix. *Cell* 83:715-724.
- Wu S, Wu Y, Capecchi MR (2006) Motoneurons and oligodendrocytes are sequentially generated from neural stem cells but do not appear to share common lineage-restricted progenitors in vivo. *Development* 133:581-590.
- Wu SX, Goebbels S, Nakamura K, Kometani K, Minato N, Kaneko T, Nave KA, Tamamaki N (2005) Pyramidal neurons of upper cortical layers generated by NEX-positive progenitor cells in the subventricular zone. *Proc Natl Acad Sci U S A* 102:17172-17177.
- Xiong JP, Stehle T, Goodman SL, Arnaout MA (2003) New insights into the structural basis of integrin activation. *Blood* 102:1155-1159.
- Xiong JP, Stehle T, Zhang R, Joachimiak A, Frech M, Goodman SL, Arnaout MA (2002) Crystal structure of the extracellular segment of integrin alpha Vbeta3 in complex with an Arg-Gly-Asp ligand. *Science* 296:151-155.
- Xiong JP, Stehle T, Diefenbach B, Zhang R, Dunker R, Scott DL, Joachimiak A, Goodman SL, Arnaout MA (2001) Crystal structure of the extracellular segment of integrin alpha Vbeta3. *Science* 294:339-345.
- Yancopoulos GD, Davis S, Gale NW, Rudge JS, Wiegand SJ, Holash J (2000) Vascular-specific growth factors and blood vessel formation. *Nature* 407:242-248.
- Yang JT, Rayburn H, Hynes RO (1993) Embryonic mesodermal defects in alpha 5 integrin-deficient mice. *Development* 119:1093-1105.

- Yang Y, Paquet, AC (2005) Preprocessing Two-Color Spotted Arrays. In: *Bioinformatics and Computational Biology Solutions Using R and Bioconductor* by Gentleman, R.; Carey, V.; Huber, W.; Irizarry, R.; Dudoit, S.: Springer Publishing.
- Yang YH, Dudoit S, Luu P, Lin DM, Peng V, Ngai J, Speed TP (2002) Normalization for cDNA microarray data: a robust composite method addressing single and multiple slide systematic variation. *Nucleic Acids Res* 30:e15.
- Yi C, McCarty JH, Troutman SA, Eckman MS, Bronson RT, Kissil JL (2005) Loss of the putative tumor suppressor band 4.1B/Dal1 gene is dispensable for normal development and does not predispose to cancer. *Mol Cell Biol* 25:10052-10059.
- Yu BP, Yu CC, Robertson RT (1994) Patterns of capillaries in developing cerebral and cerebellar cortices of rats. *Acta Anat (Basel)* 149:128-133.
- Zamir E, Geiger B (2001) Molecular complexity and dynamics of cell-matrix adhesions. *J Cell Sci* 114:3583-3590.
- Zawistowski JS, Serebriiskii IG, Lee MF, Golemis EA, Marchuk DA (2002) KRIT1 association with the integrin-binding protein ICAP-1: a new direction in the elucidation of cerebral cavernous malformations (CCM1) pathogenesis. *Hum Mol Genet* 11:389-396.
- Zhang J, Clatterbuck RE, Rigamonti D, Chang DD, Dietz HC (2001) Interaction between krit1 and icap1alpha infers perturbation of integrin beta1-mediated angiogenesis in the pathogenesis of cerebral cavernous malformation. *Hum Mol Genet* 10:2953-2960.



- Zheng X, Saunders TL, Camper SA, Samuelson LC, Ginsburg D (1995) Vitronectin is not essential for normal mammalian development and fertility. *Proc Natl Acad Sci U S A* 92:12426-12430.
- Zhu J, Motejlek K, Wang D, Zang K, Schmidt A, Reichardt LF (2002) beta8 integrins are required for vascular morphogenesis in mouse embryos. *Development* 129:2891-2903.
- Zimmerman L, Parr B, Lendahl U, Cunningham M, McKay R, Gavin B, Mann J, Vassileva G, McMahon A (1994) Independent regulatory elements in the nestin gene direct transgene expression to neural stem cells or muscle precursors. *Neuron* 12:11-24.
- Zou JX, Wang B, Kalo MS, Zisch AH, Pasquale EB, Ruoslahti E (1999) An Eph receptor regulates integrin activity through R-Ras. *Proc Natl Acad Sci U S A* 96:13813-13818.

Appendix

Generation and Characterization of Polyclonal Antisera Against the Murine Integrin $\beta 8$ Subunit



Acknowledgements

I want to thank James Linton and Zhen Huang for helpful discussions throughout this project. James has also taught me the value of patience in times that require it the most.

Abstract

Detection of the integrin $\beta 8$ subunit in the mouse has been difficult due to the absence of highly specific reagents. In order to aid biochemical and histological analysis of this integrin subunit, the cytoplasmic sequence of the mouse integrin $\beta 8$ polypeptide was fused to glutathione-S-transferase (GST) to make a fusion protein suitable for injection into rabbits. Antibodies raised against this fusion protein were purified using an affinity column containing the same mouse integrin $\beta 8$ cytoplasmic sequence tagged with maltose binding protein. While the serum contained immunoreactive antibodies against the purified mouse and human integrin $\beta 8$ cytoplasmic sequence, neither the serum nor the affinity purified antibodies were capable of detecting the integrin $\beta 8$ cytoplasmic sequence in extracts from neonatal mouse brain or in coronal slices of neonatal mouse brain.

Introduction

Since the integrin $\beta 8$ subunit was cloned in 1991 (Moyle et al., 1991), six polyclonal antibodies have been generated to detect this integrin in various biochemical or immunohistochemical assays. The first four antibodies have all been used to detect integrin $\beta 8$ in human cells and tissue. The first antibody was a polyclonal antibody, raised in rabbits, which recognized the 20 most C-terminal amino acids of the human integrin $\beta 8$ cytoplasmic sequence (Moyle et al., 1991). In an over expression assay in human kidney epithelial cells, this antibody recognized a 95 kDa polypeptide that corresponded to a heavily glycosylated integrin $\beta 8$ subunit whose unglycosylated mass is approximately 81 kDa. The second antibody was a monoclonal antibody, raised in mice that recognized a secreted form of the extracellular domain of the human integrin $\beta 8$ subunit. This monoclonal recognized the human integrin $\beta 8$ subunit when overexpressed in human kidney epithelial cells (Nishimura et al., 1994). Two additional antibodies made and distributed by Santa Cruz Biotechnologies, Inc. were polyclonal antibodies, raised in goats, that recognized either a portion of the “internal region” (Santa Cruz catalog number: sc-10817) or a fragment of the C-terminal sequence (Santa Cruz catalog number: sc-6638) of the human integrin $\beta 8$ subunit. The latter of these two antibodies has been used to characterize human integrin $\beta 8$ expression in glial tumors (Belot et al., 2001; Riemenschneider et al., 2005).

Finally, two antibodies have been used to detect integrin $\beta 8$ in rodent tissue. The first of these was generated in rabbits against the cytoplasmic domain of the human integrin $\beta 8$ subunit fused to glutathione-S-transferase (GST) (Nishimura et al., 1998). These authors report that the initial test bleeds only contained antibodies that recognized

GST so in their subsequent boosts, they used either purified full-length cytoplasmic tail not fused to GST, or synthetically generated peptide sequences of the membrane proximal region of the cytoplasmic tail and central sequence of the cytoplasmic tail. These latter two synthetic peptides were then used to affinity purify the resulting serum. Using the affinity purified antibodies, these authors localized integrin $\beta 8$ to neurons and glia within the hippocampus and the molecular and granule cell layers of the cerebellum in the adult mouse brain. The most recent polyclonal antibody was generated against the thirty-two most C-terminal amino acids of the cytoplasmic tail of the human integrin $\beta 8$ subunit (McCarty et al., 2005). This antibody was used to localize integrin $\beta 8$ within the cortex of the embryonic mouse.

Four of the six antibodies made to recognize the integrin $\beta 8$ subunit have been directed against the cytoplasmic tail of the polypeptide. This is most likely due to the fact that the cytoplasmic tail is the most unique and divergent from the other integrin β subunits (Moyle et al., 1991). All of the antibodies generated to recognize the integrin $\beta 8$ subunit thus far have been raised against the human isoform of the subunit. Although the mouse isoform and the human isoform share 84% identity in their polypeptide sequences [based on sequence information obtained from the National Center for Biotechnology website], I generated a fusion protein that consisted of the cytoplasmic domain of mouse integrin $\beta 8$ fused to GST in order to make an antibody that specifically recognized the mouse isoform of the integrin $\beta 8$ subunit. This polypeptide was injected into rabbits and the resulting serum was purified using an affinity column made of the cytoplasmic domain of mouse integrin $\beta 8$ fused to maltose binding protein (MBP) and linked to sepharose beads. While the serum contained antibodies that recognized the cytoplasmic

domain of mouse integrin $\beta 8$, it did not recognize native integrin $\beta 8$ in extracts of mouse embryonic brain.

Materials and Methods

Cloning of the mouse *itg $\beta 8$* cytoplasmic tail cDNA sequence into tag vectors. Tagging the *itg $\beta 8$* cytoplasmic tail with glutathione-S-transferase (GST). The 174 base pair (bp) *itg $\beta 8$* cytoplasmic tail cDNA sequence was subcloned into the GST vector pGEX-4T-3 (Stratagene, La Jolla, CA) using the *EcoR*I and *Not*I restriction sites available in the multiple cloning site (MCS) of the vector. PCR was used to flank the *itg $\beta 8$* cytoplasmic tail cDNA fragment with these two restriction sites using the following primers: *EcoR*I-*itg $\beta 8$* primer (5'- CCC GAATTC CAATAATAATAAAATAAAGTCCTC- 3'); *Not*I-*itg $\beta 8$* primer (5'- CCC GCGGCCGC TTAGAAGTTGCACCTGAAGG- 3'). PCR was performed using high fidelity *Pfu* DNA Polymerase (Promega, Madison, WI). The resulting PCR product and the pGEX-4T-3 vector were digested with *EcoR*I and *Not*I restriction enzymes [New England Biolabs (NEB), Ipswich, MA] after which the vector alone was treated with calf-intestinal-alkaline-phosphatase(CIP) (NEB). Both the PCR product and the vector were electrophoresed and isolated from a low melting point agarose gel. The isolated fragments were ligated using the Roche Rapid Ligation Kit (Roche, Switzerland) in a ratio of 6 μ l PCR product to 2 μ l vector. The ligated circular plasmid containing the *itg $\beta 8$* cytoplasmic tail cDNA (termed *itg $\beta 8$ cyto-GST*) was transformed into DH5 α *E. coli* bacteria (Invitrogen, Carlsbad, CA) to generate large quantities of the plasmid using standard procedures. Using a Qiagen plasmid purification kit (Qiagen, Valencia, CA) to purify the *itg $\beta 8$ cyto-GST* plasmid, its sequence was confirmed by sequencing the inserted *itg $\beta 8$* cytoplasmic tail cDNA using the following

primers derived from the pGEX-4T-3 vector sequence flanking the MCS: (5'-CAGCAAGTATATAGCATGGC- 3'); (5'-ACCGTGATGACCGAAACGCG- 3'). Tagging the *itgβ8* cytoplasmic tail with maltose binding protein (MBP). The 174 bp *itgβ8* cytoplasmic tail cDNA sequence was subcloned into the MBP vector pMAL-P2x (NEB) using the *EcoR1* and *Pst1* restriction sites available in the MCS of the vector. PCR was used to flank the *itgβ8* cytoplasmic tail cDNA fragment with these two restriction sites using the following primers: *EcoR1*- *itgβ8* primer (5'- CCC GAATTC CAATAATAATAAAATAAAGTCCTC- 3'); *Pst1*- *itgβ8* primer (5'- CCC CTGCAG TTAGAAGTTGCACCTGAAGG- 3'). PCR was performed using high fidelity *Pfu* DNA Polymerase (Promega). The resulting PCR product and the pMAL-P2x vector were digested with *EcoR1* and *Pst1* restriction enzymes (NEB) after which the vector alone was treated with CIP. Both the PCR product and the vector were electrophoresed and isolated from a low melting point agarose gel. The isolated fragments were ligated using the Roche Rapid Ligation Kit (Roche) in a ratio of 7 μl PCR product to 1 μl vector. The ligated circular plasmid containing the *itgβ8* cytoplasmic tail cDNA (termed *itgβ8cyto-MBP*) was transformed into DH5α *E. coli* bacteria (Invitrogen) to generate large quantities of the plasmid using standard procedures. Using a Qiagen plasmid purification kit (Qiagen) to purify the plasmid *itgβ8cyto-MBP*, its sequence was confirmed by sequencing the inserted *itgβ8* cytoplasmic tail cDNA using the following primers derived from the pMAL-P2x vector sequence flanking the MCS: (5'-TGTCGATGAAGCCCTGAAAG- 3'); (5'-CTGCAAGGCGATTAAGTTGG- 3').

Production of mouse integrin β8 cytoplasmic tail fusion proteins. Producing the *itgβ8* cytoplasmic tail tagged with GST fusion protein. The *itgβ8cyto-GST* plasmid was

transformed into BL-21 protease deficient *E. coli* bacteria (Stratagene) for production of the fusion protein using standard procedures. Three colonies were transferred to 2 mL liquid cultures and grown, lysed, induced, and the fusion protein purified according to the RediPack GST Purification Module protocol from Amersham Biosciences (Buckinghamshire, UK). The colony that produced the most fusion protein was regrown in a 10 mL liquid culture and diluted into a large 1000 mL liquid culture and then grown, lysed, induced, and the fusion protein purified according to the Bulk GST Purification Module protocol from Amersham Biosciences. In total, 35 mg of integrin $\beta 8$ cytoplasmic tail tagged with GST fusion protein was purified. Producing the *itg* $\beta 8$ cytoplasmic tail tagged with MBP fusion protein. The *itg* $\beta 8$ *cyto-MBP* plasmid was transformed into BL-21 protease deficient *E. coli* bacteria (Stratagene) for production of the fusion protein using standard procedures. One colony was grown in a 20 mL liquid culture and diluted into a large 2000 mL liquid culture and then grown, lysed, induced, and the fusion protein purified according to Method I of the MBP Protein Purification System from NEB. Note: it is important to use Method I because it allows the use of phosphate buffered saline (PBS) as a column buffer instead of Tris-Cl which is not an appropriate buffer for coupling the fusion protein to Sepharose beads (see below). One Mini Complete Tablet of Protease Inhibitors (Roche) was added per 25 mL of cell extract before loading the amylose column. Using a 30 mL column of amylose resin, 23 mg of integrin $\beta 8$ cytoplasmic tail tagged with MBP fusion protein was purified.

Generation of polyclonal antisera against the mouse integrin $\beta 8$ cytoplasmic tail tagged with GST. 10 mg of the integrin $\beta 8$ cytoplasmic tail tagged with GST fusion protein was sent to Covance Research Products (Denver, PA) for injection into rabbits. Covance

Research Products used an in-house standard injection protocol for immunizing two rabbits with the fusion protein. The company sent back 5 to 10 mL of antisera per bleed, which included 2 test bleeds and 1 production bleed from each animal and 7 more production bleeds from animal 1673. When animal 1673 was exsanguinated, Covance sent 25 mL of serum from this rabbit.

ELISA analysis of polyclonal antisera against the mouse integrin β 8 cytoplasmic tail tagged with GST fusion protein. Presence of antibodies against the integrin β 8 cytoplasmic tail in the serum was determined by an enzyme-linked immunosorbent assay (ELISA) using the mouse integrin β 8 cytoplasmic tail tagged with the maltose binding protein (MBP) as the capture antigen. The fusion protein was diluted to a concentration of 10 μ g/mL in 50mM carbonate buffer pH 9.6. As controls, purified maltose-binding-protein and laminin were diluted to a final concentration of 10 μ g/mL and 5 μ g/mL, respectively. Wells of a 96 well plate were coated with 100 μ L of diluted fusion protein (or control protein) and incubated for 2 hours at room temperature. Any remaining liquid was removed and 100 μ L of blocking solution (2% BSA in PBS pH 7.4) was added to the wells for 1 hour at room temperature. Each well was then washed 4 times with 0.1% Tween-20 in PBS. Sample serum and control primary antibodies were serially diluted in 1% BSA; 0.1M NaCl; 0.1M HEPES buffer pH 7.4. Control primary antibodies were laminin polyclonal antibody (pAb) (L9393, Sigma, St. Louis, MO), and MBP pAb (E8031S, NEB). 100 μ L of diluted sample serum or control antibody was applied to each well and incubated at room temperature for 1 hour. Each well was then washed 4 times with 0.1% Tween-20 in PBS. The secondary antibody used for all samples was diluted 1:5000 in 1% BSA; 0.1M NaCl; 0.1M HEPES buffer and was the same for all samples

and control wells [Peroxidase-conjugated AffiniPure Goat Anti-Rabbit IgG (Jackson Immuno Research Laboratories, West Grove, PA)]. 100 μ L of diluted secondary antibody was applied to each well and incubated at room temperature for 1 hour. Each well was then washed 4 times with 0.1% Tween-20 in PBS. 100 μ L of substrate [5mg O-phenylenediamine tablet (P-6912, Sigma) dissolved in 12 mL of 25 mM citric acid; 0.1M Na_2HPO_4 ; pH 5.0; 12 μ L of 30% hydrogen peroxide was added just prior to use] was added to each well. After 10 minutes the fluorescence from each well was read in a TiterTek Multiscan MC ELISA reader (MP Biomedicals, Irvine, CA) using a 490 nm filter. Immunoreactivity of the bleeds was estimated by determining the ratio of immunofluorescence detected in wells containing bleed serum versus immunofluorescence in wells containing pre-immunization serum.

Affinity purification of polyclonal antisera against the mouse integrin β 8 cytoplasmic tail. The integrin β 8 cytoplasmic tail tagged with MBP was covalently linked to CNBr Activated Sepharose 4B beads (Amersham Biosciences) to create an affinity column. 350 mg of CNBr beads were hydrated over a vacuum filter with 1mM HCl for 15 minutes using very light suction. 6 mg of the fusion protein was diluted in coupling buffer (0.1M NaHCO_3 ; 0.5M NaCl pH 8.3) to a final concentration of 0.75 mg/mL. In a 15 mL tube, the diluted fusion protein was mixed with the activated beads for 1 hour at room temperature (approximately 80% of the fusion protein had bound the beads as determined by spectrophotometric analysis at 280 nm). The beads were then washed once with coupling buffer and the unbound amino terminus was blocked with 0.1 M Tris pH 8.0 for 1 hour. The beads were then washed with once with 0.1 M glycine pH 2.5; once with [0.5 M NaCl; 20 mM Tris pH 7.5; 0.01% Tween-20 (TTBS)]; once with 0.1 M

Triethylamine pH 11.0; and then twice with TTBS. 10 mL of serum was diluted with 1 mL of 10X TTBS and centrifuged for 10 minutes at 3000 RPM in swinging bucket rotor in a RT600B Sorvall centrifuge. The supernatant was added to the CNBr beads covalently linked to the integrin $\beta 8$ cytoplasmic tail-MBP fusion protein and incubated overnight at 4°C on a rocker. The slurry was transferred to a 5 mL disposable column (catalog #274570D, Amersham). After the column drained, it was washed with 40 mL of 1X TTBS. 10 mL fractions were collected until the OD 280 reached 0.02. The column was then eluted with 10 mL of 0.2M glycine pH 2.5 containing 0.02% NaN₃ in 1 mL fractions. Each tube used for collecting a fraction contained 100 μ L of 1M Tris pH 8.0. The OD 280 nm was measured for each fraction and the fractions with the highest value were combined and the OD 280 nm was remeasured. 20% glycerol was added to the antibodies after dialysis with PBS overnight at 4°C.

Western Blotting and Immunoprecipitation. HT1080 cells (kind gift from S. Nishimura at UCSF) were grown to confluency on 50 cm culture plates. The cells were then scrapped from the plates and lysed in 2 mL RIPA buffer containing Mini Complete Protease Inhibitors (Roche). The cell membranes were pelleted and removed by centrifugation. The final concentration of the supernatant was determined to be 3 mg/mL by Bradford analysis. Some cells were biotinylated using the EZ-Link Sulfo-NHS-Biotinylation Kit (catalog #21420, Pierce, Rockford, IL). These cells were lysed as described above. Two P0 mouse brains were lysed in 3 mL RIPA buffer containing Mini Complete Protease Inhibitors (Roche). After disrupting the tissue by passing it through 18 gauge and 27 gauge needles, the lysate was spun at 14000 RPM in a table top Tomy MTX-152 centrifuge for 30 minutes at 4°C. The pellet was discarded and the

concentration of protein in the supernatant was determined by Bradford analysis. Western blots were performed using standard procedures and Biomax Light film (Kodak). Immunoprecipitations were performed as follows: 250 μ L of the biotinylated HT1080 cell lysate was precleared with 35 μ L of protein A/G beads (Amersham). The cleared lysate was then mixed with either 3 μ g of the affinity purified antibody against the mouse integrin β 8 cytoplasmic tail or with 3 μ g of anti- α v pAb (catalog #1930, Chemicon International, Inc., Temecula, CA) overnight at 4°C. 35 μ L of protein A/G beads were then added to the immunoprecipitation at 4°C for 30 minutes. The slurry was then spun at 14000 RPM in a table-top Tomy MTX-152 centrifuge for 1 minute. The beads were washed 4 times with ice-cold RIPA buffer and then boiled in sample buffer containing 1% β -mercaptoethanol. The samples were electrophoresed on a reducing polyacrylamide gel and transferred to nitrocellulose. Peroxidase-conjugated streptavidin (Pierce) was used at 1:100,000 to visualize the immunoprecipitated biotin-labeled proteins. This blot was stripped with 100 mM β -mercaptoethanol; 2% SDS; 10 mM Tris pH 7.4; 150 mM NaCl for 30 minutes at 50°C. The affinity purified antibody against the integrin β 8 cytoplasmic tail was used at a dilution of 1:1000 and the Peroxidase-conjugated AffiniPure Goat Anti-Rabbit IgG (Jackson Immuno Research Laboratories) was used at 1:50,000.

Immunocytochemistry of HT1080 Cells. HT1080 cells were plated at 30-40% confluency on glass cover slips and grown overnight at 37°C. The cells were washed once with PBS and then fixed with 4% PFA for 5 minutes. The cells were washed 3 times for 5 minutes each in PBS and then permeabilized for 10 minutes in 0.1% Triton-X 100 (Sigma). The cells were washed once with PBS and then blocked for 1 hour in 10%

goat serum. After rinsing with PBS the cells were incubated with integrin $\beta 8$ cytoplasmic tail polyclonal serum from production bleed 8 diluted 1:1000 in PBS for 2 hours at room temperature. The cells were then washed 3 times for 5 minutes each in PBS followed by incubation with goat anti-rabbit Texas Red (1:500, Invitrogen) fluorescent secondary antibody in blocking buffer for 1 hour at room temperature. The cells were washed 3 times for 5 minutes each in PBS and the coverslips were mounted on slides using Antifade (Invitrogen). Cells were analyzed using a Zeiss LSM 5 Pascal confocal microscope.

Results

Generation of polyclonal antisera against the mouse integrin $\beta 8$ cytoplasmic tail

The cDNA region of the mouse integrin $\beta 8$ cytoplasmic tail was cloned into a GST vector for expression in bacteria. The plasmid was then transformed into protease deficient bacteria for production of the fusion protein. After purifying thirty-five milligrams of the fusion protein using glutathione beads, ten milligrams was sent to Covance Research Products for injection into New Zealand rabbits to make polyclonal antisera.

Two rabbits were initially injected, numbered 1672 and 1673. After screening the first two test bleeds and the first production bleed by an enzyme-linked immunosorbent assay (ELISA) using a fusion protein composed of the integrin $\beta 8$ cytoplasmic tail tagged with the maltose binding protein (MBP) (Fig. A-1B, C), only bleeds from rabbit 1673 were taken beyond the first production bleed since the titer of antibody seemed to be slightly higher in the sera from this animal. This animal, in the end, provided eight production bleeds (Fig. A-1D). As shown in figure A-1C, production bleeds three and

eight had the highest titers of antibody directed against the cytoplasmic tail of mouse integrin $\beta 8$.

Functional analysis of polyclonal antisera against the mouse integrin $\beta 8$ cytoplasmic tail

To test the functionality of the antibodies contained in the serum collected from rabbit 1673, I obtained a human epithelial cell line (termed HT1080 cells) from Dr. Steve Nishimura (UCSF) stably transfected with human *itg $\beta 8$* . If the antisera contained antibodies directed against the cytoplasmic tail of mouse integrin $\beta 8$, they would likely recognize the human integrin $\beta 8$ cytoplasmic tail because the polypeptide sequences of these two isoforms share 93% homology [based on a blast comparison of the two polypeptide sequences found on the National Center for Biotechnology website]. These cells were grown in culture to a confluent density and then lysed in the presence of protease inhibitors to assay the presence of integrin $\beta 8$. Lysates, as well as purified mouse integrin $\beta 8$ cytoplasmic tail tagged with MBP, were electrophoresed on a reducing polyacrylamide gel. Using the antisera from test bleed number two, no integrin $\beta 8$ protein was detected in the lysate from these HT1080 cells (Fig. A-2A). However, using serum from production bleed eight, an 85 kDa band was detected in the *itg $\beta 8$* transfected lane that was not present in the mock transfected control cell lysate. This 85 kDa band corresponds to the approximate mass of the integrin $\beta 8$ protein (Moyle et al., 1991). To determine if the antisera would stain integrin $\beta 8$ protein on live cells, transfected HT1080 cells were directly labeled by immunocytochemistry. Staining the cells with antisera from production bleed eight resulted in a polarized staining pattern limited to the cell membrane that was not seen in control cells (Fig. A-2D). Therefore, it seemed very

likely that production bleed eight contained antibodies directed against the cytoplasmic tail of integrin $\beta 8$.

Affinity purification of polyclonal antisera against the mouse integrin $\beta 8$ cytoplasmic tail

Since the antisera seemed to contain antibodies that recognize the cytoplasmic tail of mouse and human integrin $\beta 8$ by Western blot and in immunocytochemistry assays, the antibodies were purified from the serum by affinity purification. The fusion protein of the mouse integrin $\beta 8$ cytoplasmic tail was fused to MBP and then linked amylose resin to create an affinity column. Polyclonal sera from production bleed 3 and production bleed 8 were diluted and run over the column in batches. The column was eluted using free maltose in solution and fractions were collected and assayed by spectrophotometry to determine the fractions that contained the highest concentration of purified antibodies. To test these purified antibodies, the *itg $\beta 8$* transfected HT1080 cell lysate was electrophoresed on a polyacrylamide gel and transferred to nitrocellulose for Western blotting using the purified antibodies. While the affinity purified antibodies did recognize the purified mouse integrin $\beta 8$ cytoplasmic tail tagged with MBP, they did not recognize any human integrin $\beta 8$ protein in the *itg $\beta 8$* transfected HT1080 cell lysate (Fig. A-3A). This was surprising since the unpurified sera recognized a band corresponding to the molecular mass of the integrin $\beta 8$ subunit (Fig. A-2). In addition, mouse P0 brain lysate was also electrophoresed on a polyacrylamide gel, transferred to nitrocellulose, and Western blotted using the affinity purified antibodies. However, no native mouse integrin $\beta 8$ protein was detected (Fig. A-3B).

It is possible that during the affinity purification procedure specific antibodies that recognized the integrin $\beta 8$ cytoplasmic tail were lost. However, it is also possible that the antibodies were so dilute they did not provide adequate signal for the chemiluminescent film to detect. To test this possibility, the *itg $\beta 8$* transfected HT1080 cells were biotinylated and lysed to create a pool of surface labeled molecules which should include the human integrin $\beta 8$ protein. The affinity purified antibodies were used to immunoprecipitate the integrin $\beta 8$ protein from that biotinylated lysate. As control, a polyclonal antibody against the 25kDa light chain of the human αv integrin protein was used to immunoprecipitate the αv integrin subunit and associated proteins. The affinity purified mouse integrin $\beta 8$ antibodies pulled down three bands, one of which corresponded to the 85kDa band of the integrin $\beta 8$ protein (Fig A-4A). The αv integrin antibody pulled down six bands one of which corresponded to the 85 kDa band of the integrin $\beta 8$ protein, but no 25kDa band was detected indicating this pull down may not have worked properly (Fig. A-4A). In either case, this blot was stripped with β -mercaptoethanol and SDS and then reprobed with the integrin $\beta 8$ cytoplasmic tail affinity purified antibodies. In both the integrin $\beta 8$ and αv integrin pull-down lanes, an 85kDa band was present indicating that both of these antibodies had, either directly or indirectly, pulled down integrin $\beta 8$ protein (Fig. A-4B).

The immunoprecipitation experiment indicated that the affinity purified antibodies do recognize the human integrin $\beta 8$ cytoplasmic tail. To test whether these antibodies would recognize native mouse integrin $\beta 8$ protein in immunohistochemistry, coronal P0 sections of mouse brain were stained with these affinity purified antibodies. Unfortunately, no specific staining of native mouse integrin $\beta 8$ protein was detected

under any condition or dilution (data not shown). Moreover, these antibodies did not seem to recognize the mouse integrin $\beta 8$ protein from lysates derived from neonatal mouse brain tissue in spite of their success in recognizing human integrin $\beta 8$ protein expressed in *itg $\beta 8$* transfected HT1080 cells.

Discussion

This study was intended to generate a specific polyclonal antibody that would recognize the mouse isoform of the integrin $\beta 8$ subunit. I generated a mouse integrin $\beta 8$ cytoplasmic domain-GST fusion protein that was injected into rabbits. The serum produced by these rabbits contained antibodies that recognized purified cytoplasmic tail of mouse integrin $\beta 8$ protein (Fig. A-1). Moreover, it recognized the cytoplasmic domain of the human integrin $\beta 8$ protein overexpressed in human airway epithelial cells (Fig. A-2). This was not unexpected since the human and mouse integrin $\beta 8$ cytoplasmic domains share 93% identity in their polypeptide sequences. The serum was affinity purified using a mouse integrin $\beta 8$ cytoplasmic domain-MBP fusion protein, but the affinity purified antibodies failed to recognize native integrin $\beta 8$ in P0 mouse brain lysate (Fig. A-3) or in coronal sections of P0 mouse brain (data not shown). We did attempt use of an antigen retrieval protocol on P0 sections of mouse brain to test the possibility that the cytoplasmic domain of integrin $\beta 8$ was difficult to access inside the cell, but did not see specific staining. However, the affinity purified antibodies were able to immunoprecipitate human integrin $\beta 8$ protein that was overexpressed in human airway epithelial cells (Fig. A-4). These results indicate that while this strategy successfully generated antibodies that could recognize human integrin $\beta 8$ when overexpressed *in vitro*, they were not capable of recognizing native mouse integrin $\beta 8$ expressed *in vivo*.

One of the problems with this strategy may be that the integrin $\beta 8$ cytoplasmic domain is not immunogenic enough to generate a sufficient immune response. Certainly, compared to the GST protein to which it was fused, it is a very small polypeptide. Thus, the majority of antibodies present in the serum collected in these experiments most likely recognized GST, not the integrin $\beta 8$ cytoplasmic tail. While the serum did contain antibodies that recognized the integrin $\beta 8$ cytoplasmic domain, they were most likely in such low concentration that they were extremely difficult to purify. One way to get around this problem in future experiments may be to inject the GST-integrin $\beta 8$ cytoplasmic domain fusion protein to generate an initial immune response. Then, in subsequent immunizations inject only the integrin $\beta 8$ cytoplasmic tail polypeptide. In theory, proteins as small as 3000-5000 daltons are capable of generating an immune response (Harlow, 1988). This may help selectively up-regulate production of antibodies by the plasma cells producing antibodies against the integrin $\beta 8$ cytoplasmic domain.

While other antibodies to this integrin subunit have been generated, all of them have been directed against the human isoform of the protein. Since most of the *in vivo* integrin $\beta 8$ research has been done in the mouse, it is important that a specific antibody against the mouse integrin $\beta 8$ protein be generated. In general, rabbit polyclonal antibodies offer the distinct advantage of low background when used directly on mouse tissue. However, most of the strategies used to generate a polyclonal antibody against integrin $\beta 8$ have targeted the cytoplasmic domain [including one commercial antibody made by Santa Cruz Biotechnology Inc., (Moyle et al., 1991; Nishimura et al., 1998; McCarty et al., 2005)]. However, none of these antibodies work with repeatable results or irrefutable specificity for immunohistochemical detection of the protein *in vivo*.

Perhaps the problem lies in the fact that the integrin $\beta 8$ cytoplasmic tail may be difficult to access inside the cell. If this hypothesis is accurate, then perhaps future strategies should focus on targeting the extracellular domain of integrin $\beta 8$. One such monoclonal antibody has been made against the extracellular domain of human integrin $\beta 8$ (Nishimura et al., 1994), but since it has not been used in any subsequent studies, it is either no longer available or it may not recognize the mouse isoform of the protein.

One of the barriers to making antibodies directed against the extracellular domain of integrin subunits is that to have the proper three dimensional conformation, integrin subunits must be expressed with their appropriate partner. Secondly, they must be expressed without their transmembrane domains so that they will be secreted from the cell allowing the soluble dimer of the integrin subunits to be purified from the cell culture supernatant. Several strategies exist to accomplish this in various cell systems. One method involves dimerizing the integrin subunits using the Jun/Fos dimerization motif and has been used successfully to express a soluble form of the extracellular domains of $\alpha v\beta 5$ integrin in insect cells (Mathias et al., 1998). A second method that has been used to successfully express the ectodomains of the $\alpha 5\beta 1$ integrin in Chinese hamster ovary cells uses a covalent linkage created by complementary α -helical coiled coil peptides (Takagi et al., 2001). The latter method may be the most useful since it allows expression of the secreted integrin heterodimer in mammalian cells.

Generating specific antibodies against the mouse integrin $\beta 8$ will facilitate our ability to understand its function *in vivo*. These antibodies could potentially be used for many applications such as immunoprecipitation and immunohistochemistry which may

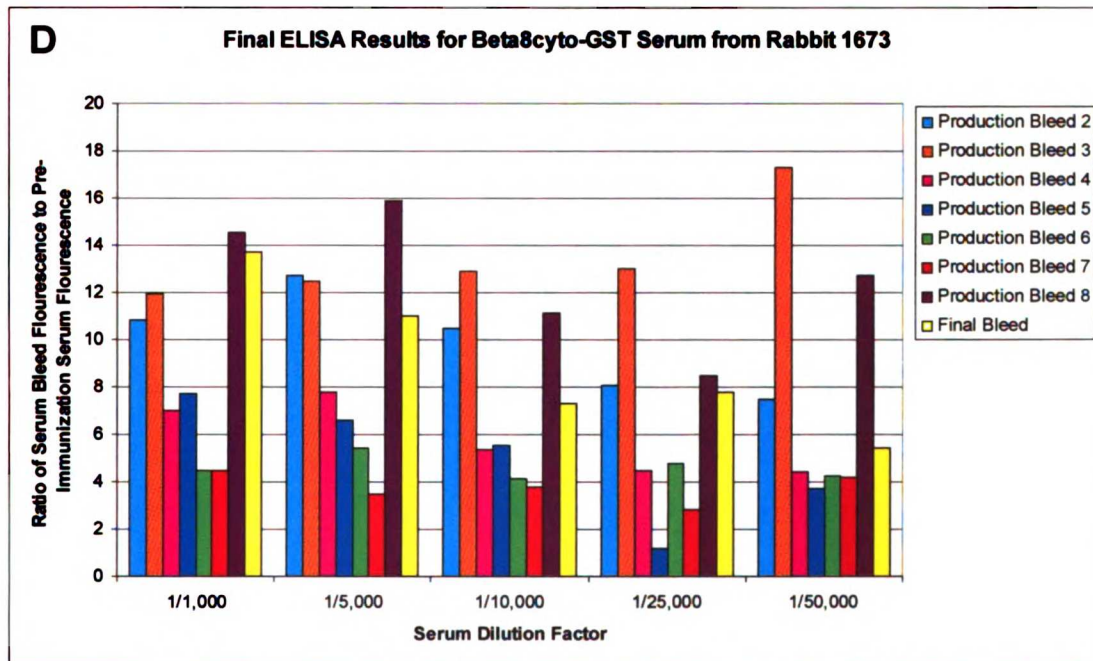
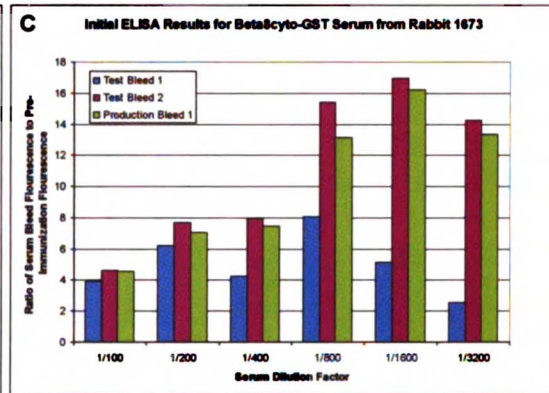
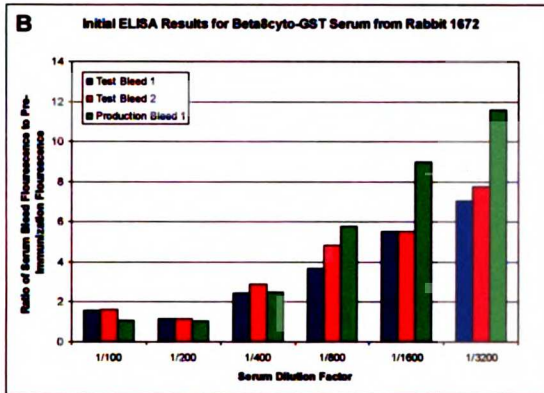
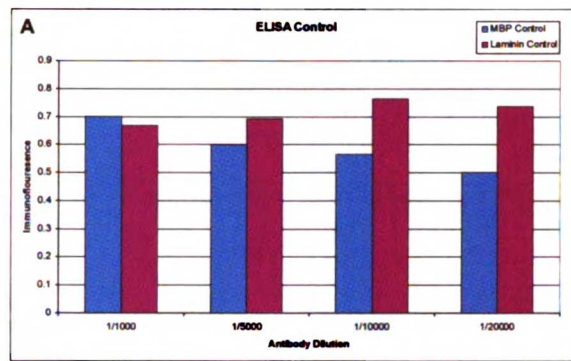


Figure A-1. ELISA results for serum obtained from rabbits immunized with the GST-tagged mouse integrin $\beta 8$ cytoplasmic tail.

Figure A-1. ELISA results for serum obtained from rabbits immunized with the GST-tagged mouse integrin $\beta 8$ cytoplasmic tail.

Two rabbits, numbered 1672 and 1673, were immunized with the cytoplasmic tail of integrin $\beta 8$ tagged with GST. Over a period of 10 weeks, each rabbit was bled 3 times in two test bleeds and one production bleed which was a larger bleed than the two prior test bleeds. Presence of antibodies against the integrin $\beta 8$ cytoplasmic tail in the serum was determined by an enzyme-linked immunosorbent assay (ELISA) using the integrin $\beta 8$ cytoplasmic tail tagged with the maltose binding protein (MBP) as the capture antigen. Immunoreactivity of the bleeds was measured as a ratio of immunofluorescence detected in wells containing bleed serum versus immunofluorescence in wells containing pre-immunization serum. *A*, Control ELISA performed with either maltose binding protein as a capture antigen and a polyclonal antibody against the maltose binding protein as the primary detecting antibody or laminin as the capture antigen and a polyclonal antibody against laminin as the primary detecting antibody. Notice the high immunofluorescence detected even at large dilutions. Note: since no pre-immunization serum was available for these commercially available antibodies, no ratio was calculated. The values shown are a fraction of the maximal possible absorbance. *B*, initial ELISA results from test bleeds 1 and 2 and production bleed 1 from rabbit 1672. *C*, initial ELISA results from test bleeds 1 and 2 and production bleed 1 from rabbit 1673. Since the ratio of immunofluorescence detected in wells containing bleed serum versus immunofluorescence in wells containing pre-immunization serum was higher for rabbit 1673, only serum from that animal was collected over the subsequent 21 week period. *D*, final ELISA results

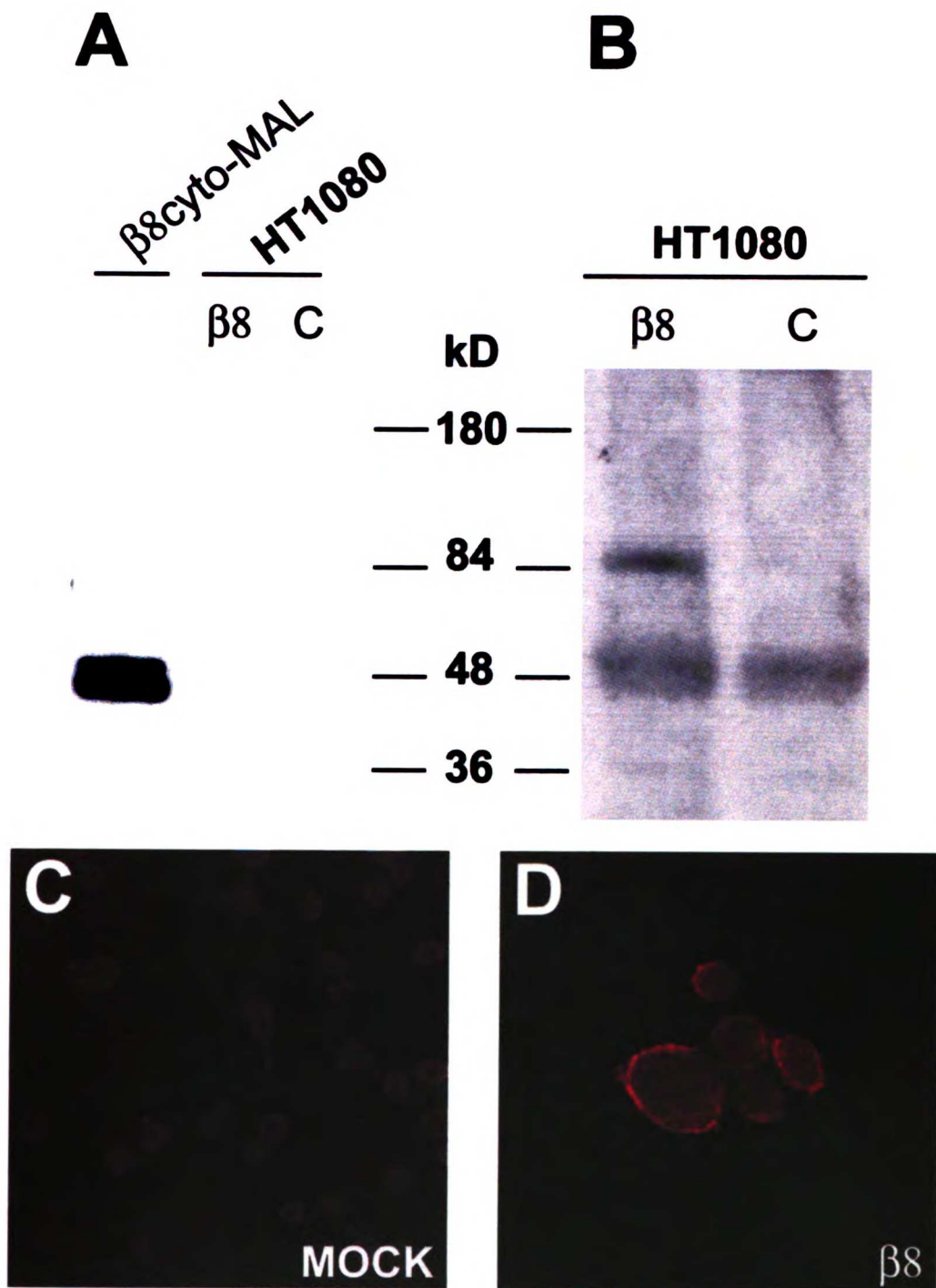


Figure A-2. Western blot and immunocytochemistry of HT1080 cells transfected with human integrin $\beta 8$.

Figure A-2. Western blot and immunocytochemistry of HT1080 cells transfected with human integrin $\beta 8$.

Western blots were performed using serum from rabbit 1673. *A*, Western blot using serum from test bleed 2. Lane one contains purified integrin $\beta 8$ cytoplasmic tail tagged with MBP. Lane two contains lysate from HT1080 cells transfected with integrin $\beta 8$ and lane three contains lysate from mock transfected HT1080 cells (control). *B*, Western blot using serum from production bleed 8 on the same HT1080 lysates. Notice the prominent band in the integrin $\beta 8$ transfected lane at approximately 85 kDa where integrin $\beta 8$ is expected to run. *C*, Mock transfected HT1080 cells stained directly with serum from production bleed 8. *D*, integrin $\beta 8$ transfected HT1080 cells stained directly with serum from production bleed 8. Notice the intense polarized membrane staining.

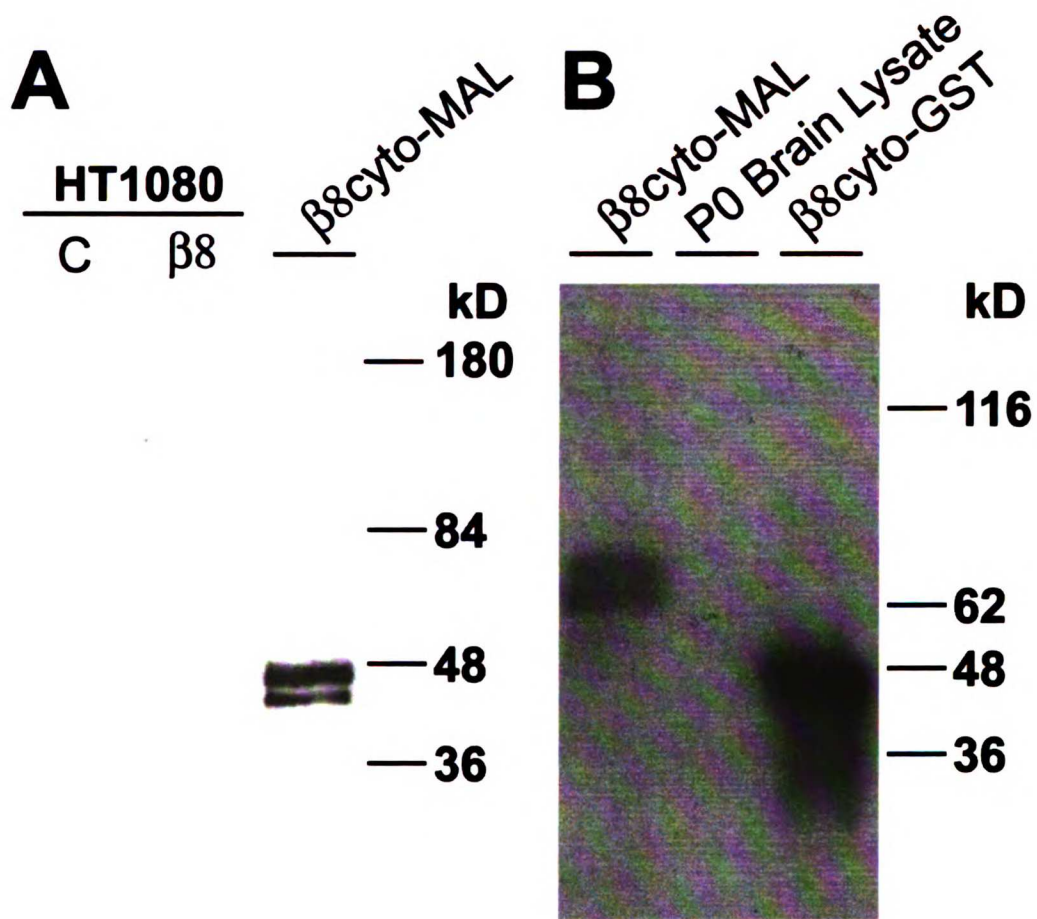


Figure A-3. Affinity purification of antibodies against the mouse integrin $\beta 8$ cytoplasmic tail tagged with GST from serum obtained from rabbit 1673.

Figure A-3. Affinity purification of antibodies against the mouse integrin $\beta 8$ cytoplasmic tail tagged with GST from serum obtained from rabbit 1673. Serum from production bleed 3 and production bleed 8 were affinity purified on a column containing the mouse integrin $\beta 8$ cytoplasmic tail tagged with MBP. Western blots using the affinity purified antibodies. *A*, Lane one contains lysate from HT1080 cells transfected with human integrin $\beta 8$, lane two contains lysate from mock transfected HT1080 cells (control), and lane three contains purified integrin $\beta 8$ cytoplasmic tail tagged with MBP. *B*, Lane one contains purified mouse integrin $\beta 8$ cytoplasmic tail tagged with MBP. Lane two contains lysate from P0 brain lysate and lane three contains purified mouse integrin $\beta 8$ cytoplasmic tail tagged with GST, the original antigen.

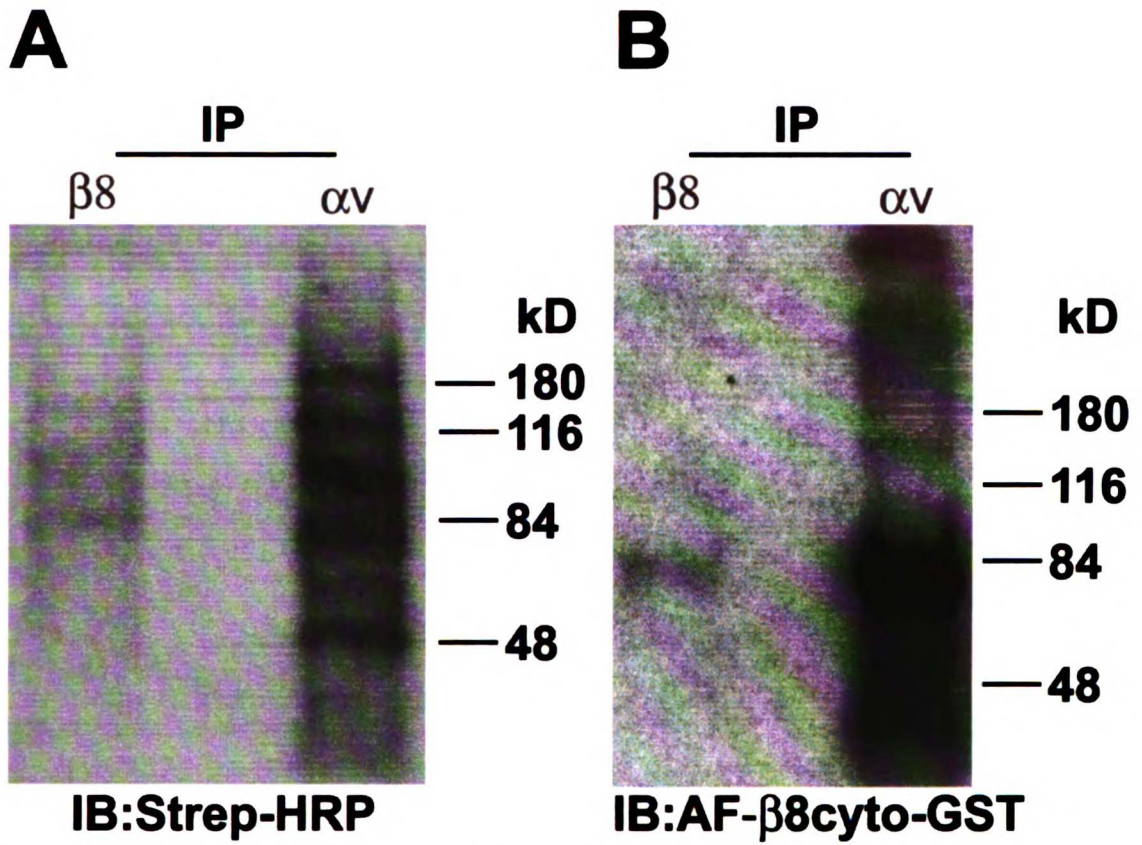
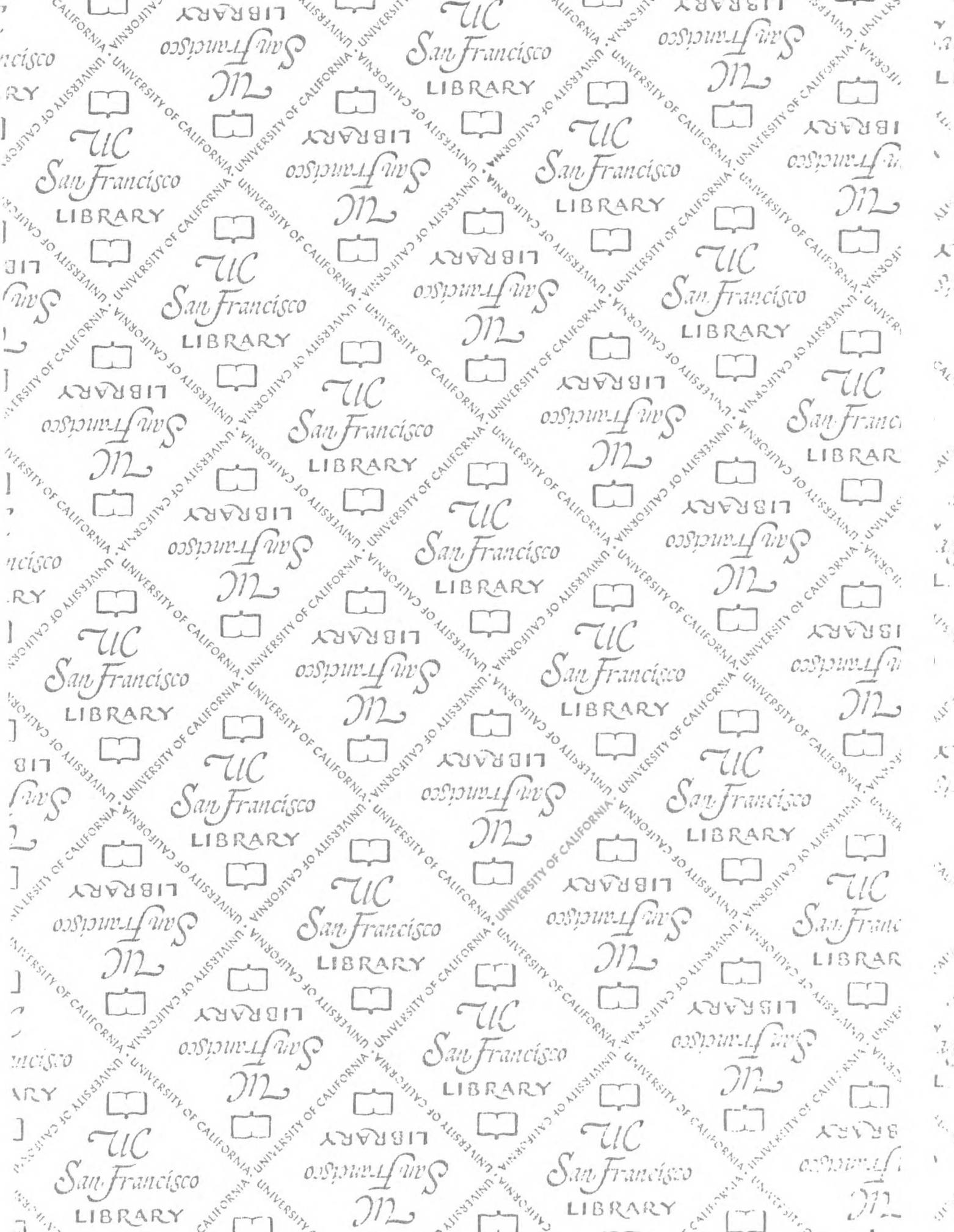


Figure A-4. Immunoprecipitation using affinity purified antibodies against the mouse integrin $\beta 8$ cytoplasmic tail.

Figure A-4. Immunoprecipitation using affinity purified antibodies against the mouse integrin $\beta 8$ cytoplasmic tail.

The affinity purified mouse integrin $\beta 8$ cytoplasmic tail antibodies were used to immunoprecipitate proteins from lysate obtained from biotinylated HT1080 cells transfected with human integrin $\beta 8$. *A*, Western blot using horseradish peroxidase conjugated streptavidin. Lane one contains proteins immunoprecipitated using the affinity purified mouse integrin $\beta 8$ cytoplasmic tail antibody. Lane two contains proteins immunoprecipitated using a polyclonal antibody against integrin αv that recognizes the 25 kDa light chain moiety of the mature 150 kDa αv protein. Notice the presence of the 85 kDa band in both lanes. *B*, The Western blot in *A* was stripped and reprobed using the affinity purified mouse integrin $\beta 8$ cytoplasmic tail antibody. Notice the presence of the 85 kDa band corresponding to integrin $\beta 8$ in both lanes.



7537775



3 1378 00753 7775

For reference

Not to be taken
from the room.

